Functional analysis of a cytoplasmic male sterility in Arabidopsis thaliana

Noémie Dehaene

Thèse de doctorat
de l'Université Paris-Saclay
préparée à l'Université Paris-Sud

Ecole doctorale n°567
Sciences du végétal : du gène à l'écosystème
Spécialité de doctorat : Biologie

par

Noémie Dehaene

Functional analysis of a cytoplasmic male sterility in *Arabidopsis thaliana*

Thèse présentée et soutenue à Versailles, le 15 Novembre 2017.

Composition du Jury :

M.	Pascal Touzet	PR	Président du jury
		Polytech'Lille, EEP Lille	
M.	David Logan	PR	Rapporteur
		Université Angers, IRHS Angers	
M.	Stephan Greiner	Group leader	Rapporteur
		MPIMP, Golm	
Mme	Hélène Vanacker	MCF	Examinatrice
		Université Paris-Sud	
Mme	Françoise Budar	DR	Directrice de thèse
		INRA, IJPB Versailles	

Remerciements (Acknowledgments)

Ces trois années de thèse ont été très stimulantes et riches, tant sur le plan professionnel que personnel. La participation et le soutien de beaucoup de personnes m'ont permis de mener à bien ce projet doctoral, et je tenais à les remercier ici.

Françoise, je te remercie de m'avoir introduite à la CMS, en m'ayant proposé un sujet de recherche très intéressant, impliquant des approches variées. Merci aussi pour ton soutien, pour ton optimisme indéfectible et ta disponibilité, ainsi que ton aide au laboratoire, en serre, et tes relectures de ma thèse.

Un grand merci aussi à Clément pour m'avoir co-encadrée et avoir préparé mon arrivée, ainsi que pour m'avoir tout montré à mes débuts dans le laboratoire, tout en faisant montre de beaucoup de patience.

Matthieu, ton aide précieuse (pour les clonages, les broyages, la cyto...) notamment au moment où la fin de mon travail approchait, accompagnée d'une conversation sympathique et de ton retour d'expérience sur ta propre thèse, m'a beaucoup apporté.

Merci aussi à Christine, Stéphanie et Anthony pour les discussions avec Françoise lors des réunions CMS, les idées stimulantes pour prolonger mes réflexions sur mon sujet. J'ai beaucoup apprécié nos intéractions nucléo-cytoplasmiques, qui ne révélaient pas l'ombre d'une incompatibilité.

Im Laufe meiner Promotion habe ich zwei Monate in Bonn verbracht, im Labor von Markus Schwarzländer. Erst möchte ich Ihm für die Beistellung der netten ratiometrischen Sensoren und für die Hilfe bei der Einstellung danken. Für die Vorbereitung der Pflanzen vor meiner Ankunft sowie seine Hilfe mit dem konfokalen Mikroskop möchte ich Thomas meinen tiefen Dank aussprechen. Das ganze Team soll außerdem begrüßt sein: Markus, Thomas, Philippe, Marlene, Stephan und Valentina, vielen Dank für euren freundlichen Empfang, die stets interessanten Diskussionen und die gespannte Forschungsatmosphäre. Philippe, ganz herzlichen Dank für deine Hilfe am Fahrradfinden sowie für die großartige Fahrradtour im schönen Rheinland-Pfalz!

Résumé en français

Les angiospermes, ou plantes à fleurs, sont majoritairement à reproduction sexuée. Leur reproduction implique l'alternance entre une génération sexuelle et une génération asexuelle. La génération asexuelle correspond à la croissance végétative du sporophyte diploïde sur lequel une forme de vie haploïde très réduite, appelée le gamétophyte, se développe. Le gamétophyte femelle correspond au sac embryonnaire, tandis que le gamétophyte mâle correspond au grain de pollen. La fonction principale des gamétophytes est de produire les gamètes, qui réalisent la double fécondation et créent un nouvel individu diploïde. Si la majeure partie des espèces sont hermaphrodites (elles portent les organes reproducteurs mâles et femelles sur une même fleur bisexuelle), il existe beaucoup de systèmes de reproduction différents. Dans le système gynodioïque, des plantes hermaphrodites coexistent avec des plantes femelles dans une population. Dans ces populations, les individus femelles ont en fait perdu la capacité de produire du pollen viable - elles sont mâle-stériles. Dans la plupart des cas, ces stérilités mâles sont liées à un facteur de stérilité porté par le génome cytoplasmique, donc à hérédité maternelle, d'où la dénomination de stérilité mâle cytoplasmique (SMC). Le noyau peut quant à lui être de deux types : il est dit mainteneur (de stérilité) s'il permet l'effet du gène de stérilité, et restaurateur (de fertilité) s'il contrecarre cet effet. Les gènes nucléaires restaurateurs sont sélectionnés en réponse à la présence du cytoplasme stérilisant car ils rétablissent la fertilité mâle. Les SMC résultent d'une incompatibilité entre les génomes nucléaire et cytoplasmiques. Jusqu'à présent, tous les gènes cytoplasmiques associés à des SMC naturelles qui ont été identifiés sont mitochondriaux. Les systèmes de SMC sont très répandus. D'une part, on trouve 275 genres d'angiospermes qui contiennent au moins une espèce gynodioïque. D'autre part, la fixation d'allèles restaurateurs dans le noyau masque parfois les SMC, qui sont révélées à la suite de croisements mettant en présence le cytoplasme d'une espèce ou d'une accession, et le noyau "naïf" sans allèles restaurateurs d'une autre espèce. Ces SMC invisibles car ne provoquant pas de dimorphisme sexuel dans leur population d'origine, sont appelées cryptiques.

Les SMC sont utilisées depuis les années 30 en agriculture pour la production d'hybrides, et les facteurs génétiques conduisant à ces stérilités commencent à être bien compris, pour avoir été abondamment étudiés chez les espèces d'intérêt agronomique. Cependant, les mécanismes physiologiques aboutissant à l'avortement du gamétophyte mâle, alors que la croissance végétative de la plante n'est pas affectée, sont encore mal comprises. En effet, si le gène de stérilité est exprimé constitutivement dans bien des systèmes de SMC, le seul phénotype visible qu'il induit est l'avortement du grain de pollen. Cette "spécificité mâle" du phénotype est encore largement incomprise. Les SMC sont classifiées en deux types, selon que le gène de stérilité agit sur la génération sporophytique (SMC sporophytique) ou gamétophytique (SMC gamétophytique). Dans le cas des SMC sporophytiques ce sont les cellules du tapis de l'anthère qui présentent le défaut primaire, et le dysfonctionnement provoque la mort du pollen, tandis que dans le cas des SMC gamétophytiques le défaut se produit au niveau du grain de pollen. Plusieurs hypothèses ont été proposées pour expliquer l'avortement du pollen. Parmi celles-ci, la plus communément acceptée est "l'hypothèse de l'ATP", selon laquelle un dysfonctionnement mitochondrial lié au gène de stérilité conduirait à une production diminuée d'ATP, la monnaie énergétique de la cellule. Cette déficience en ATP serait délétère pour la gamétogenèse mâle, qui est une étape du développement particulièrement énergivore. Cette hypothèse est néanmoins controversée pour plusieurs raisons. Il paraît notamment difficile d'imaginer comment un manque d'énergie n'aurait pas de conséquences sur d'autres processus développementaux que la gamétogenèse mâle, alors qu'ils peuvent également demander beaucoup d'énergie. D'autres hypothèses impliquent un rôle particulier que joueraient les mitochondries dans la gamétogenèse mâle, la présence d'un facteur X présent uniquement dans les cellules du tapis ou du grain de pollen qui interagirait avec le facteur de stérilité pour induire la stérilité, et une surproduction de dérivés réactifs de l'oxygène (ROS) qui conduiraient à l'induction de la mort cellulaire prématurée des cellules du tapis ou à l'avortement du gamétophyte mâle.

Une SMC gamétophytique cryptique a été découverte par l'équipe chez l'espèce modèle *Arabidopsis thaliana*. Le cytoplasme de l'accession Shahdara, ou Sha (Tadjikistan) est stérilisant, et le noyau de l'accession Cvi-0 (Cap Vert) est mainteneur de stérilité. Une phase ouverte de lecture codant possiblement un peptide composé de 117 acides aminés, appelée *orf117Sha*, a été identifiée comme facteur de stérilité candidat par une approche de génétique d'association. La protéine possiblement encodée par l'*orf117Sha* est similaire à 69 % au produit potentiel de l'*orf108*, qui a été identifié comme gène inducteur de SMC dans le système *mori* (cytoplasme de *Moricandia arvensis* et noyau de *Brassica juncea*). Au cours de ma thèse, j'ai cherché à valider le rôle de l'*orf117Sha* comme inducteur de stérilité, et à comprendre comment une anomalie mitochondriale pouvait

induire cette stérilité mâle. J'ai utilisé essentiellement la lignée au cytoplasme Sha et au noyau Cvi-0, notée [Sha]Cvi-0 comme lignée mâle stérile, la lignée [Kz-9]Cvi-0 comme contrôle (l'accession Kz-9 porte un cytoplasme très proche de celui de Sha, mais n'est pas inducteur de stérilité), l'accession Cvi-0 comme lignée mainteneuse, et l'accession Sha comme lignée restaurée.

Pour valider l'*orf117Sha* comme gène associé à la SMC, j'ai étudié son expression dans l'accession Sha et la lignée [Sha]Cvi-0. Je n'ai pas détecté de différence d'accumulation de l'ARN messager, ni de modification de cet ARN messager selon le fonds nucléaire. Par contre, grâce à un anticorps que j'ai développé, j'ai observé une différence d'accumulation de la protéine ORF117SHA, qui est présente uniquement dans la lignée stérile, support-ant l'hypothèse de son rôle dans la stérilité. Afin de construire un outil qui permettrait d'étudier le lien entre structure et fonction de l'ORF117SHA, j'ai cherché à phénocopier la stérilité à l'aide de plantes transgéniques exprimant l'ORF117SHA adressée à la mi-tochondrie. Lorsque le promoteur utilisé dans la construction est constitutif, les plantes transgéniques obtenues ont deux types de phénotypes : certaines d'entre elles présentent du pollen mort et ne transmettent pas l'insert, suggérant l'induction par l'ORF117SHA d'une possible létalité du gamétophyte femelle en plus du gamétophyte mâle ; d'autres ne présentent ni mortalité pollinique, ni biais de transmission de l'insert. Nous avons supposé que des différences d'expression du transgène étaient responsables de ces deux types de comportement. Ces deux approches appuient l'hypothèse selon laquelle l'*orf117Sha* serait responsable de la SMC, bien qu'elles ne permettent pas d'exclure l'existence d'autres gènes candidats qui pourraient expliquer l'avortement pollinique.

Afin de comprendre comment un défaut mitochondrial pouvait conduire à la mort pollinique sans être délétère à la croissance végétative de la plante, j'ai utilisé plusieurs types d'approches. J'ai d'abord décrit l'avortement du pollen à l'aide d'observations cy-tologiques. Des grains de pollen mort sont détectés dans les plantes stériles à partir du stade binucléé, et leur proportion augmente au cours du développement pour atteindre environ 100 % de pollen mort au stade trinucléé. J'ai également observé les mitochon-dries du gamétophyte mâle au cours du développement, pour la première fois, à l'aide d'une GFP adressée aux mitochondries. Dans la lignée stérile, j'ai observé à partir du stade uninucléé un gonflement des mitochondries qui semble évoluer vers l'éclatement de celles-ci. De plus, j'ai vérifié le bon déroulement des mitoses polliniques à l'aide d'une GFP marquant spécifiquement les noyaux de la lignée germinale (cellule générative et cellules spermatiques) du grain de pollen chez les plantes stériles. Environ la moitié des grains de pollen subit la première mitose pollinique, et seulement 3 % la seconde mitose pollinique. Le gonflement puis l'éclatement des mitochondries semble provoquer l'arrêt du développement, car la proportion de grains de pollen ayant des mitochondries anormales

correspond à la proportion de grains de pollen n'ayant pas de noyau germinatif différencié au stade binucléé. De la même façon, d'après les proportions observées seuls les grains de pollen qui ont encore des mitochondries normales au stade binucléé semblent pouvoir subir la deuxième mitose pollinique. Dans la lignée stérile, au stade binucléé la plupart des grains de pollen ont des mitochondries anormales et leur développement paraît bloqué avant la seconde mitose pollinique. Ils évoluent vers un stade binucléé tardif qui dégénère.

D'autre part, j'ai évalué plus en profondeur le fonctionnement mitochondrial dans les lignées stérile et fertiles. J'ai d'abord analysé le fonctionnement global des mitochondries dans la plante entière. Les complexes du système de phosphorylation oxydative apparaissent être accumulés de la même manière dans les lignées stérile et fertiles. De plus, la voie de l'oxydase alternative, généralement déclenchée en cas de dysfonctionnement mitochondrial, ne semble pas induite chez les plantes stériles. J'ai ensuite évalué le fonctionnement mitochondrial spécifiquement dans certains tissus, à l'aide d'approches innovantes en microscopie confocale. J'ai pour cela utilisé des senseurs fluorescents génétiquement encodés, qui m'ont permis de comparer le niveau d'ATP cytosolique disponible pour la cellule ainsi que l'état redox du glutathion. Les mesures ont été effectuées sur des tissus végétatifs : des cellules d'épiderme d'hypocotyle de plantules *in vitro* ; ainsi que sur le pollen. Aucune différence n'est détectable dans le niveau d'ATP entre les plantes fertiles et stériles, que ce soit dans les tissus végétatifs ou dans le grain de pollen. Ce résultat va à l'encontre de "l'hypothèse de l'ATP". Par contre, le glutathion mitochondrial se trouve dans un état plus oxydé dans les mitochondries des cellules d'épiderme d'hypocotyle de la lignée stérile que dans les lignées fertiles, ainsi que dans les mitochondries et le cytosol des grains de pollen de la lignée stérile. Nous supposons que la suroxydation du glutathion résulte d'une production de ROS plus importante dans la lignée stérile, liée à la présence du gène de stérilité. Dans des hybrides restaurés, le glutathion n'est plus suroxidé ni dans les mitochondries des cellules d'épiderme d'hypocotyle, ni dans le grain de pollen, ce qui suggère un lien entre cette suroxydation et la SMC.

Dans la SMC Sha d'*A. thaliana*, il semble qu'un défaut mitochondrial conduise à l'avortement progressif du grain de pollen, possiblement en relation avec une suroxydation continue du gamétophyte mâle, un changement de la morphologie mitochondriale et l'arrêt prématuré du développement. Les évènements conduisant à la mort pollinique rappellent ceux décrits dans l'induction de mort cellulaire programmée dans d'autres systèmes.

Avec cette étude, j'apporte des arguments en faveur du rôle de l'*orf117Sha* dans l'induction de la SMC Sha d'*A. thaliana*, et je décris les évènements préalables à l'avortement du grain de pollen dans cette SMC gamétophytique. Mes résultats permettent une avancée de la compréhension des mècanismes physiologiques de la stérilité mâle, en suggérant un rôle des ROS et en écartant l'hypothèse d'une déficience en ATP.

Contents

List of Figures

List of Tables

Abbreviations

AOX =	Alternative Oxidase
ADP =	Adenosine Di Phosphate
ATP =	Adenosine Tri Phosphate
BLAST =	Basic Local Alignment Search Tool
bp =	Base Pairs
CaMV =	Cauliflower Mosaic Virus
cDNA =	Complementary DNA
CFP =	Cyan Fluorescent Protein
CMS =	Cytoplasmic Male Sterility
Col-0 =	*A. thaliana* accession Columbia-0
Cvi-0 =	*A. thaliana* accession Cvi-0
DAPI =	4',6-DIamino-2PhenylIndole
DNA =	DesoxyriboNucleic Acid
EDTA =	EthyleneDiamine-Tetraacetic Acid
Fx =	Filial generation x
Fr =	Fertility restorer
FRET =	Fluorescent Resonance Energy Transfer
Genta =	Gentamycin
GFP =	Green Fluorescent Protein
GSH =	Glutathione reduced form
GSSG =	Glutathione oxidized form
Grx1 =	human Glutaredoxin-1
Kana =	Kanamycin
Kz-9 =	*A. thaliana* accession Kz-9
LB =	Lysogeny Broth
MOPS =	3-(N-MOrpholino)Propane Sulfonic acid
mRNA =	Messenger RNA
Mn-SOD =	Manganese dependent SuperOxide Dismutase

MPTP =	Mitochondrial Permeability Transition Pore
Mr-0 =	*A. thaliana* accession Mr-0
OD =	Optical Density
ORF =	Open Reading Frame
OXPHOS =	OXidative PHOSphorylation
PCD =	Programmed Cell Death
PCR =	Polymerase Chain Reaction
pDNA =	Plasmidic DNA
PI =	Propidium Iodide
PPR =	PentatricoPeptide Repeat
PVDF =	PolyVinyliDene Fluoride
qRT-PCR =	Quantitative Real-Time Polymerase Chain Reaction
Rak-2 =	*A. thaliana* accession Rak-2
Rf =	Restorer of fertility
RFLP =	Restriction Fragment Length Polymorphism
Rif =	Rifampicin
RNA =	RiboNucleic Acid
RT-PCR =	Reverse-Transcription PCR
ROS =	Reactive Oxygen Species
Sha =	*A. thaliana* accession Shahdara
SDS =	Sodium Dodecyl Sulfate
Tx =	Transformed plant, generation x
TAE =	Tris-Acetate-EDTA
T-DNA =	Transfer-DNA
Tris =	TRIS-(hydroxymethyl)-aminomethane
UTR =	UnTranslated Region
UV =	UltraViolet
YFP =	Yellow Fluorescent Protein
[X]Y =	Cytoline combining the cytoplasm from the accession X with the nucleus from the accession Y

Nitrogenous base

A =	Adenine
T =	Thymine
C =	Cytidine
G =	Guanine
U =	Uridine

1 — Introduction

1.1 Cytoplasmic male sterilities in the context of flowering plant reproduction

Angiosperms, or flowering plants, are often appreciated in nature because of their flowers, that are extremely diverse in shape, colors, and odors. Linnaeus, in his *Praeludia sponsaliorum plantarum*, described the petals as the nuptial beds, and drew a parallel between the reproductive organs of animals and plants. His writing on plant sexuality earned him comparison with the most "obscene romance writer" by his contemporaries. Yet, he was one of the first to recognize the biological importance of sexual reproduction in plants, and to classify them according to morphological features of their reproductive organs [1]. The female reproductive organs are the pistils, whereas the male reproductive organs are the stamens. In the following sections, I describe some of the many reproduction systems in flowering plants, before discussing a peculiar case: gynodioecy. Because my study focuses on one particular male sterility, I also describe more precisely male gametophyte development.

1.1.1 Reproduction systems in flowering plants

Angiosperms reproduce mostly sexually, even though they are capable of asexual reproduction. Unlike animals that produce primordial germ line in early embryogenesis, higher plants alternate asexual and sexual generations. Asexual generation consists on the growth of a diploid sporophyte organism, on which a highly reduced form of haploid organism, named the gametophyte, develops. The major function of the gametophyte is to produce the gametes. The alternation between the two generations is achieved through meiosis to form the haploid gametophyte, and double fertilization to create the new diploid zygote. The female gametophyte is named megagametophyte or embryo sac, whereas the male gametophyte is named microgametophyte or pollen grain.

Flowering plants have outstandingly high diversity of different sexual reproduction

systems. Most species (70 %) are hermaphroditic: plants carry female (pistil) and male (stamens) organs on a bisexual flower [2]. Other species (5-6 %) are called dioecious: male and female flowers are separated on different individuals. In 1877, C. Darwin [3] proposed that these plants "are descended from plants which formerly had the two sexes combined in the same flower. It is a curious and obscure problem how and why such hermaphrodites have been rendered bisexual". He proposed that the reproduction systems that he called polygamous (with male, female, and hermaphroditic plants co-existing) and gynodioecious (with female and hermaphroditic plants co-existing) would be an evolutionary step towards the separation of sexual types on different individuals in dioecious species. Since Darwin, it has been proven that monoecy (an individual carries female and male organs on different flowers) is positively linked to dioecy regarding the number of genera including monoecious and dioecious species [2]. Furthermore, recent studies suggest that gynodioecy is also positively linked to dioecy, with more genera including gynodioecious and dioecious species than expected by random [4]. The monoecy and gynodioecy evolving pathways to dioecy are presented in figure 1.1.

1.1.2 Gynodioecy and cytoplasmic male sterility

Gynodioecy is widespread among angiosperms: 275 angiosperm genera contain at least one gynodioecious species [2]. In gynodioecious populations, the female plants are male sterile, *i.e.* they have lost the ability to produce pollen. In most gynodioecious systems, the sterilizing factor is cytoplasmic. It was first shown in flax that such male sterility was the result of combination of nuclear genes inherited in a Mendelian way, together with cytoplasmic factors [6]. Then, M. Rhoades described the same phenomenon in maize, and demonstrated the cytoplasmic inheritance of a male sterility used in breeding programs [7, 8]. His work contributed to the denomination of Cytoplasmic Male Sterility (CMS). Although male infertility can be caused by many factors, gynodioecy is most often linked to cytoplasmically transmitted determinant with interaction of nuclear gene(s) [9].

CMS is of agronomic interest, as females are widely used to facilitate hybrid seed production. Hybrids benefit from the "heterosis", or hybrid vigor, phenomenon: hybrid crops can produce up to 50 % higher yields than inbred varieties [10]. Moreover, the breeding of different varieties or species is an important genetic resource for crop improvement. Many crops such as maize, rice, sorghum, and rapeseed are cultivated as hybrids. To produce hybrid seeds, it is necessary to emasculate one line to prevent self pollination. The use of CMS lines avoids manual labor, machine and chemical treatments to perform emasculation and is therefore extremely convenient for breeders [11].
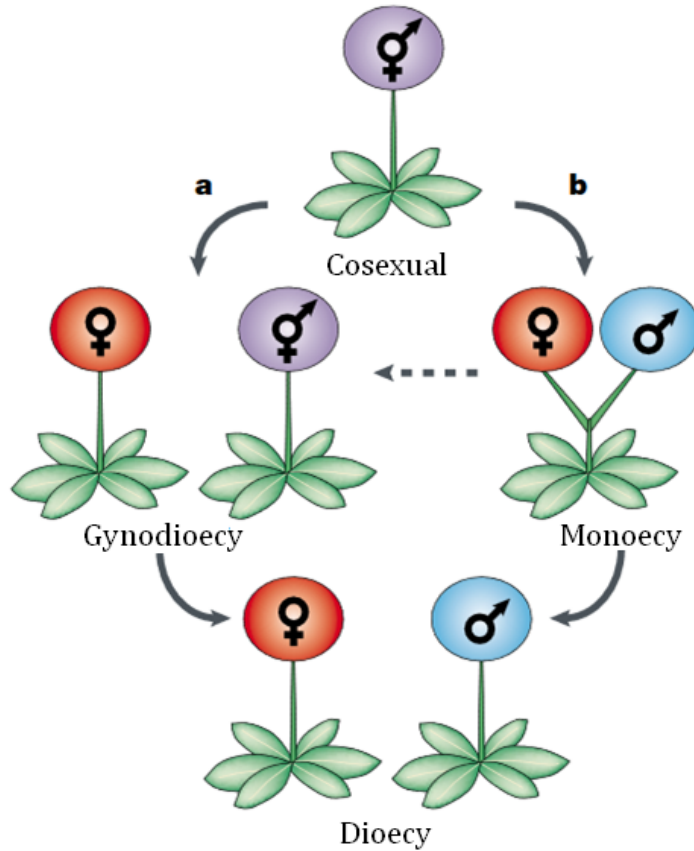
Figure 1.1: Main evolution pathways from hermaphroditism to dioecy. In the gynodioecy pathway (a), an intermediate stage between hermaphroditism (firstly all individuals in one population are hermaphroditic, the plants are named cosexual) and dioecy is composed of gynodioecious populations with hermaphroditic and female individuals. In the monoecy pathway (b), an intermediate stage is composed of plants with unisexual flowers. Another pathway might involve monoecy evolving to gynodioecy (dashed line). Modified from S. Barrett (2002) [5].

CMS is also an interesting model to study cytonuclear incompatibilities because they result from cytoplasmically inherited sterilizing gene, and the nucleus can restore the fertility or maintain the sterility, as detailed in section 1.2.

1.1.3   Male gametophyte development

In this study, I was particularly interested in understanding events leading to cytoplasmic male sterility. In this regard, the description of male gametophyte development is necessary. The male gametophyte, or pollen grain, is produced in the anthers of the sporophyte. The male gametogenesis requires tight cooperation between gametophyte (pollen grain) and sporophyte (tapetal cells) tissues to develop. The tapetal cells provide nutrients to the gametophyte during early stages of development and degenerate at a precise time point, contributing to the formation of the pollen coat. A premature or delayed tapetum degeneration results in male gametophyte abortion [12]. Two successive phases are distinguished for male gametophyte development, that are named microsporogenesis and microgametogenesis. The microsporogenesis consists of the production of the four haploid spores grouped in a tetrad with a callose wall, from meiosis of the mother diploid sporogenous cells. Then, during microgametogenesis the microgametophyte develops until it is released from the anthers at anthesis. First, the callose wall is degraded by the callase (secreted by the tapetum), thus releasing the uninucleate microspores. Individual microspores grow and a large vacuole is formed. The nucleus migrates to the edge of the pollen grain at the vacuolated microspore stage. The first pollen mitosis, which is a highly asymmetric division, occurs to produce the binucleate pollen grain carrying two unequal cells. This pollen grain is composed of a small generative cell (the male germline) engulfed in the cytosol of the large vegetative cell. Then, there are two types of behavior considering the species: in those that shed bicellular pollen, the binucleate pollen grain maturates and dehydrates after the first pollen mitosis and is released from the anther. In species that shed tricellular pollen, such as *A. thaliana*, the generative cell undergoes a second round of pollen mitosis and produces twin sperm cells. The trinucleate pollen grain dehydrates and is subsequently released at anthesis. Successful pollination results from landing on a compatible stigma, hydration and germination. The vegetative cell elongates to produce the pollen tube. In species that shed binucleate pollen, the second pollen mitosis occurs in the pollen tube. In both cases, the pollen tube elongates in the stylar tissues to deliver the twin sperm cells to the embryo sac, to perform double fertilization and form the new diploid zygote and the albumen (triploid tissue of the seed that provides nutrients to the embryo) [13]. The pollen grain development is represented in figure 1.2.

4
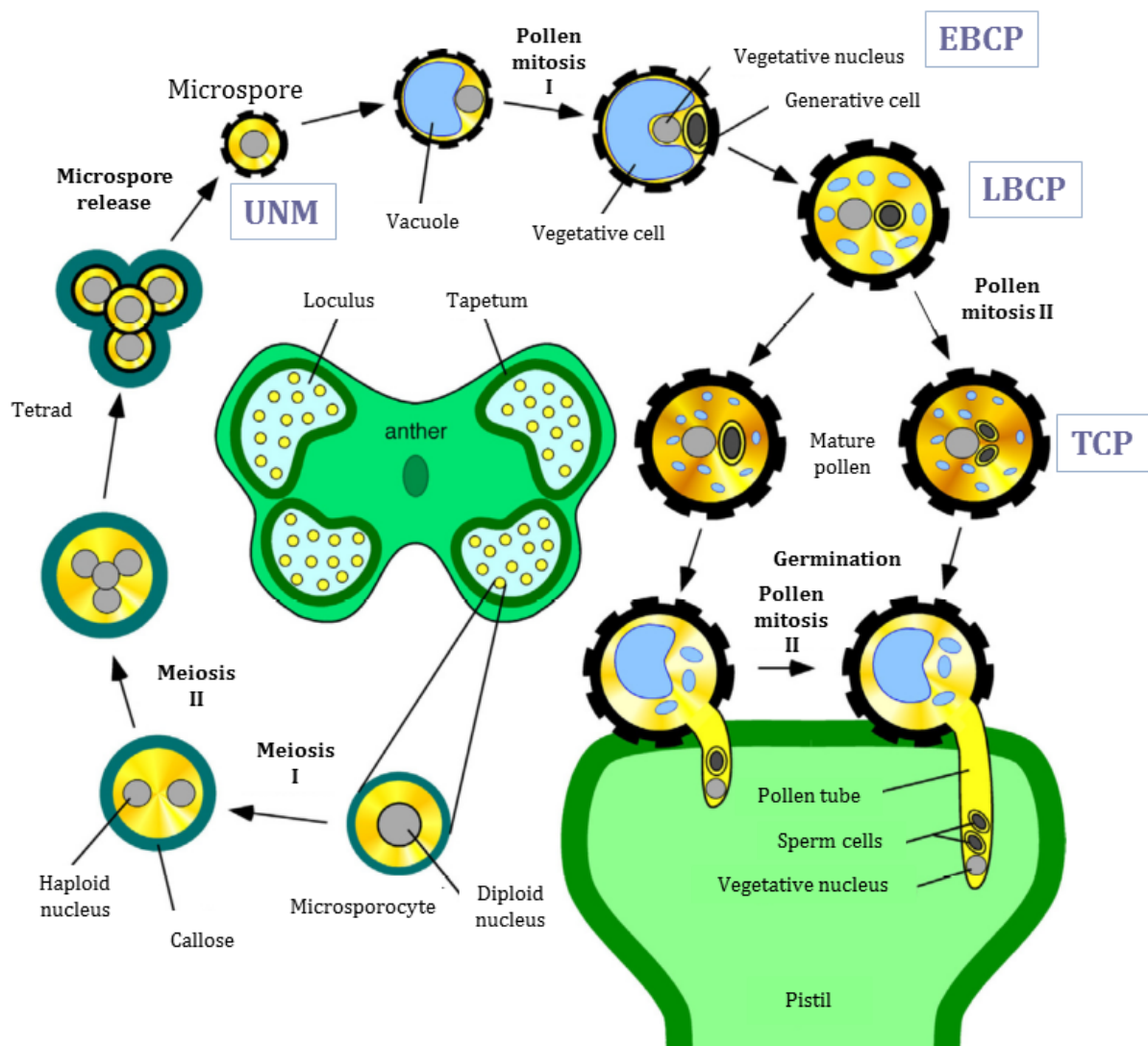
Figure 1.2: Male gametophyte development. Male gametophyte development takes place in the anthers. Firstly, sporophytic cells differentiate into microsporocytes, that undergo meiosis and ultimately form four haploid spores grouped with callose in tetrads. The microspores are then released and form four uninucleate microspores. The tapetal cells start to degenerate. A big vacuole appears in the microspore and the nucleus is found at its edge at the vacuolate stage. A first asymmetric mitosis produces bicellular pollen grain containing a big vegetative cell and a small generative cell. At this stage, the tapetal cells degenerate. Then, according to the species, the generative cell undergoes the second pollen mitosis either before or after germination, to form the spermatic cells. For both types of species, the pollen tube is formed by elongation of the vegetative cell, that delivers the two spermatic nuclei to the embryo sac to perform double fertilization. From D. Honys et al. (2006) [14]. The developmental stages that are investigated in this work are indicated in blue color and framed. UNM: uninucleate microspore; EBCP: early binucleate pollen grain; LBCP: late binucleate pollen grain; TCP: trinucleate pollen grain.

The male gametophyte development requires the tight developmental co-regulation of the sporophytic and the gametophytic cells, and there are many critical steps that could be impaired and result in pollen abortion. Two major phases can be identified during male gametophyte development, according to their transcriptomic profiles. A transcriptomic study in *A. thaliana* Landsberg *erecta* showed that during the early phase, that starts at the uninucleate stage and ends at the binucleate stage, more genes are expressed compared to the late phase composed of the trinucleate and mature stages [15]. In the late phase, less genes are transcribed and the proportion of pollen-specific genes increases. These genes are involved in cell wall metabolism, cytoskeleton functions and cell signaling [15]. Molecular control of male gametophyte development is reviewed in M. Borg et al. (2009) [13].

1.2 Cytoplasmic male sterilities are the result of a cytonuclear incompatibility

As it was mentioned in section 1.1.2, CMS is of special interest in agronomy. The genetics behind this sterility has been widely studied since the discovery of the maize CMS-T, and later on in other crop species. Even though the sterilizing determinant is challenging to identify, some studies succeeded. In 1927, R. Chittenden and C. Pellew showed that CMS is the result of combination of nuclear genes together with cytoplasmic factors [6]. In fact, the sterilizing factor is mostly comprised in the cytoplasmic fraction, whereas the nucleus can counter-act its effect. This section aims at explaining in detail these interactions: where they come from, and their consequences.

1.2.1 The plant cell is composed of three genomes that must cooperate and have co-evolved

At least three genomes are present in the plant cell, that have different inheritance patterns. Other genomes can be present, such as those of endosymbionts, parasites or viruses, but they are not taken into consideration here. The plant genomes have different inheritance patterns: most species inherit mitochondria and plastids maternally [16]. There are few exceptions: some species, for example those of the *Oenothera* genera, perform maternal and bi-parental plastid inheritance [17]. In *Medicago sativa* plastids are inherited paternally [18], whereas in cucumber mitochondria are inherited paternally [19]. Nevertheless such bi-parental or paternal inheritance is scarce. The differential inheritance of the three genomes of plant cells is represented in figure 1.3.
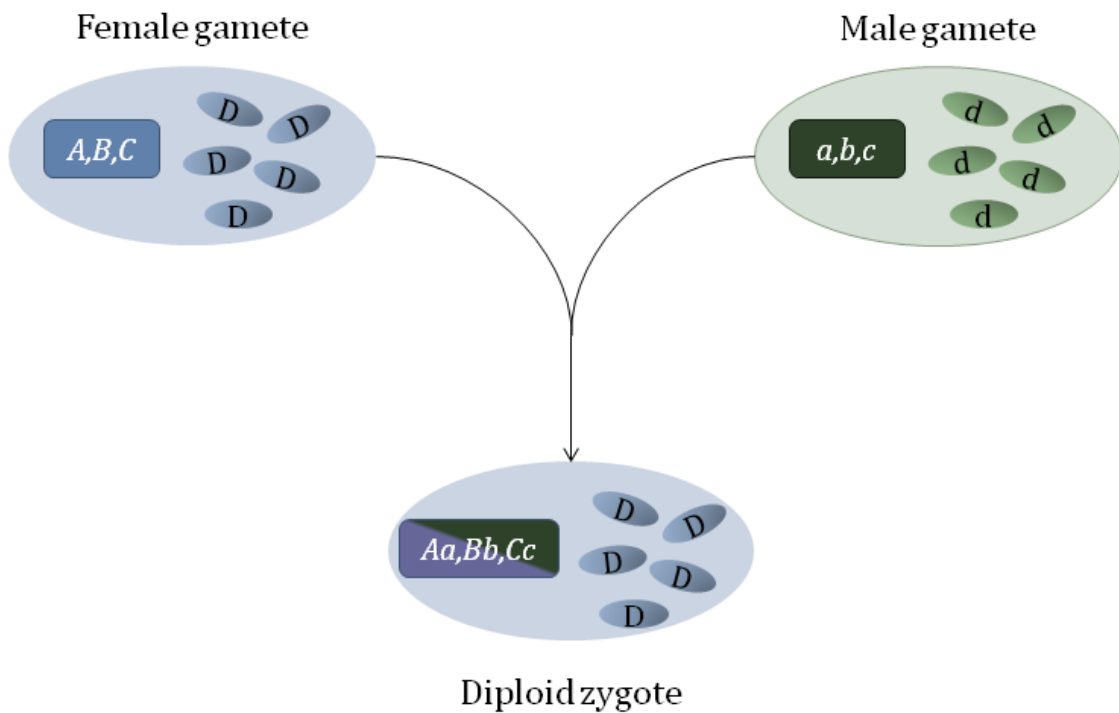
Figure 1.3: Differential inheritance of the nucleus and cytoplasmic compartments in sexual reproduction. The female gamete carries the nuclear genome A,B,C and the cytoplasmic genome D; the male gamete carries the nuclear genome a,b,c and the cytoplasmic genome d. The fertilization results in the formation of a new diploid zygote carrying half of the nuclear genome from the mother and half from the father Aa,Bb,Cc, and the cytoplasmic genome from the mother D.

It is generally accepted that plastids and mitochondria evolved from free-living prokaryotic organisms that were integrated into host cells (likely an archea) through endosymbiosis [20, 21]. Mitochondria derive from a proteobacteria which association with its host contributed to eukaryogenesis [22]. Chloroplasts descend from cyanobacteria that were engulfed by a non-photosynthetic eukaryote [23]. During the evolutionary process that transformed the original endosymbionts into organelles, profound genetic and functional integration took place that profoundly modified the genomes and metabolisms of the partners.

In particular, a massive transfer of genes occurred between compartments, essentially from organelles to nucleus [24]. Nevertheless, both mitochondria and plastids have conserved a core set of genes mostly encoding factors involved in gene expression or energy metabolism [25], hence the costly necessity for the cell to maintain and express organelle genomes. The maintenance in mitochondria and chloroplasts of similar sets of genes amongst highly diverged phyla led to the "CoRR" hypothesis proposing that the colocation of gene and product allows an efficient redox regulation of gene expression [26].

However, the sets of genes contained in organelle genomes are far from being sufficient to allow proper function of the organelles. For example, chloroplast and mitochondrion proteome sizes in *A. thaliana* are estimated at 2000 and 2700 proteins respectively [27], whereas plastome (genome in chloroplast) and chondriome (genome in mitochondrion) carry only 100 possible genes [28] and 57 identified genes [29] respectively.

As a consequence, major cellular processes that take place in organelles, including organelle biogenesis and division, photosynthetic apparatus and respiratory complexes, and organelle gene expression [30, 31, 32, 33], rely on nuclear-encoded proteins that have to be accurately addressed to, and imported into the organelles after their synthesis in the cytosol. Not only the right organelle itself must be targeted, but also the right position relative to the two organellar membranes. The majority of nuclear-encoded proteins addressed to the inner compartments of chloroplasts and mitochondria are imported through TOC/TIC and TOM/TIM complexes, respectively. These important multimeric complexes recognize and translocate through the outer (TOC and TOM) and inner (TIC and TIM) membranes of the organelles the precursors of the imported proteins [34]. The recognition of precursors by the TOC and TOM complexes is generally ensured by an N-terminal targeting peptide that is eventually cleaved by dedicated peptidases after import [35]. In plants, the mitochondrial processing peptidase is part of the bc1 complex [36]. Structural, but nor primary sequence, features of precursor signal peptides are thought to be crucial both for the recognition and discrimination by the chloroplast and mitochondrial import complexes. Indeed, these signal peptides are sufficient to address

new engineered proteins to organelles [37] and have been instrumental to the functional study of these organelles [38, 39, 40] .

The massive protein import from the cytosol to the organelles is considered as the anterograde part of the signalling pathways between the nucleus and organelles. In return, chloroplasts and mitochondria send signals to the nucleus, called retrograde signals [41, 42]. The anterograde-retrograde signalling pathways are crucial for the normal development and for the response of plants to their environment [43].

On the evolutionary scale, the involvement of nuclear and organellar encoded factors in many multiprotein complexes mandatory for photosynthesis and respiration and primary metabolic assimilation drives the coadaptation between the cell genomes, which ensures a tight cooperation between the co-evolved compartments to fine-tune cell functions [44]. By performing inter- or intra-specific crosses, followed by recurrent backcrosses, cytoplasmic and nuclear genomes that diverged can be gathered because of the differential inheritance of the genetic compartments (the cytoplasm from the mother is placed in an unprecedented nuclear background from the recurrent father). Cytonuclear incompatibilities are often highlighted in these new genetic combinations but may also appear in the early hybrid generations [44, 45, 46]. The mechanism by which incompatibilities arise can be explained under the Dobzhansky-Muller model, as shown in figure 1.4 [44]. Cytonuclear incompatibilities can lead to a decrease fitness of the hybrid, hybrid mortality or hybrid sterility, thus creating reproductive barriers between species or populations. Among cytonuclear incompatibilities, CMS, which is a defect in pollen production whereas the overall fitness of the plant is normal, often occurs.

Ancestral genotype and plasmotype

Nuclear-cytoplasmic co-evolution in isolated populations

Fixation of mutations in the nuclear and organellar genomes

Nuclear-cytoplasmic incompatibility upon hybridization
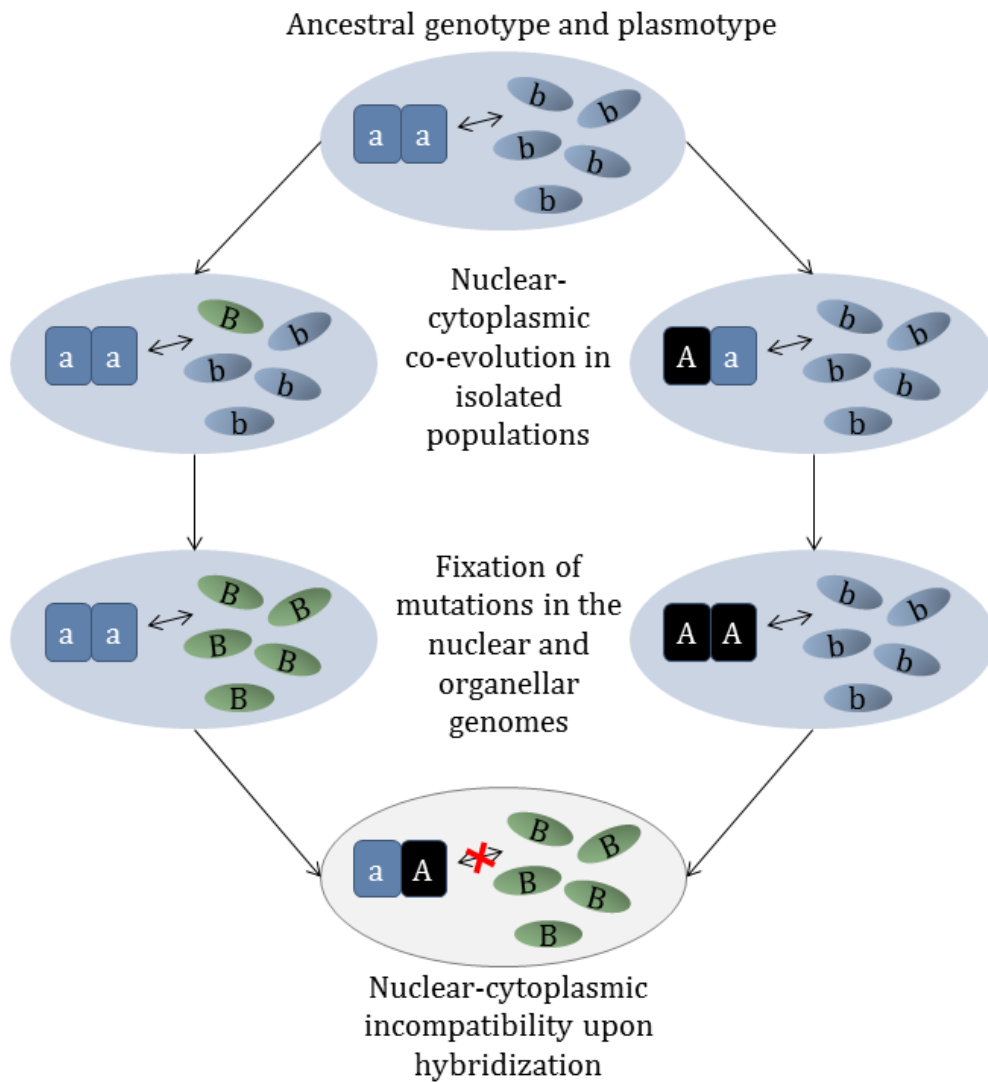
Figure 1.4: The Dobzhansky-Muller model of hybrid incompatibility for nuclear-cytoplasmic interactions. In an ancestral population, the nuclear (aa) and cytoplasmic (b) genomes are co-adapted and interact functionally (double arrow). A population split results in reproductive isolation, and independent mutations can arise in the nuclear (AA) and the cytoplasmic genome (B). After fixation of the mutations in the different genomes, hybridization of two individuals from both subpopulations that differently evolved produce individual carrying an unprecedented combination of nucleus and cytoplasm. This hybridization can lead to incompatibility between the A allele and the B cytoplasm, either in the F1 progeny in the case in which the newly evolved allele is dominant, or in the F2 progenies carrying a AA nucleus in the case in which the newly evolved allele is recessive. From S. Greiner and R. Bock (2013) [44].

1.2.2 Genomic conflict in cytoplasmic male sterilities

The arising of a sterilizing gene in cytoplasmic genomes has to be explained in the light of the genomic conflict theory from L. Cosmides and J. Tooby (1981) [47]. In most cases, the cytoplasmic genomes, *i.e.* the plastome and the chondriome are inherited maternally whereas the nuclear chromosomes are inherited following Mendelian's segregation (see figure 1.3). Therefore, the plant genome can be divided into fractions, the fitness of all genes in a fraction being maximized in the same way. Each fraction is selected in a way that the genes comprised in it maximally propagate, possibly in a deleterious way for the other fractions' genes [47]. Cytoplasmic genes are not disadvantaged by the male sterility (as long as the plant can be pollinated by a male-fertile plant), whereas nuclear genes are [48]. In response to the presence of the sterilizing cytoplasm, the nuclear genome can evolve to counter-act the effect of the sterilizing gene [49]. The nuclear genes counteracting the sterilizing gene effect are called restorers of fertility, and they are historically labeled *Fr* or *Rf* depending on the species. In CMS systems, the nucleus can be of two types: restorer (of fertility) if it carries restorer genes counter-acting the sterilizing factor, or maintainer (of sterility) if it allows the sterilizing factor effect.

Females can spread and persist in natural populations for two reasons. Firstly, it is widely accepted that female plants in gynodioecious populations have better female fertility (for example more seeds, or higher germinating seeds) than their hermaphroditic counterparts [50, 51]. This "female advantage" might be explained by the arrest of male gametophyte development at early developmental stage that thus saves resources that are re-allocated for female gametophyte production [52]. In some species however, the CMS individuals do not produce more or better seeds. In these species, the persistence of females can be explained in the light of the "restoration cost" phenomenon: in the absence of the sterilizing gene, the restorer (of fertility) alleles are counter-selected in a population [53]. This cost is different in the CMS systems considered, regarding the specificity of the restorer allele. For example, some restorers have deleterious pleiotropic effects, and are therefore counter-selected when they are not in presence of the sterilizing cytoplasm [54]. In other CMS systems, the restorer evolved from nuclear genes that regulate cytoplasmic gene expression, called "housekeeping" genes. Hemizygous plants for these restorers carrying the sterilizing cytoplasm are restored, and the non-mutated restorer allele can perform its housekeeping role simultaneously. Now, fixation of such restorer has a cost, as the housekeeping duty of the non mutated restorer allele is not achieved [54].

To sum up, cytoplasmic male sterility results from an incompatibility between two cell fractions that have different interests, the cytoplasmic and the nuclear compartments.

The cytoplasm can be either sterilizing or non sterilizing, whereas the nucleus can carry maintainer (of sterility) or restorer (of fertility) alleles, allowing or counter-acting the effects of the sterilizing gene, respectively. The different possible combinations of cytoplasms and nuclei in one CMS system are presented in figure 1.5. It is noteworthy that individuals carrying the sterilizing cytoplasm can be hermaphroditic if they have restorer alleles, so that the effect of the sterilizing protein is hidden in these individuals. Actually, the high frequency at which CMS appears when breeding different species or genera [55] indicates that sterilizing cytoplasms might be common, but their effect is hidden because of the fixation of restorer alleles. Indeed, if the female advantage is too low, or if the restoration is not costly, the restorer allele is eventually fixed [56]. The intra- or inter-specific hybridization in this case leads to co-adaptation disruption (see section 1.2.1), the restorer alleles are not present anymore to counter-act the sterilizing factor effect and male-sterile plants arise. These cytoplasmic male sterilities are called cryptic [56]. Therefore, a "naive" nucleus in contact with a sterilizing cytoplasm results in female plants and gynodioecious populations.

Alloplasmy, which is the phenomenon wherein cells have the cytoplasm from one species and the nucleus from another species, often results in CMS [53]. While energy metabolism deficiency during pollen formation is often suggested to explain alloplasmic CMS, some studies pointed towards cryptic cytoplasmic genes silenced by fixed restorers in the cytoplasmic donor, but active in the alloplasmic line whose "naive" nuclear genome lacks restorers [53, 57]. In crop species, CMS are often discovered by breeding different hermaphroditic species and can thus be considered as cryptic. For example, creation of CMS in wheat can be performed by crossing wild wheat *Triticum timopheevii* or related species such as *Aegilops* with common wheat followed by successive backcrosses [58]. Sunflower CMS has been obtained by breeding wild relative male fertile species: *Helianthus petiolaris* and *Helianthus annuus*. Moreover in wild populations, a cryptic CMS has been highlighted in *Mimulus guttatus* when it was crossed with *M. nasutus* [59]. All described populations of *M. guttatus* are hermaphroditic, so the CMS is called cryptic. Another cryptic CMS has been discovered in *A. lyrata* [60]. All these findings indicate that cryptic CMS are more common than previously thought, and so sterilizing factors which are silenced by the restorer nucleus.

In the previous section, I attempted to explain generally how a cytonuclear interaction could be involved in CMS. Hereafter, I bring more detailed elements on the nuclear and cytoplasmic partners involved in CMS, based on well-studied CMS systems.

Figure 1.5: Combination of cytoplasms and nuclei in CMS systems. CMS systems are characterized by two types of cytoplasms and two types of nuclei. The nucleus is called maintainer of sterility or restorer of fertility, whereas the cytoplasm is non sterilizing or sterilizing. Individuals carrying the sterilizing cytoplasm and maintainer nucleus are male sterile, whereas all the other combinations result in hermaphroditic individuals.

1.3 Cytoplasmic male sterility associated genes and nuclear restorers

1.3.1 Cytoplasmic genes associated to male sterility

1.3.1.1 Characteristics of cytoplasmic male sterility associated genes

Well before the discovery of mitochondrial and plastidic genomes in 1964 [25], M. Rhoades (1950) proposed that mitochondria were responsible for the sterility in CMS [61]. The identification of a mitochondrial trait governing male sterility in angiosperms was one of the arguments advanced to set up the uniparental inheritance model of mitochondria [62]. It was then verified that all non engineered CMS-associated genes identified are mitochondrial [52]. Why CMS genes are related to mitochondria and not chloroplasts, and why CMS are so frequent in plants are intriguing questions. CMS gene appearance might come from the large size of plant mitochondrial genomes, as well as the high recombination frequency of the chondriome [63]. In comparison, the plastome is much more condensed and conserved. The origin of CMS-associated sequences is still a mystery. Yet, in a recent study on rice WA-CMS, H. Tang et al. (2016) proposed a model for the WA-CMS associated gene to arise, that could be generalized [64]. Their study indicates that the functional sterilizing gene formation involved multiple and complex evolutionary processes including recombinations among conserved genes, substoichiometric shifting and sequence variation of CMS protogenes until functionalization occurred [64].

Identified CMS-associated genes share general features. First of all, they contain sequences that are specific to each sterilizing cytoplasm [52], with few exceptions. The CMS-related genes in BT- and HL-type CMS of rice, *orf79* and *orfh79*, are 98 % identical [65]. Also, the sorghum A3 CMS-related gene putatively encodes a protein for which the 49 C-terminal predicted amino acids are 57 % identical to those of *orf79* [66]. Finally, *orf224* and *orf222*, that are respectively associated with the *pol* and *nap* CMS in *B. napus*, encode predicted proteins sharing 79 % identity [67].

Another characteristic of CMS-associated genes is their close proximity and possible co-transcription with essential mitochondrial genes. The close proximity with essential mitochondrial genes might facilitate expression of the CMS-related genes by using expression signals from the essential mitochondrial genes [68]. Interestingly, many of the CMS-associated genes have been found to be co-transcribed with complex V respiratory chain subunits. For example, the first CMS gene identified, the *urf13* related to maize CMS-T, is co-transcribed with *atp4* [52]. The *orf108* that is associated with *mori* CMS

in *Brassica juncea* is co-transcribed with *atp1* [69]. The Ogura CMS gene *orf138* is co-transcribed with a gene firstly designated as *orf158* [70], and which was later on identified as *atp8* [71]. HL-CMS rice *orfh79* is co-transcribed with *atp6* [72], the common bean *orf239* is co-transcribed with *atp1* [73]. In other cases, other essential mitochondrial genes are involved in co-transcription with CMS genes as for example in *Petunia* the *nad3* subunit of complex I is co-transcribed with the sterilizing gene *pcf* [74]. Yet, CMS-associated genes are not always co-transcribed with any essential mitochondrial gene, as it is the case for the sorghum A3-CMS related gene *orf107* [66].

If the co-transcription of CMS genes with essential mitochondrial gene is not universal, it is not rare to find the presence of parts of such essential mitochondrial genes in the coding sequence of CMS genes [52]. For example the sorghum A3-CMS related gene *orf107* harbors a part of *atp9* gene in its coding region [66]. The *Petunia pcf* also presents parts of *atp9* and *cox2* in its coding region [75]. Also, CMS-related factors often present large hydrophobic domains or predicted transmembrane domains in their predicted amino-acid sequences [52, 76] . Some identified CMS genes and their specific features are presented in figure 1.6.

Finally, the expression profiles of CMS-genes usually present specific patterns. Firstly, transcription profile is often altered by the presence of restorer genes. Also, an intriguing feature of CMS-related genes is their constitutive expression, whereas the induced phenotype is restricted to male gametophyte production [77]. This leads to the "male specificity" paradox: why the CMS-related gene, that is constitutively expressed, has an effect on reproductive organs without being deleterious to the other tissues?

1.3.1.2 Identification and validation of cytoplasmic male sterility associated genes

In the previous section, I detailed the common features of CMS-related genes. Formally identifying them is often tricky. Approaches that have been employed are reviewed in M. Hanson and S. Bentolila (2004) [52]. Two approaches allow unequivocal identification of a mitochondrial sterilizing gene. The first strategy consists in using comparative genomics: by comparing sterilizing mitochondria with closely related fertile revertants, one can identify a DNA region that would be specific for the sterilizing genome. Unfortunately, this method is often limiting as it is difficult to find mitochondrial genomes that recently diverged and just differ at the CMS locus. Maize CMS-T *urf13* [79, 80] and CMS-S *orf355/orf77* [81] as well as common bean *pvs* [73] sterilizing genes have been identified in this way. Another strategy is to search for the segregation of a DNA sequence inducing the male sterility phenotype.
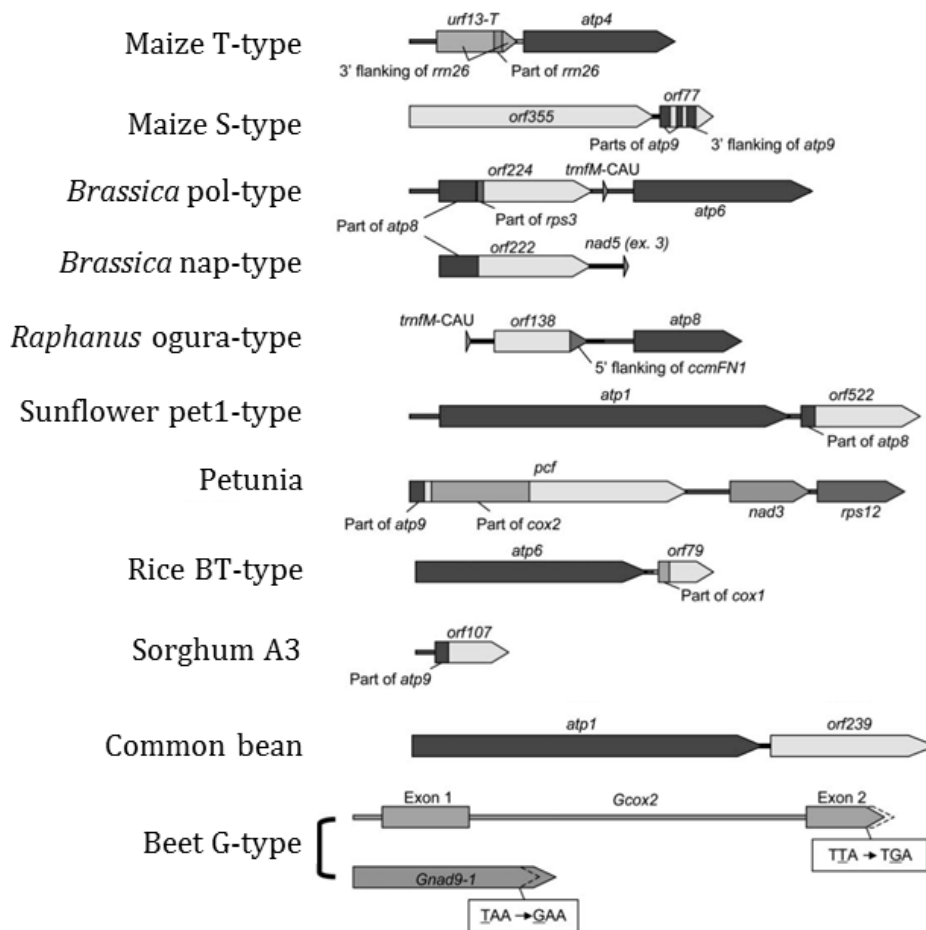
Figure 1.6: Main features of some identified CMS-associated genes, detailed in the text. Modified from T. Kubo et al. (2011) [78].

As the cytoplasmic compartment is maternally inherited in most species, this approach is made possible by the technique of protoplast fusion.

This technique breaks the monoparental inheritance and allows recombinations. For example, recombined mitochondrial genomes of rapeseed cybrids were used in addition to comparison of fertile revertants to identify *orf138* as the sterilizing gene in Ogura CMS [70, 82, 83].

In most cases, genetic proofs such as recombinant or revertant fertile plants are not available. In this instance, several lines of evidence from different approaches are necessary to validate the sterilizing gene. Comparing mitochondrial genomes and transcript profiles, and researching for unusual recombinants at the same time provide good hints on a candidate. The comparison of mitochondrial genomes is fastidious, as plant chondriomes are very large [84] and new orfs that could potentially induce CMS are common [85, 86]. As it was detailed in the previous section, CMS-related genes are often co-transcribed with essential mitochondrial genes. Therefore, looking at transcription profiles of these essential genes can highlight CMS-related candidate genes. Yet, these approaches are often not sufficient, and they need to be supported by other lines of evidence. I already mentioned that CMS was determined by cytonuclear epistasis. The nucleus can carry restorer alleles, whose identity and mode of action will be presented in detail in section 1.3.2.2. Yet, it is interesting to mention that they often silence the sterilizing factor by acting on its expression. Therefore, investigating the candidate expression in sterile and restored lines could give clues to formally identify the CMS factor. Indeed, most of the fertility restorer genes alter the sterilizing gene expression [87]. However, a restorer can modify the expression profile of genes other than the sterilizing one [88], so this method cannot prove alone the identity of the sterilizing gene neither.

Examples of multiple clues that had to be advanced to formally identify CMS-related genes are detailed hereafter. The factor responsible for CMS-WA was identified *via* the study of mitochondrial transcription profiles by RNA blotting: the mRNA profile detected with an *rpl5* probe was different between the CMS-WA line and a fertile line. It was then shown that this mRNA was affected in a restored nuclear background, and its sequence revealed an ORF of unknown origin, named *wa352*. This ORF led to male sterility when it was transgenically expressed in the nucleus and its product addressed to mitochondria. Altogether these results were considered sufficient to validate the role of this ORF in WA-CMS [89]. Another example is the identification of the *orf108* sterilizing gene associated with *mori* CMS in *Brassica juncea*. Longer *atp1* transcripts in the CMS line were detected. The *atp1* region was sequenced and the 5' and 3' mRNA ends were identified in fertile, CMS and restored lines. A new orf was detected, which was expressed in the CMS and restored lines but had a modified expression in the restored background

17

[69]. Transgenic *A. thaliana* plants expressing *orf108* were sterile, supporting the *orf108* role in sterility [90]. Moreover, mutations in *orf108* blocked the *M. arvensis* restoration of fertility, suggesting that the restorer could not interact with its cytoplasmic partner anymore and thus further supporting *orf108*'s role in *mori* CMS [91]. Finally, one more example is the BT-type CMS, for which an additional copy of the *atp6* region containing a predicted ORF named *orf79* was identified. It was proven that this ORF was transcribed and translated in the CMS line, and that the two restorers of fertility act on its expression either at the transcriptional or the translational level. Also, transgenic plants expressing the *orf79* phenocopied the CMS. These pieces of evidence validated the role of *orf79* in BT-type CMS [92].

1.3.2   The restoration of fertility

In the previous section, the cytoplasmic factors involved in cytonuclear incompatibilities leading to CMS were outlined. This section aims in presenting the nuclear factors of CMS systems. As it was already mentioned, the sterilizing factor is cytoplasmic, and more precisely mitochondrial in most cases. However, the nucleus can carry restorer (of fertility) or maintainer (of sterility) alleles. According to the type of CMS, the restoration of fertility (also simply called "restoration") has to occur either in the sporophyte or in the gametophyte generation.

1.3.2.1   Gametophytic and sporophytic cytoplasmic male sterilities and their restoration

As I mentioned in section 1.1.3, male gametophyte development is tightly regulated, and it requires the cooperation of gametophytic and sporophytic tissues. In gametophytic CMS the defects occur in the male gametophytes. In sporophytic CMS, the tapetal cells are the primary targets of the sterility factor. The genetic behavior of restoration can allow to distinguish between these two cases, since a plant that is heterozygous for the restorer allele *Rf*, called *Rf/rf*, does not segregate *Rf* and *rf* similarly in gametophytic and sporophytic CMS. In sporophytic CMS, the presence of one *Rf* allele is sufficient to rescue the male fertility of all pollen grains whatever their allele at the restorer locus. The *Rf/rf* plant thus presents 100 % of viable pollen. The *Rf* and *rf* alleles segregate according to Mendel's laws of genetic inheritance, and so one fourth of this *Rf/rf* plant's offspring will be male sterile. Now, in gametophytic CMS the presence of one *Rf* allele rescues the fertility only in the gametophytes carrying it. Therefore, heterozygous *Rf/rf* plants present half dead pollen. The *rf* allele is never transmitted *via* the pollen, but it is transmitted *via* the egg cell according to Mendel's laws, and so a segregation bias is

expected with half of the progenies that are homozygous for the restorer allele Rf/Rf, and the other half that are heterozygous Rf/rf. No male sterile progeny is observed. The inheritance patterns of alleles at the restorer locus in the two different CMS systems is represented in figure 1.7. As the two different types of CMS are widespread, and as the two tissues on which a defect occurs are very different, it is not known whether the same functional mechanisms lead to pollen abortion in gametophytic and sporophytic CMS.

1.3.2.2 Mechanisms of fertility restoration

In most studied CMS systems, the restoration of fertility is mediated by disturbing the expression of the sterilizing gene [76]. The first findings were made on CMS gene expression, that was found to be modified in restored lines compared to steriles [66, 93, 94, 95, 96, 97]. The first cloned restorer of fertility that acts on disturbing CMS-gene expression was the restorer Rf in *Petunia* CMS [98]. In lines containing the Rf allele, the sterilizing *pcf* mRNA profile is altered, and subsequently the accumulation level of the PCF protein is reduced. In this study, authors identified the Rf allele to be composed of tandem copies of a gene containing repeats of the pentatricopeptide repeat (PPR) motif, that was described in *A. thaliana* shortly before and hypothesized to have a function in mRNA processing [99]. The corresponding PPR protein, *PPR592*, is very similar in maintainer and restorer lines but a polymorphism in the promoter avoids its expression in floral buds in the maintainer background, so that the *pcf* and PCF accumulations are possible and the male gametophyte development stops. Since the cloning of *Petunia*'s Rf, many restorer genes that have been identified code for PPR proteins [87]. For example, the restorer of fertility RFo in Ogura CMS is a PPR protein inhibiting *orf138* mRNA translation [100]. In the rice BT-type CMS, the two identified restorers *Rf1a* and *Rf1b* encode PPR proteins that restore male fertility via endonucleotic cleavage or degradation of the sterilizing mRNA [92]. Finally, some restorers of fertility do not code for PPR proteins but they interact with them and allow the alteration of CMS factor expression. For example, the *Rf2* restorer in rice LD-type CMS encodes a glycine-rich protein that might form a complex possibly targeting the CMS protein [101].
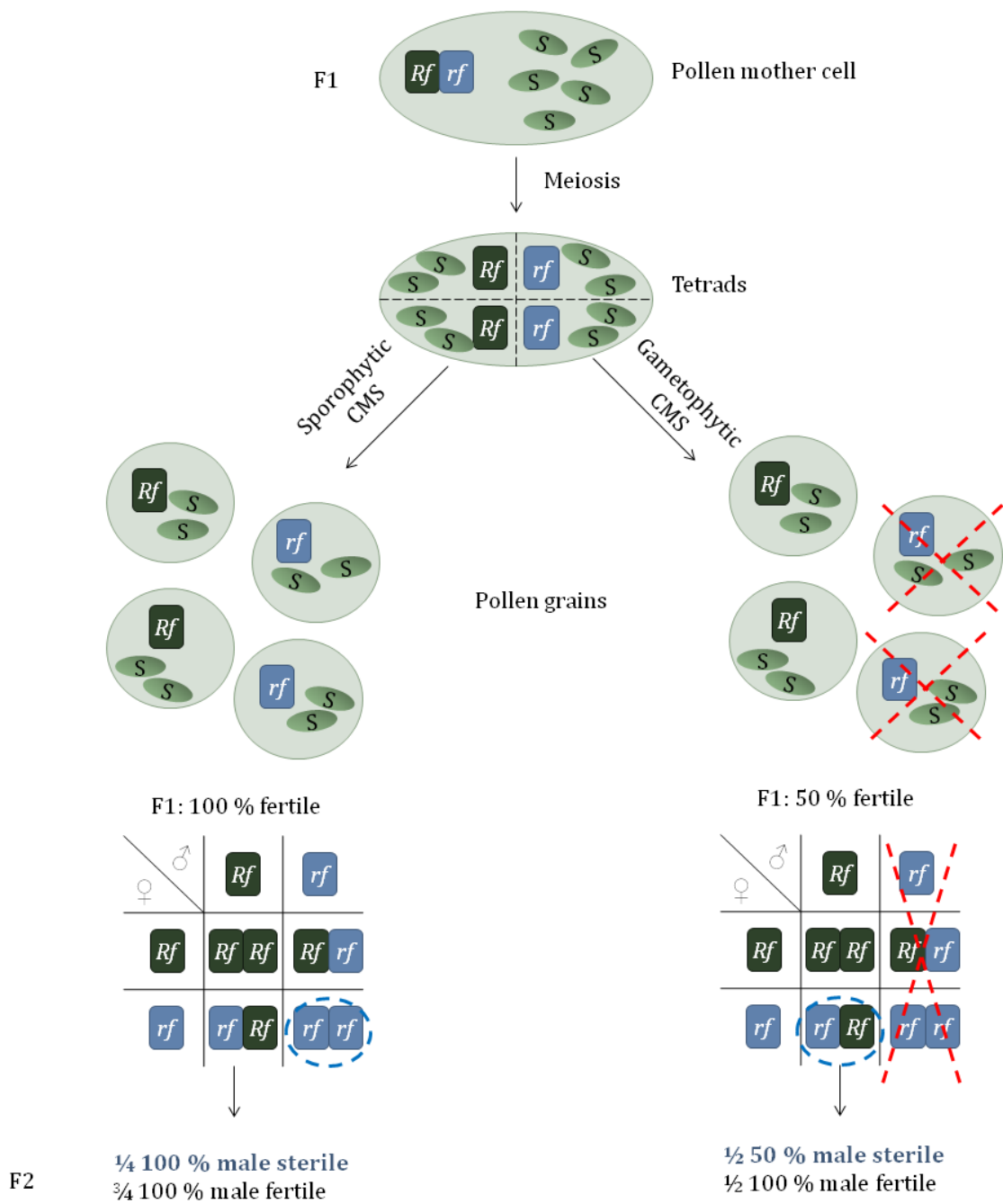
Figure 1.7: The different inheritance patterns of sporophytic and gametophytic CMS. The pollen of F1 is derived from a pollen mother cell, PMC, which forms tetrad through meiosis. In sporophytic CMS, all pollen grains are fertiles in the heterozygous Rf/rf F1 and in gametophytic CMS the 50 % of pollen grains that carry the rf alleles abort and do not contribute to the next offspring. Consequently, in sporophytic CMS one fourth of the progenies harvest the rf/rf genotype and are 100 % male sterile, whereas in gametophytic CMS the rf allele can be passed on by the female but not male gametophyte, and so half of the progenies carry both Rf and rf alleles and present half of dead pollen.

20

All the restorers that are described above act post-transcriptionally to silence the sterilizing gene and inhibit its action. Other identified restorers of fertility involve other mechanisms than post-transcriptional restoration events, and they do not always code for PPR proteins. The common bean restorer *Fr* reduces the sterilizing *pvs* mtDNA region to substoichiometric level, thus reducing the amount of sterilizing DNA [102]. In rice CW-type CMS, the RMS restorer in the *Rf17* locus is a "loss of function" restorer allele. Indeed, a SNP in the restorer allele promoter leads to a lower expression of *RMS*, which results in male fertility restoration. *RMS* is hypothesized to be involved in a retrograde signaling pathway, as its mRNA accumulation depends on the cytoplasmic genome. It encodes an acyl carrier protein [103]. Another known "loss of function" restorer allele is the maize S-CMS *rfl1*, for which accumulation of mitochondrial ATP synthase subunit α protein is reduced in haploid microspores, maybe avoiding a necessary interaction with the sterilizing factor to cause sterility [104]. Another hypothesis would be that this restorer has an effect on the expression of both on *atp1* and the sterilizing factor. Finally, the *Rf2* restorer allele in maize CMS-T, that was the first restorer to be cloned, does not act on the post-transcriptionnal level neither [105]. Actually, it does not silence the sterilizing gene at all, but it rather "detoxify" its effect, by encoding an aldehyde dehydrogenase that is suspected to remove oxidative stress caused by URF13 [106].

To sum up, plant mitochondria genomic shuffling often results in new ORFs production that can be deleterious to the male gametophyte. The nucleus evolutionary response is the formation of restorer of fertility alleles that can rescue male fertility [76]. The restoration of fertility can have a cost, as restorer alleles are sometimes recruited in "housekeeping" nuclear genes that regulate mitochondrial gene expression, or because they have pleiotropic effects affecting expression of essential mitochondrial genes [49]. Some CMS systems and their identified nuclear and mitochondrial factors are summarized in table 1.1. As CMS genetics have been studied for decades by breeders, the genetic processes behind these phenomena start to be better understood, and general patterns can be drawn. Yet, the physiological mechanisms leading to the male gametophyte abortion without affecting plant general fitness remain mysterious.

Table 1.1: Cytoplasmic and nuclear genes involved in different CMS

CMS type	Species	Restoration type	Sterilizing gene	Identified restorer	Mechanism of restoration	Ref
CMS-S	Maize	Gametophytic	orf355	Rf3	mRNA degradation	[81]
CMS-T	Maize	Sporophytic	urf13	Rf1 / Rf2	mRNA control / detoxification	[79, 80, 107, 108, 109, 105]
CMS-C	Maize	Sporophytic	atp6-C	Rf4	?	[110]
HL-CMS	Rice	Gametophytic	orfH79	Rf5	mRNA maturation	[72, 111]
BT-CMS	Rice	Gametophytic	orf79	Rf1a / Rf1b	mRNA maturation / mRNA degradation	[112, 113, 114, 115, 116]
LD-CMS	Rice	Gametophytic	orf79	Rf2		[117, 101, 118]
CW-CMS	Rice	Gametophytic	orf307?	Rf17	mitochondria-to-nucleus signaling?	[119, 120]
WA-CMS	Rice	Sporophytic	WA352	Rf3 / Rf4	translation inhibition / Reduction of transcripts	[121, 89]
CMS-Pol	Brassica	Sporophytic	orf224	Rfp	transcript level control	[93, 122]
CMS-Nap	Brassica	Sporophytic	orf222	Rfn	transcript level control	[67]
CMS-Ogura	Brassica	Sporophytic	orf138	Rfo	protein level control	[82, 70, 83, 100]
mori-CMS	Brassica	Gametophytic	orf108	?	post-transcriptionnal inhibition	[69, 90, 91]
G-CMS	Wild beet	?	cox2?	RfG1, RfG2	?	[123]
CMS-sprite	Common bean	Gametophytic	orf98-orf239	Fr	mtDNA alteration	[73, 95, 102]
CMS-PET1	Sunflower	Sporophytic	orf522	Rf1	mRNA degradation	[124, 125, 96, 126]
	Pepper	?	orf456	?	?	[127]
	Pepper	?	orf507	CaPPR6?	?	[128, 129, 130]
	Petunia	?	urfS	Rf-PPR592	mRNA maturation? translation inhibition?	[131, 75, 98, 132]
CMS-A3	Sorghum	Gametophytic	orf107	PPR13?	mRNA processing	[66, 133]
CMS-IM62	Mimulus	?	orf141?	Rf1, Rf2	translation inhibition	[134, 135]

1.4 The plant mitochondria functions and their role in cytoplasmic male sterilities

In the previous section, I detailed the genetics behind CMS with the identified cytoplasmic and nuclear factors involved in different systems. The physiological mechanisms by which pollen abortion occurs remain mysterious until now. As all naturally-occurring CMS genes described so far are localized in the mitochondrion, it is assumed that mitochondria might fulfill a specific role in the male gametophyte production. Firstly, I summarize some of the plant mitochondria functions, with focuses on those that could participate in the phenomenons leading to pollen death. In addition to their functions in energy production, redox signalling and homeostasis, which are described below, mitochondria also play roles in organic acid and amino acid metabolism, as well as biosynthesis of essential compounds, reviewed in [136]. I also present features displayed by mitochondria during the cell cycle, as they have recently been suggested to take part in the control of meiosis and mitoses during plant reproduction. In the last part of this section, the main hypotheses proposed to explain CMS are reviewed.

1.4.1 Energy production through oxidative phosphorylation

The eukaryotic cell is highly compartmentalized, and each compartment fulfills a specific function. Mitochondria are often defined as the "powerhouse" of the cell as they are the main producers of Adenosine Tri Phosphate (ATP), which is the energy currency for the cell, together with chloroplasts. Yet, it is noteworthy to mention that ATP is also produced in the cytosol *via* glycolysis, the metabolic pathway by which glucose is converted into pyruvate while producing two molecules of ATP. Nevertheless, in non-photosynthetic cells, the ATP production necessary for all cell functions relies mainly on mitochondria. Mitochondria have a complex internal structure. They are compartmentalized by two membranes, the outer and inner membranes. The space between the two membranes is called the inter-membrane space. Inside the inner membrane is found the matrix, that contains the mitochondrial DNA and has a high protein content. The two membranes have very different properties. The outer membrane controls the exchanges of molecules between the mitochondria and the cytosol. It is permeable to ions and small molecules through protein-based pores and carries the TOM complex that translocates mitochondrial proteins synthesized in the cytosol. It also carries the proteins involved in mitochondria dynamics thus controlling their shape and size [137]. The inner membrane is very impermeable and supports the transmembrane potential which drives ATP synthesis by the ATP synthase. It presents many invaginations that form the *cristae*,

that increase the exchange surface. Moreover, it carries the oxidative phosphorylation (OXPHOS) system complexes, and its properties allow the maintainance of a transmembrane potential. Most of the proteins encoded by the mitochondrial genome are part, or involved in the assembly, of OXPHOS system complexes.

In mitochondria, aerobic respiration is the main pathway to produce ATP [138]. The respiration process leads to the reduction of oxygen to water, the release of carbon dioxide and the phosphorylation of ADP to ATP. The main steps of the respiration process are the Krebs cycle, taking place in the mitochondrial matrix, and the oxidative phosphorylation. The Krebs cycle involves acetyl-coA oxidation. Acetyl-coA is notably produced from decarboxylation of the pyruvate produced during glycolysis. Glycolysis ocurs in the cytosol, but also in mitochondria, where it would directly provides pyruvate that will be used as a respiratory substrate [139]. The Krebs cycle reactions produces, *inter alia*, NADH and $FADH_2$ molecules that will be oxidized by the respiratory complexes that compose the electron transport chain. The plant OXPHOS system is composed of five complexes supplemented with proteins allowing bypasses pathways.

The complex I, or NADH-Ubiquinone oxidoreductase is composed of a mixture of nuclear and mitochondrial-encoded proteins so that genomes coordination must be tightly regulated in order to form a complex with the correct stoichiometry [140]. Complex I is the main entrance point of electrons into the respiratory chain: it transfers them to the ubiquinone using NADH as an electron source [141]. Concomitantly, it translocates four protons from the matrix to the inter-membrane space. Complex II, or succinate dehydrogenase, is the second entrance point of electrons, as it transfers electrons from succinate to ubiquinone without simultaneous protons translocation. Complex III, or cytochrome c reductase, transfers electron from the reduced ubiquinone (called ubiquinol) to cytochrome c. Simultaneously, four protons are translocated from the matrix to the inter-membrane space. Complex IV, or cytochrome c oxidase, is the terminal complex of the respiratory chain. It transfers the electrons from the cytochrome c to oxygen, simultaneously reduces the latter to water, and translocates two more protons from matrix to the inter-membrane space. The electron transport *via* respiratory chain results in a proton gradient across the inner membrane, which is the motor for complex V, or ATP synthase, to produce ATP. The OXPHOS system complexes can form supercomplexes [141], that might provide kinetic advantage and thus prevent reactive oxygen species (ROS) production [142].

Besides the five complexes of the OXPHOS system, the plant mitochondria have specific features compared with animal mitochondria. They possess alternative electron transport pathways. These pathways were identified because plant mitochondria can

respire even in the presence of rotenone and cyanide, that are complexes I and IV inhibitors respectively. The cyanide-insensitive respiration is catalyzed by the alternative oxidase (AOX), that oxidizes ubiquinol and reduces oxygen to water without proton translocation. AOX is an antioxidant, it is induced by oxidative stress and participates in the stress response [143]. The alternative NAD(P)H dehydrogenases are located on either side of the inner mitochondrial membrane, and they oxidize NAD(P)H without proton translocation [138]. Together, any NAD(P)H dehydrogenase and the AOX form an alternative electron transport chain [143]. The OXPHOS system and the alternative pathways are presented in figure 1.8.

The alternative electron transport chain function is to limit mitochondrial ROS production by keeping the ETC oxidized. However, a ROS production is inherent to mitochondrial function, and mitochondria are the major source of ROS in the plant cell. More specifically, complexes I, II and III are implicated in superoxide production, because of electron leaking and single electron reduction of oxygen to superoxide [144].
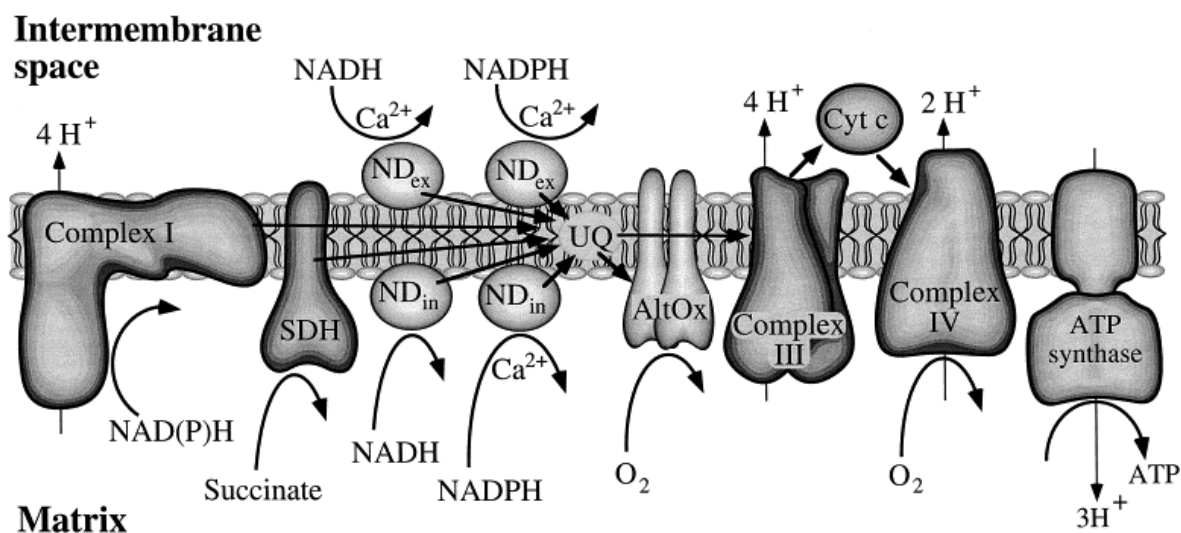
Figure 1.8: OXPHOS system and alternative electron transport chain in plant mitochondria. From A. Rasmusson et al. (1998) [140].

1.4.2 Redox homeostasis in the regulation of cellular processes and response to stress: a central role for mitochondria

1.4.2.1 ROS production in mitochondria and redox biology

At high concentrations, ROS are deleterious to the cell. Their major targets are nucleobases (DNA), disulfure bounds and methionine in proteins, and unsaturated fatty acids. At high concentration they are thought to induce cell death, when the rate of oxidative damage to cellular components exceeds their repair or replacement. Numerous lines of evidence indicate that mitochondria are involved in cell death in animals [145, 146]. In plants, the involvement of mitochondria and chloroplasts in triggering programmed cell death (PCD) is highlighted by increasing pieces of evidence. In mitochondria, pro-death signals involve ROS production, that trigger signals leading to the opening of mitochondrial permeability transition pore (MPTP), dissipation of the mitochondrial membrane potential and a burst of ROS production from the electron transport chain, dysfunction and finally disintegration of the organelle. Proteins normally contained in the inter membrane space and that are cell death signals, such as cytochrome c, are released in the cytosol [147]. Thus, continuous oxidation leads to cell death, but it is important to note that this effect is cell type dependent [147].

Nevertheless, even though ROS are deleterious to the cell when they are produced in too high amount to be efficiently scavenged, they are also signaling molecules involved in many biological processes [148, 149]. They are early signals in many stress responses, and they are necessary for the cell to survive [150]. ROS signaling controls many cell processes, such as gene expression and metabolism [151]. It also mediates flower senescence, root architecture formation, polar cell growth in pollen tube and root hair cells [152], cell growth [153], and certainly many other processes that we have not identified so far. As mitochondria produce superoxide and hydrogen peroxide, but also are central actors in their control through efficient redox couples, they play a central role in such ROS signaling. It is not known whether ROS are directly signaling molecules on their own, or if they initiate a redox signaling cascade from their metabolism. Both can be possible, as oxidation of transcription factors have been reported, and a small shift in the glutathione redox potential is associated with changes in gene expression and plant development [154].

In addition, hydrogen peroxide also participates in many defense mechanisms against various stresses, *via* induction of defense and resistance genes [155]. ROS production are thought to protect cells from stress by triggering a redox signalling cascade that leads to the appropriate response in the appropriate compartment [154]. Mitochondria are involved in this stress response [138]. Perturbations of the mitochondrial electron

transport chain can result in altered pathogen resistance, likely by their effect on the redox status. For example, the *Nicotiana sylvestris* CMSII line has a deficiency in complex I and a resulting increase in mitochondrial ROS production, and this line has higher resistance to tobacco mosaic virus than the wild type [156]. Also, *A. thaliana* mutant in complex II subunit SDH1-1 show less mitochondrial ROS production and a higher susceptibility to several pathogens [156]. Finally, the *slo2* mutant for which a reduction in complexes I, III and IV as well as an increased mitochondrial ROS production has been reported, is more susceptible to *Botrytis cinerea* [156]. A tight and accurate regulation of the cellular redox status is therefore needed to mediate pathogen attack response. Finally, the AOX, which is involved in mitochondrial regulation of ROS production, has also been reported to participate in plant defense [157].

The maintenance of a basal level of ROS for proper cell function is illustrated in figure 1.9. Redox biology is involved in many cell processes. A tight balance of ROS is needed for proper redox biology, and cytostatic / cytotoxic conditions are deleterious to the cell. Several molecules are involved in ROS scavenging, such as the ascorbate and the glutathione.
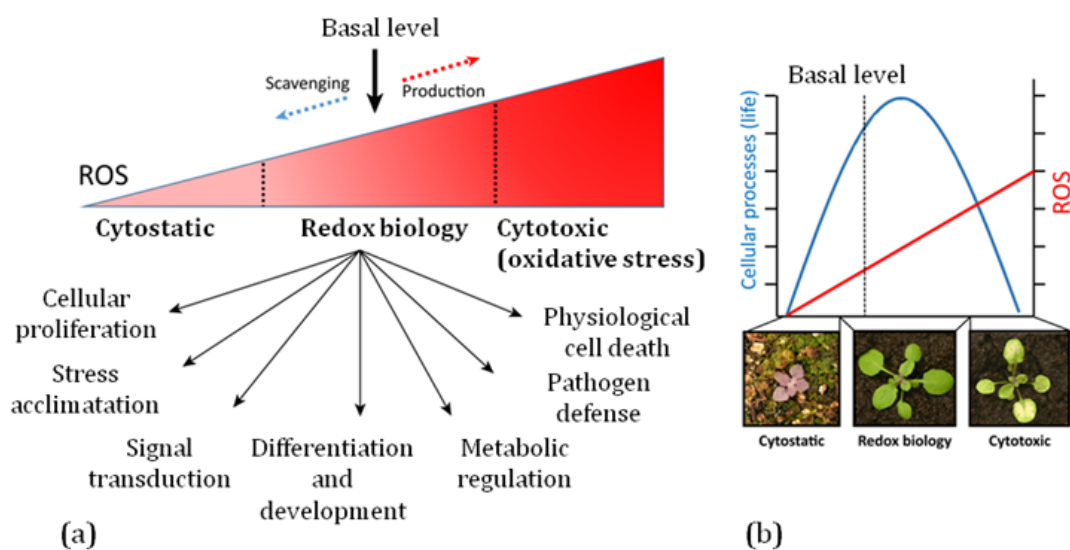
Figure 1.9: **Maintaining a basal level of ROS in cells is essential for proper cellular function.** (a) the effect of different levels of ROS on the regulation of different cellular processes. ROS levels that are too low are thought to be cytostatic for cells, whereas ROS levels that are too high are cytotoxic. A basal level of ROS is therefore required for proper ROS and redox signaling in cells, and this level is maintained by the balance between ROS production and ROS scavenging. (B) The dependency of cellular functions and viability on ROS concentrations. A bell-shaped curve is hypothesized to represent the dependency of maintaining proper cellular processes on increasing ROS concentrations. Normal plant metabolism requires therefore an optimum range of ROS levels that enable the plant to achieve its maximal growth and developmental potential. From R. Mittler (2017) [150]

1.4.2.2   Glutathione is at the centre of redox homeostasis in mitochondria

During normal functioning, ROS are scavenged *via* enzymatic or non-enzymatic pathways. The primary defense against superoxide is the manganese dependent superoxide dismutase (Mn-SOD), located in the mitochondrial matrix. Mn-SOD detoxifies superoxide into hydrogen peroxide. Hydrogen peroxide is in turn scavenged by catalase (resulting in water and oxygen formation), ascorbate glutathione cycle (resulting in the formation of reduced glutathione (GSH) and $NAD(P)^+$), and glutathione peroxidase cycle (resulting in the formation of GSH and $NAD(P)^+$) [158]. The hydrogen peroxide can be detoxified in the mitochondrial matrix as well as in other compartments (notably in cytosol and peroxisomes), as it is able to diffuse freely through membranes. The catalase has been found mostly in peroxisome and in maize mitochondrial matrix [159, 160]. Yet, mitochondrial location seems marginal as no catalase has been reported in matrix mitochondria in other species [161]. The ascorbate glutathione cycle occurs in chloroplast stroma and mitochondrial matrix, and it is the main ROS detoxification pathway in plant mitochondria [162]. The glutathione peroxidase (GPX) is found in the cytosol [155]. The main enzymatic pathways of ROS detoxification are presented in figure 1.10.

The tight control of reactive oxygen, both to prevent cell damages and to ensure efficient signalling, relies mainly on few redox couples that are at the centre of the complex hub integrating metabolic information and environmental stimuli. C. Foyer and G. Noctor developed the idea that glutathione plays a central role in the redox hub, defined as an "interconnected core of reactions and components able to mediate a cross-talk between essential bioenergetics processes and signalling pathways" [163]. Glutathione is mainly in reduced form under normal conditions [164], and the reduced state of the cytosolic glutathione pool is actively and robustly maintained in a broad range of organisms [165]. It is a major ROS scavenger in the cell, linked to peroxide metabolism by specific enzymes. The oxidized form of glutathione is relatively stable, enabling changes in the GSSG:GSH ratio to trigger cell redox responses. This ratio thus represents the dynamic equilibrium between the ROS scavenging activity of GSH and the activity of glutathione reductases (GR), relying on NAD(P)H as electron donors to enzymatically GSSG recycled to the GSH reduced form. Therefore, the redox potential of the glutathione pool is indicative of the level of ROS production in the cell. In addition, it was shown to be independently regulated in the cytosol, mitochondrial matrix and mitochondrial intermembrane space in yeast [166], which possibly enables an independent control of the redox signalling trigger from different compartments.
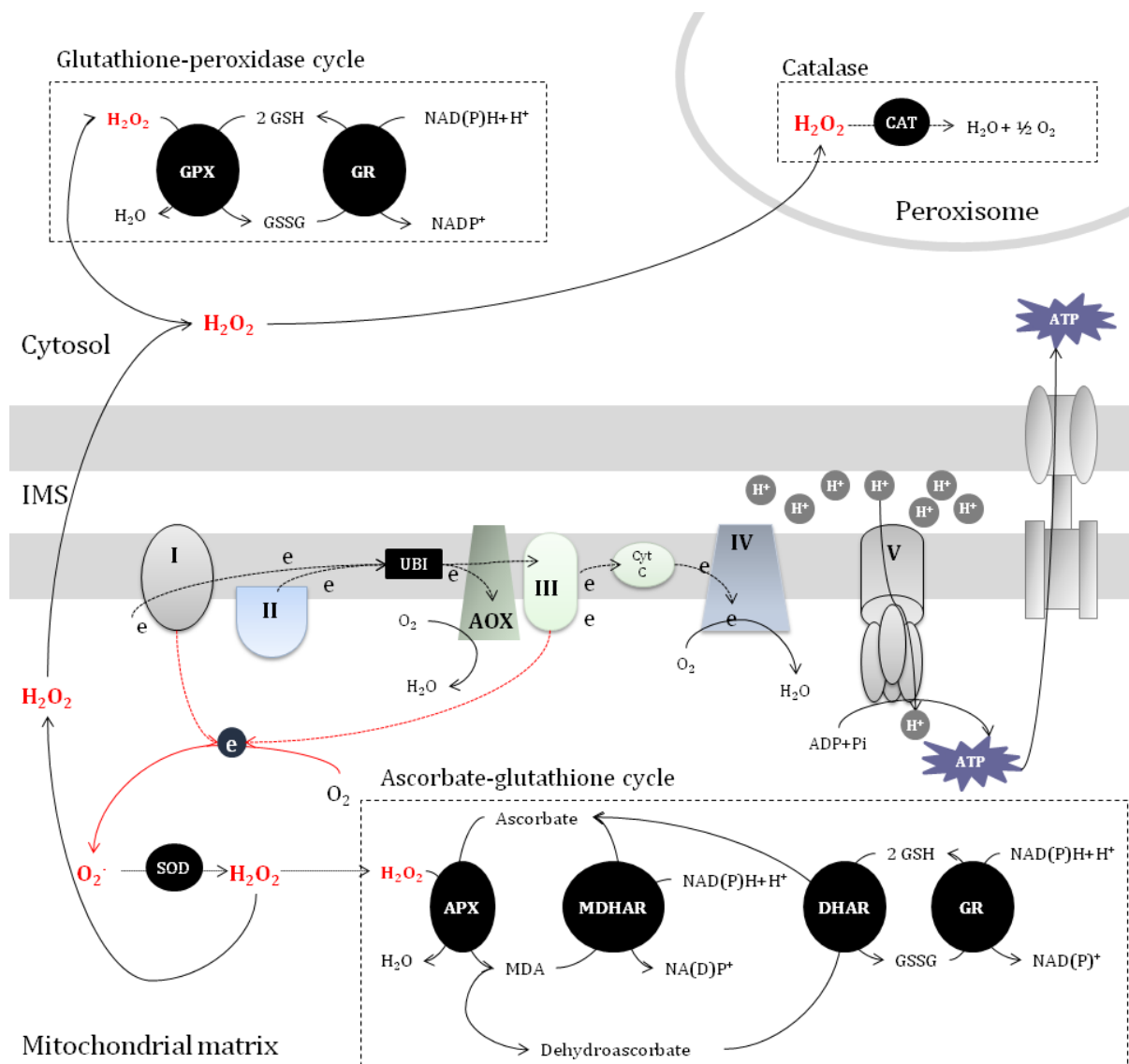
Figure 1.10: Enzymatic pathways involved in ROS scavenging. ROS are notably produced in plant mitochondria by respiratory complexes I, II, and III *via* electron leakage and oxygen reduction to superoxide. Different pathways are involved in ROS detoxification. The first involves reduction of superoxide into hydrogen peroxide, catalyzed with SOD (superoxide dismutase). Thereafter, hydrogen peroxide is further detoxified in the peroxisome *via* catalase, in the mitochondrial matrix *via* ascorbate glutathione cycle, or in the cytosol *via* glutathione peroxidase cycle. The ROS are indicated with red color. Dashed arrows, black: electron transfer; dashed arrows, red: electron leakage; red arrows, plain: hydrogen peroxide movements. CAT: catalase; APX: ascorbate peroxidase; MDA: monodehydroascorbate; MDAR: MDA reductase; GSH: glutathione (reduced form); GSSG: glutathione (oxidized form); GR: glutathione reductase; GPX: glutathione peroxidase; IMS: intermembrane space.

29

In the frame of this study, it is interesting to note that, among the two GRs encoded in *A. thaliana*, the GR2, dually-targeted to the chloroplast and mitochondria, is mandatory for embryo development [167], whereas the cytosolic GR1 seems to be required for pollen tube germination and elongation in the absence of NADPH-dependent thioredoxin reductases (NRTA and NRTB) [168]. These reinforce the idea that the redox equilibrium of the cell is crucial in both gametophyte and sporophyte, and is, at least in part, dependent on the redox status of the glutathione pool.

1.4.3 Mitochondria and the cell cycle

Recent studies suggest that mitochondria might fulfill a specific role in plant cell during meiosis and mitosis according to their number, size and morphology changes during these events, as mitochondria are highly dynamic organelles that are capable of fission and fusion [169]. For example, in cultured cells mitochondrial morphology change occurs during G1/S boundary phase and controls the cell cycle [170]. In *A. thaliana* shoot apical meristem and leaf primordia, a large mitochondrion wrapping the nuclear pole, called the "tentaculate mitochondrion", together with small round shaped mitochondria distributed in the cell, are observable at the G1/S stage. In G2, mitochondria double their volume and the tentaculate mitochondrion surrounds the nucleus. During mitosis, 60 % of the small round-shaped mitochondria fuse with the large mitochondrion to form a cage-like mitochondrion, that divides in two independent tentaculate mitochondria during cytokinesis. After fission, newly small round-shaped mitochondria are formed. The existence of the tentaculate/cage mitochondria is hypothesized to facilitate genetic information exchange between the different mitochondria, therefore mixing DNA content that changed because of high recombination rate of plant mitochondrial DNA, and thus homogenizing the chondriomes inherited by the daughter cells [171]. This morphology change seems however to be dependent on the cell type, as no cage mitochondria was detected in *A. thaliana* root-tip meristem, highlighting the different mitochondrial behavior in different cell types. Moreover, mitochondria might play a role in plant reproduction as ROS are thought to be involved in processes of plant reproductive development, for example by controlling the transition from mitosis to meiosis, and the development and mitoses of the gametophytes [172].

In this section, I summarized some mitochondrial functions in cell development and signaling, with a specific interest on the consequences of mitochondrial ROS production and subsequent redox biology. According to the CMS genetics and the known roles of mitochondria, some hypotheses that might explain the physiological defects leading to pollen abortion are detailed hereafter.

1.4.4 Main hypotheses to explain cytoplasmic male sterilities

In the past years, several hypotheses have been proposed to explain how a mitochondrial defect could lead to pollen abortion. The most accepted one is the "ATP hypothesis", which postulates that male gametogenesis is highly energy demanding and that a decrease of ATP production due to the sterilizing gene would cause pollen abortion [52]. This hypothesis came from the observations that (1) mitochondrial gene expression is particularly high during pollen development [173, 174], and (2) CMS genes are often co-transcribed with, and/or often contain in their coding sequence, parts of essential mitochondrial genes encoding subunits of the OXPHOS complexes. It was proposed that this latter feature could provoke a decrease in ATP production, as the expression of the sterilizing gene could interfere with expression and regulation of linked essential mitochondrial genes on one hand, and as parts of the sterilizing protein corresponding to parts of OXPHOS subunits could interact with complexes on the other hand [52]. The "ATP hypothesis" was experimentally supported by a study on sunflower CMS for which a decrease in the activity of the ATP synthase was detected [175]. In rice HL-CMS, a decrease in ATP level was also reported [176]. Yet, it is interesting to note that in sunflower CMS only the mitochondrial ATP synthase activity has been investigated, in mitochondria isolated from etiolated seedlings and florets. Also, in rice HL-CMS, ATP level was measured in mitochondria isolated from seedlings. Therefore, in both cases only the mitochondrial ATP production or concentration was under investigation and the cytosolic ATP level available for the cell (for example the ATP produced during glycolysis) was not monitored. Moreover, the analyses were performed in vegetative tissues, or in a mixture of reproductive and vegetative tissues. Thus, there is no direct evidence of an energy depletion in male reproductive organs in these CMS lines. The "ATP hypothesis" is controversial for several reasons. One is that many other developmental steps are highly energy demanding and they are not affected in CMS lines. Moreover, respiratory mutants that have a default in ATP synthesis present not only male gametophyte but also female gametophyte defects, and vegetative growth retardation. Thus, an energy deficiency cannot explain alone the male specificity of the CMS phenotype. Furthermore, inducible knock down mutants for ATP synthase subunits do not present a decrease in pollen fitness [177]. Also in maize CMS-S, the *rfl1* restorer decreases the ATP1 accumulation in pollen, and yet it confers fertility to the pollen carrying it [104].

It was also proposed that the sterilizing protein could interact with a still unknown X-factor specifically present in the pollen grain and/or the tapetum and that this interaction would be deleterious for the cell. This hypothesis is in accordance with our knowledge on the CMS-T from maize, where the sterilizing protein URF13 likely forms

a pore in the inner mitochondrial membrane, which opens in the presence of the T-toxin from the fungus *Cochliobolus heterostrophus* [178]. R. Flavell (1974) proposed that some biosynthetic product only found in young anthers would interact with URF-13 as does the T-Toxin, leading to the T-URF13 pore opening and subsequent cell death [179]. However, such X-factor has not been identified so far.

Also, it is proposed that mitochondria may fulfill a specific role in pollen production, for example by producing precursors necessary for its development [177], although no such precursor was identified to date. However, the fact that *A. thaliana* mutants affected in nuclear genes encoding mitochondrial proteins present organ-specific plant phenotypes (delayed development and flowering, altered leaf morphology and/or photosynthetic capacity, alteration in root morphology and respiration rate...) [138] indicates that mitochondria could play a specific role in each of these tissues. R. Jacoby et al. (2012) hypothesized that such differences in the tissues would come from either "the inability of mitochondria to meet energy demands in a particular tissue", and/or a mutation in the mitochondrial proteome that might require the expression of particular isoforms of proteins for tissue-specific functions [138]. Transcriptomic and proteomic studies highlighted differential gene transcription and protein isoform accumulation for mitochondrial proteins in the different tissues [180, 181]. Mitochondria from flowers tend to have a specialized role in metabolism other than the TCA cycle, such as the maintenance of mitochondrial redox state (for example thioredoxin reductases and aldehyde dehydrogenase).

Another hypothesis for the CMS mechanism involves a ROS burst in mitochondria, that would induce PCD and lead to pollen abortion. In sporophytic CMS, such a ROS burst is thought to induce premature tapetal layer degeneration *via* early PCD. For example, in the sporophytic rice WA-type CMS, the sterilizing protein WA352 interacts with OsCOX11, a complex IV subunit, triggering a ROS burst and a premature tapetal cells PCD, which results in male gametophyte abortion at the uninucleate stage [89]. The interaction of the sterilizing gene with a respiratory subunit could lead to an increase in ROS production because of complex dysfunction, or disorganization of the supercomplexes. In maize CMS-C, a ROS burst as well as a PCD phenomenon was also detected [182]. In Ogura CMS and maize CMS-T, the sterilizing protein likely forms a pore in the inner mitochondrial membrane [178, 179, 183], leading to premature PCD of the tapetal cells and microspore abortion, at the vacuolate microspore stage in Ogura CMS [184]. The only gametophytic CMS system for which the mechanism of pollen abortion has been investigated is the HL-type CMS of rice [176]. The ORFH79 sterilizing protein interacts with the P61 subunit of complex III. A lower activity of the complex III as well as a decrease in mitochondrial ATP concentration was detected in the sterile line, as well as

the inhibition of expression of cell-cycle related genes. Authors proposed a model for this CMS, according to which the interaction of the sterilizing protein with complex III leads to a ROS burst coupled with an ATP production decrease, both producing retrograde signals repressing the nuclear genes related to cell cycle that allows the second pollen mitosis [176].

Physiological mechanisms leading to pollen abortion elucidated in some sporophytic and gametophytic systems are presented in table 1.2. Sporophytic CMS have been widely studied, and general patterns including a ROS burst and premature PCD of tapetal layer are highlighted. Conversely, there are few studies on gametophytic CMS and the mechanism by which pollen aborts in these systems is still poorly understood.

Table 1.2: Abortion stages and identified mechanisms in different sporophytic and gametophytic CMS

	CMS type	Species	Abortion stage	Mechanism	Ref
Sporophytic system	WA-CMS	Rice	Uninucleate	Complex IV interaction, early PCD of tapetal cells	[89, 185]
	CMS-C	Maize	Tetrad	ROS over-accumulation, PCD	[182, 186]
	CMS-T		Tetrad	Pore formation in the inner mitochondrial membrane	[178, 179, 187]
	CMS-Ogura	Brassica	Vacuolate	Pore formation in the inner mitochondrial membrane, early PCD of tapetal cells	[183, 184]
	CMS-PET1	Sunflower	Tetrad	ATPase activity reduction, early PCD of tapetal cells	[188]
Gametophytic system	CW-CMS		Germinating	?	[189]
	LD-CMS		Trinucleate	?	[118]
	BT-CMS	Rice	Trinucleate	?	[118]
	W11-CMS		Germinating	?	[120]
	HL-CMS		Binucleate	Complex III interaction, ROS accumulation ATP decrease and cell cycle arrest	[176]
	CMS-S	Maize	Binucleate	?	[190]

1.5 The Sha cryptic cytoplasmic male sterility of *A. thaliana*

A. thaliana is a model plant that has been used in research since the early 50's. Its short life cycle, its relatively small nuclear genome (158 millions of base pairs on five chromosomes), its autogamous reproduction as well as its propensity to produce many seeds make it attractive for genetic studies. Moreover, the diversity of genetic resources is very large in *A. thaliana*, with many accessions and mutants available. It was the first plant organism for which the genome was sequenced [191], and 1,135 accessions were later on sequenced [192]. A cryptic cytoplasmic male sterility has been discovered in *A. thaliana* after reciprocal crosses between far-related accessions [193]. Investigating CMS in *A. thaliana* allows the use of many techniques developed on this model plant, and could possibly bypass technical issues that render difficult the study of pollen mitochondria in CMS.

1.5.1 A gametophytic cytoplasmic male sterility system in *A. thaliana*

A cryptic CMS has been discovered by our team, as part of Nicolas Gobron's thesis, by crossing two distantly related accessions Shahdara (Sha, originating from Tajikistan) and Mr-0 (originating from Italy) [193]. Reciprocal crosses gave progenies with different behavior, as they were sterile in the Sha x Mr-0 cross, whereas they were fertile in the Mr-0 x Sha cross. The hand pollination of F1 from the Sha x Mr-0 cross resulted in elongated siliques, highlighting a male sterility depending on the cytoplasmic genome. The finding that the Sha x Mr-0 F1 is fully male-sterile was intriguing if only caused by CMS, which would necessarily be sporophytic: the Sha restorer allele(s) would have to be recessive in order to explain the sterility of the heterozygous hybrids, and recessive restoration is scarce. The hybrid sterility of this F1 was later shown to be due to the genetic co-localization of factors that cause segregation distortion, "pollen killers", with nuclear loci involved in a gametophytic CMS [194, 195]. As part of Matthieu Simon's thesis [194], three nuclear loci, located on chromosomes 1, 3, and 5, were found to carry simultaneously Sha restorer alleles, and pollen-killer loci [195].

In order to detect other maintainer nuclei, reciprocal crosses were firstly performed with the smallest core-collection of Versailles Arabidopsis Stock Center: Blh-1, Bur-0, Ct-1, Cvi-0, Ita-0, Jea and Oy-0. Reciprocal crosses gave only fertile F1 individuals, and after three paternal backcrosses sterile progenies were detected in the Sha x Cvi-0 descendants.

This indicated that the Cvi-0 accession carries a maintainer nucleus, whereas all the other accessions harbored a restorer nucleus. Moreover, the fertility of the Sha x Cvi-0 F1 indicates that there is no pollen killer co-localized with the CMS-related nuclear loci in this cross. [Sha]Cvi-0 (Sha cytoplasm and Cvi-0 nucleus) and [Sha]Mr-0 (Sha cytoplasm and Mr-0 nucleus) cytolines were constructed through seven backcrosses. The cytolines were used to detect other maintainer nuclei: they were used as the mother in crosses with different accessions; the progenies are expected to be sterile in the case in which the tested accession carries a maintainer nucleus, and fertile otherwise.

The Sha CMS system is influenced by unidentified environmental conditions, as many other CMS systems [9]: the [Sha]Cvi-0 cytoline was fertile in field experiments [45], and both [Sha]Cvi-0 and [Sha]Mr-0 cytolines produce selfed seeds in non-heated greenhouse conditions during winter (unpublished results). However, several tests with fluctuating temperatures and/or photoperiod parameters did not allow us to determine the environmental conditions leading to reversion of the phenotype to partial fertility.

1.5.2 The mitochondrial *orf117Sha* is strongly suspected to cause cytoplasmic male sterility

Cytoplasms able to induce the sterility phenotype were looked for among several accessions from the collection. Firstly, twenty accessions geographically to Sha, or having a cytoplasm similar to that of Sha, were crossed with Mr-0 in both ways. Ten produced a sterile F1 when used as the female, and all of these accessions carried the same chlorotype as Sha. Among the 10 accessions not inducing sterility, only the Kz-9 accession carried the same chlorotype as Sha.

Because Kz-9 and Sha have similar cytoplasms, although Kz-9 is not sterilizing, mitochondrial structural variations were investigated in these two accessions by comparing DNA hybridization profiles with twenty-three gene probes. This approach revealed in the Sha mitochondrial genome the duplication of 1025 bp from the *cob-rpl5* region close to 400 bp of unknown origin absent from the Kz-9 genome. This latter fragment comprises an ORF putatively encoding a 117 amino acid peptide, and therefore named *orf117Sha*. The ORF117SHA protein sequence shares 56 % identity and 69 % similarity with the ORF108 protein sequence, which is known to cause sterility in *B. juncea* [69, 90, 91].

An association genetics approach was performed to support the identification of the *orf117Sha* as the sterilizing gene. The presence of the *orf117Sha* was first tested on the 20 accessions closely related to Sha that I mentioned above, and supported with 26 novel accessions. All of these accessions were crossed with Mr-0 in both ways in order to detect

a sterilizing cytoplasm, and the presence of the *orf117Sha* was tested by PCR analysis. Among these 46 tested accessions, 28 gave fully fertile F1 when crossed with Mr-0 as the male parent and were negative for the presence of *orf117Sha*. Eighteen accessions possessed the *orf117Sha*, among which 14 gave sterile F1 when crossed with Mr-0 as the male parent. The four remaining *orf117Sha* carrying accessions produced fertile F1 in similar crosses. These F1 were backcrossed by Mr-0, and half of the paternal backcross progenies were found to be male sterile, indicating a gametophytic CMS without pollen killer effect in these crosses [195]. All the F1 from crosses with Mr-0 as the mother parent were fertile.

The Sha CMS system is cryptic, as no gynodioecious population has been reported in natural *A. thaliana* populations, suggesting a fixation of restorers in accessions carrying the sterilizing cytoplasm. As *A. thaliana* is essentially autogamous, the male sterile plants would not be efficiently pollinated in natural populations. Moreover, the restorer alleles are present in many distantly related genotypes, even though they do not carry the sterilizing cytoplasm. Such a phenomenon is also observed in Mimulus cryptic CMS [59]. This finding suggests that these accessions derived from populations that formerly harbored the sterilizing gene, evolved restorer alleles and potentially lost the sterilizing gene. The discovery of a CMS system in *A. thaliana* is in accordance with the idea that cryptic CMS might be much more common that previously thought.

1.5.3 Objectives of the study

The aim of this work was to provide clues to better understand the mechanism(s) that lead to pollen abortion in the Sha CMS. To this purpose I undertook two types of experimental approaches, both relying on the maintainer nuclear background of the Cvi-0 accession, although dormant, because it is early flowering, oppositely to the Mr-0 accession.

In a first part, I tried to test the hypothesis of the *orf117Sha* being the sterilizing gene in the Sha CMS. In this regard, I attempted to provide functional evidence for its role in the CMS and to build tools for molecular analyses of its product *in vivo*. I used [Sha]Cvi-0 sterile plants, carrying the sterilizing cytoplasm of Sha and the nuclear background of Cvi-0, and the Sha accession, with restored pollen fertility, in order to assess the effects of the fertility restoring nuclear background on the *orf117Sha* expression. I used Cvi-0 plants in a transgenic approach developed in order to phenocopy the male sterility by addressing the ORF117SHA protein to mitochondria.

In a second part, I investigated cytological features of the pollen development in sterile and fertile control plants, independently from the nature of the sterilizing gene. In this

part, the genotypes used all possessed the Cvi-0 nuclear background and the possible effects of the sterilizing cytoplasm of Sha, compared to the non-sterilizing cytoplasms of Cvi-0 and Kz-9, were tested. The Kz-9 cytoplasm appeared the best fertile control as it is the closest to Sha known not to induce sterility: it prevented possible confounding effects due to a disruption of cytonuclear coadaptation to be mixed up with effects of the sterilizing factor of the Sha cytoplasm. For this approach, I used tools that allowed observation of mitochondria in the developing pollen, for the first time in my knowledge, and of nuclei of the germline cells. I could test whether the morphology of mitochondria and/or the mitoses were affected in the pollen of sterile plants. Then, using innovative genetically encoded fluorescent sensors, I investigated whether the cytosolic ATP content and the redox state of the mitochondrial glutathione pool were similar in the pollen of sterile and fertile plants.

2 — Results

The major aims of this study were to determine the molecular and cytological events leading to male gametophyte abortion in *Arabidopsis thaliana* Sha CMS, and to describe mitochondrial functions in normal and impaired pollen development. For this purpose, I developed two different types of approaches. Firstly, I used strategies relying on the hypothesis of the *orf117Sha*'s role as the sterilizing gene: I attempted to determine its expression profile, as well as the effect of restoration on it. In addition, I tried to phenocopy the CMS in transgenic plants in order to bring functional evidence of the involvement of *orf117Sha* in this CMS, and pave the way for structure-function studies of its product. Secondly, I used approaches that were totally independent from the identity of the sterilizing gene in order to elucidate the events leading to pollen abortion. I first described cytological phenomenons prior to pollen death. Then, I evaluated mitochondrial functions in the different lines, in whole plant with biochemical methods on the one hand, and specifically in the pollen grains by confocal microscopy imaging of fluorescent sensors on the other hand.

Before the start of this work, the cytolines [Sha]Cvi-0, [Sha]Mr-0 and [Kz-9]Cvi-0 were available. The cytolines are described in part 4.1.1 and their main characteristics are detailed in table 4.2. The two cytolines [Sha]Cvi-0 and [Sha]Mr-0, presenting the CMS phenotype, were described in F. Roux et al. (2016) [45] and M. Simon et al (2016) [195], respectively. The control cytoline [Kz-9]Cvi-0 was developed for this study. As the cytoplasm from the accession Kz-9 is very close to that from Sha, but does not carry the sterilizing gene [193], it is the fertile control closest to the sterile line [Sha]Cvi-0 used to characterize *A. thaliana* CMS in this study.

2.1 Analysis of the *orf117Sha* gene expression in different nuclear backgrounds

In this part, an analysis of the expression of *orf117Sha*, in maintainer and restorer nuclear backgrounds is presented. In CMS systems that have been studied, identified

restor of fertility genes often code for PPR proteins, as described in section 1.3.2.2. These proteins usually act on the expression efficiency of the mitochondrial sterilizing genes, either at the RNA level, or at the protein level [87]. Thus, I evaluated *orf117Sha* mRNA accumulation in different tissues of the sterile and fertile lines, and I searched for differentially processed transcripts. In collaboration with Nathalie Vrielynck, I developed an antibody that recognizes the ORF117SHA protein, in order to possibly detect it in the different lines.

2.1.1 *orf117Sha* mRNA accumulation in sterile and fertile lines, and in vegetative and reproductive tissues

First, I tested the presence of the *orf117Sha* mRNA in leaves and floral buds of the sterile lines [Sha]Cvi-0 and [Sha]Mr-0, the restored lines Sha and the fertile accession Cvi-0 as a negative control. Total RNA was extracted from leaves and floral buds, and used for RT-PCR experiments. As there is no intron in *orf117Sha*, a control was performed by running in parallel RT-PCR reaction with the retrotranscriptase enzyme (RT+) and the same reaction without the retrotranscriptase enzyme (RT-). The *orf117Sha* mRNA was detected in floral buds and leaves (figure 2.1a) of the sterile and restored lines, and not in the negative control.

Then, I evaluated further the *orf117Sha* mRNA accumulation. As the sterilizing gene is constitutively transcribed in vegetative and reproductive tissues in other CMS systems even though the phenotype is specific to the male gametophyte [77], I wanted to determine whether the *orf117Sha* mRNA was equally accumulated in these different tissue types. Thus, total RNA was extracted from leaves and floral buds of [Sha]Cvi-0 and Sha lines to perform qRT-PCR analysis, with three biological replicates and two technical replicates. The oligonucleotides used to quantify the *orf117Sha* accumulation were located in the 3' region of the coding sequence (no overlap with the 5'-UTR shared with the *cob* gene), and are referenced in table 4.6. The accumulation of the *orf117Sha* RNA was normalized by the mitochondrial *rrn26S* mRNA level. This normalized expression is not significantly different between floral buds and leaves (figure 2.1b). Thus, the *orf117Sha* mRNA seems to be equally accumulated in leaves (vegetative tissue) and floral buds (mixture of vegetative and reproductive tissues). Because the fertile Sha accession carries the *orf117Sha* gene as well as nuclear restorers, I also wanted to compare mRNA accumulation of this gene in Sha and sterile plants. No significant difference in mRNA accumulation is visible between the lines neither in vegetative tissue nor in floral buds (figure 2.1b).
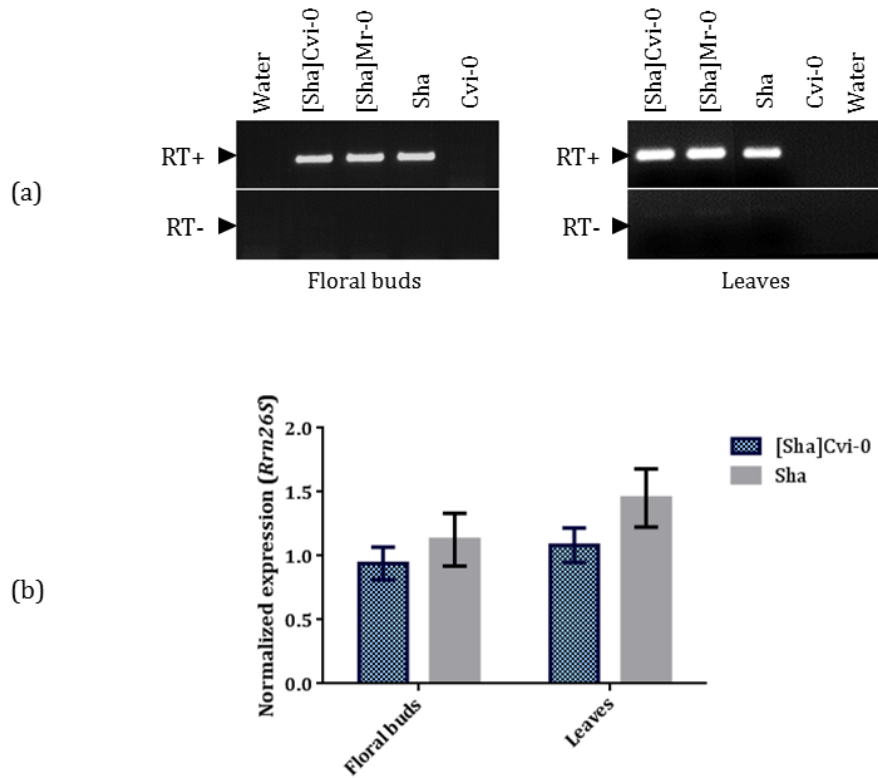
Figure 2.1: *orf117Sha* mRNA accumulation in sterile, restored and fertile lines. (a) RT-PCR analysis. Total RNAs of floral buds and leaves were extracted from sterile ([Sha]Cvi-0 and [Sha]Mr-0), restored (Sha) and fertile (Cvi-0) lines, and DNase treated. RT-PCR reaction (RT+) was performed in parallel with a negative control reaction lacking the retrotranscriptase enzyme (RT-); (b) qRT-PCR analysis. Total RNAs of leaves and floral buds were extracted from sterile ([Sha]Cvi-0) and restored (Sha) lines, and DNase treated. The amount of *orf117Sha* mRNA was normalized by the *rrn26S* mRNA level. The error bars represent $\pm$ SEM. Three independent biological replicates were performed (*n=3*). No significant difference was detected between the populations' distributions (Mann & Whitney test, α= 5 %).

To sum up, there is no detectable difference in mRNA accumulation in the fertile and restored lines in the investigated tissues. Nevertheless there might be some qualitative differences between the mRNA molecules accumulated in restored and sterile lines, due to differential processing events for example.

2.1.2   *orf117Sha* transcript processing in the sterile and restored lines

I first attempted to detect differences in the *orf117Sha* RNA molecules accumulated in the sterile cytoline [Sha]Cvi-0 and the restored accession Sha, by northern blot analysis. The *atp8* mRNA was used as a loading control. The results are presented in figure 2.2. Experiment was repeated twice with independent individuals. No major band for *orf117Sha* mRNA is detectable neither in the sterile line nor in the restored line, but rather several weak bands of different sizes between 500 bases and 2 kb, whereas the *atp8* mRNA bands (expected sizes 754 and 825 bases) [196] give strong signals, merged in figure 2.2, but clearly distinguishable in shorter expositions. This could be explained by the coexistence of multiple *orf117Sha* RNAs, as explained later.

In order to better analyze the extent of the different sized mRNAs detected in the northern blot, I mapped the *orf117Sha* mRNA extremities with the cRT-PCR approach [197]. Briefly, the principle of this method is to ligate the extremities of the processed RNA molecules, and to use the resulting circularized RNA as a matrix in an RT reaction. The cDNA carries the ligated RNA extremities that can be amplified in a PCR reaction with divergent primers. The sequencing of cloned PCR products allows the identification of 3' and 5' ends of the same RNA molecule. This approach brought clues on the sterilizing gene and about the restoration mechanism, for example in the *mori* CMS and the *hau* CMS in *B. juncea*, and the BT-CMS in rice [69, 198, 116]. cRT-PCR analysis was performed on [Sha]Cvi-0 and Sha. PCR amplification of the cDNA from circularized RNA produced multiple fragments with a wide range of different sizes (figure 2.3), suggesting multiple mRNA sizes for *orf117Sha* in accordance with the northern results. Experiment was repeated twice with independent individuals. In the gel, no clear difference was observed between the genotypes. After in gel purification and cloning of the PCR products, 24 and 15 clones were sequenced for the [Sha]Cvi-0 line and the Sha accession, respectively. A major 3' end could be determined in the sterile and fertile lines, located 234 bases downstream of the *orf117Sha* stop codon. No clear major 5' end could be determined with this approach: the clones carried 5' ends distributed from 0 to 516 bases upstream of the *orf117Sha* start codon. In addition, no clear difference in sequenced 5' and 3' extremities is detectable between the restored and fertile lines, as

represented in figure 2.4. According to these results, the *orf117Sha* RNAs have multiple different sizes, which is consistent with the profile of cRT-PCR products and northern blot analysis. These results did not allow me to highlight any difference in *orf117Sha* mRNA processing in the restored background compared with the CMS line.

2.1.3 ORF117SHA protein accumulation in sterile and restored lines

In order to test the presence of the ORF117SHA protein in the sterile and restored lines, we produced a polyclonal antibody against the recombinant ORF117SHA protein expressed in *E. coli*. Several pre-immune sera were tested to check for any aspecific band. We selected two rabbits for which no signal was detected on mitochondrial extracts in western blot analysis with the pre-immune sera. The produced antibodies were tested on pure recombinant protein, and on a mixture of mitochondrial proteins from the [Kz-9]Cvi-0 cytoline (that does not carry the *orf117Sha* gene) and different amounts of the recombinant ORF117SHA protein. In the mixture of mitochondrial proteins extract and the recombinant protein, aspecific bands were observed. Therefore the antibody was purified. After purification, the antibody was similarly tested. The protein is detected at the expected size (13 kD), at a minimal quantity of 50 ng, with a small decrease of the band intensity when the protein is mixed with mitochondrial proteins. The resulting blot is presented in figure 2.5. Even though the aspecificity decreased after purification, some aspecific bands are still visible but not at the same size as the ORF117SHA. The purified antibody could therefore detect the ORF117SHA in western blots, but with a quite weak sensitivity .

After validation of the purified antibody, western bot analysis was performed on [Sha]Cvi-0, [Kz-9]Cvi-0 and Sha mitochondrial protein extracts. After whole-plant mitochondria isolation, 50 μg of proteins were loaded on a 15 % SDS-gel. The Cytochrome C protein (which is soluble, as predicted for ORF117SHA from its primary sequence) was used as a loading control. Even though the proteins had been quantified before loading, it appears that the [Sha]Cvi-0 line was not as much loaded as the other lines (figure 2.6). Different levels of contamination by proteins from other organelles in the samples could cause a bias in the quantification of real mitochondrial protein amounts. Nevertheless, the ORF117SHA protein is detectable in the sterile line [Sha]Cvi-0 at the expected size of 13 kDa, and neither in the negative control [Kz-9]Cvi-0, nor in the restored line Sha. Thus, despite its unusual profile, the *orf117Sha* mRNA appears to be translated. The absence of signal in the Sha sample suggests that the ORF117SHA protein is not accumulated at the same level in this restored genotype compared to the sterile [Sha]Cvi-0.
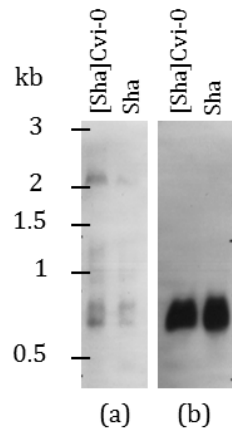
Figure 2.2: RNA hybridization analysis of the *orf117Sha* RNA. Total RNAs were extracted from floral buds, separated in a 1.5 % agarose gel containing 8 % formaldehyhde, blotted onto membranes and hybridized to an *orf117Sha* or an *atp8* probe. Experiment was repeated twice with independent RNA individuals.
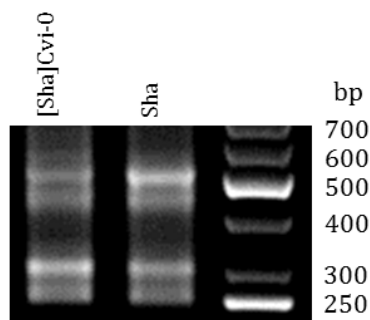
Figure 2.3: PCR amplification on the cDNA obtained from circularized *of117Sha* mRNA. Total RNAs were extracted from floral buds of sterile ([Sha]Cvi-0) and restored (Sha) lines. mRNA was circularized and reverse transcribed. The resulting cDNA was used as the matrix for PCR amplification with divergent primers on the *orf117Sha* sequence, and the PCR product loaded on a 2% agarose gel.
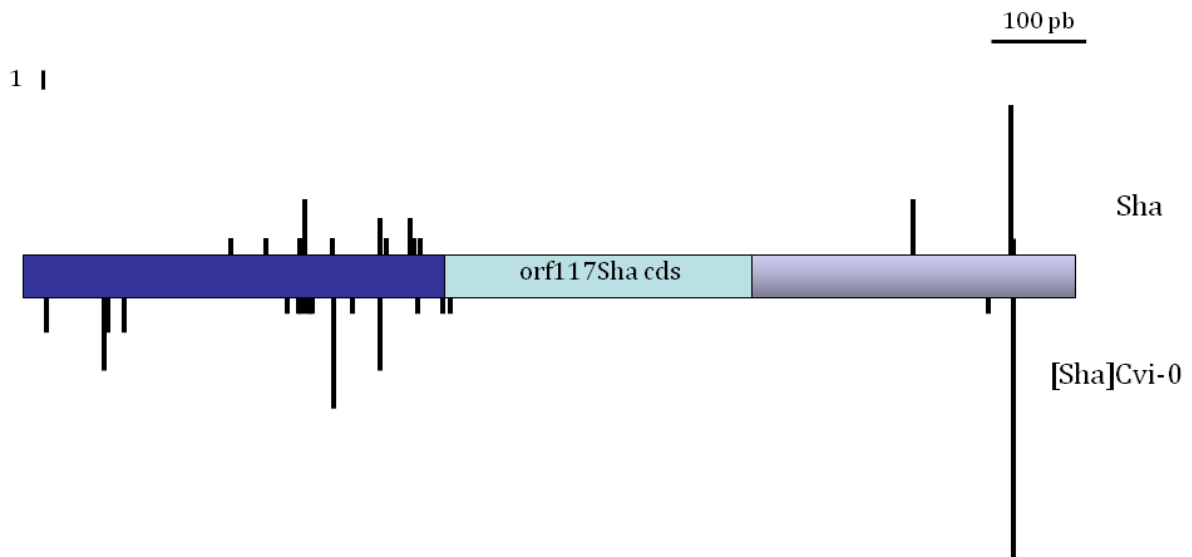
Figure 2.4: 3' and 5' extremities of the *orf117Sha* RNAs detected by cRT-PCR in sterile and restored lines. In both fertile and sterile lines, a clear major 3' but no major 5' end could be determined. This figure summarizes the results of the 24 clones obtained for [Sha]Cvi-0 (below gene boxes) and the 15 clones obtained for Sha (above gene boxes). The height of the vertical bar is proportional to the number of clones carrying the corresponding identified end (scale in the top left of the figure).

This result was obtained a once, and needs repetition to be confirmed.

In this part, I showed that there is no detectable difference in the *orf117Sha* mRNA accumulation between leaves and floral buds, as well as between sterile and restored plants. Also, I could establish with cRT-PCR that *orf117Sha* mRNAs are composed of molecules with similar 3' ends but variable 5' ends. Finally, I highlighted an ORF117SHA protein production in sterile lines and a possible difference in protein accumulation in restored and sterile lines.
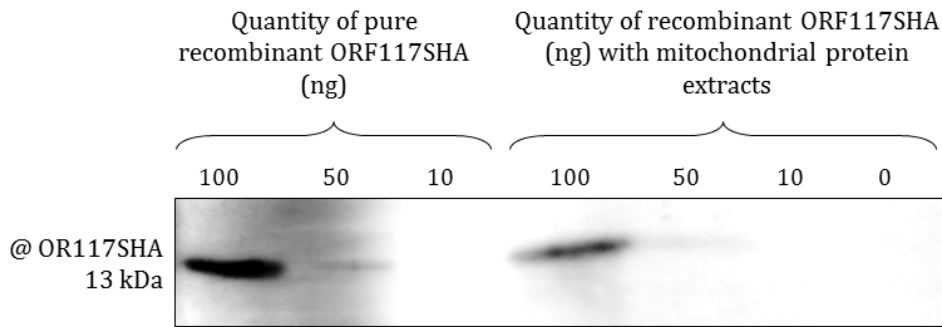
Figure 2.5: Validation of the ORF117SHA purified antibody. Pure recombinant ORF117SHA protein (left panel) and recombinant ORF117SHA protein mixed with 40 μg of mitochondrial proteins from [Kz-9]Cvi-0 (right panel) were separated on 15 % SDS-PAGE. Proteins were blotted onto a 0.20 μm PVDF membrane and probed with the purified ORF117SHA antibody. Experiment was repeated twice.
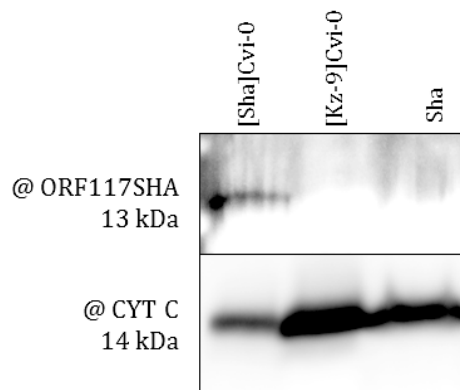
Figure 2.6: ORF117SHA protein detection in the sterile line. Mitochondrial proteins were isolated from whole plants and separated by a 15 % SDS-PAGE. 50 μg of proteins were blotted onto 0.20 μm PVDF membrane and probed with the purified ORF117SHA (top) or CYT C (bottom) primary antibodies. The ORF117SHA band appears in the sterile line at the expected size of around 13 kDa. This result was obtained once, and needs repetition to be confirmed.

2.2 Production of transgenic plants to phenocopy the CMS

We already accumulated several lines of evidence pointing towards the role of the *orf117Sha* in the *A. thaliana* Sha CMS system, as detailed in part 1.5. Indeed, the perfect correlation of its presence with the sterilizing ability of an accession's cytoplasm and the similarity of the encoded protein with the ORF108 CMS protein [193] strongly support the role of the *orf117Sha* gene in the CMS. In the previous part, I obtained results suggesting that the ORF117SHA protein accumulates more in the sterile line [Sha]Cvi-0 than in the restored accession Sha. In order to bring functional evidence of the involvement of the *orf117Sha* gene in sterility, and in view of developing a tool for structure-function analysis of its role in pollen abortion, I constructed transgenic lines producing the ORF117SHA or ORF108 proteins.

Mitochondria transformation is not technically feasible yet, so I used constructs for nuclear transgenesis and added the mitochondria-targeting sequence of the β ATPase from *N. plumbaginifolia* to the sterility gene [38, 39]. This mitochondria-targeting sequence was successfully used previously in the team [199]. As controls, I also produced lines with genes encoding either sterilizing protein not targeted to mitochondria. We excluded the CaMV 35S promoter, which is not active in pollen [200]. I used the constitutive promoter pUBQ10 from *A. thaliana* [201], because we observed a signal in mature pollen grains with the construct pUBQ10::SHMT-roGFP2-Grx1 (see section 2.4.3) in preliminary experiments, and the pollen-specific promoter pM32 from rapeseed described as specific for the male gametophyte [202].

2.2.1 Expression profile of the promoters in pollen development

I checked the expression profile of the two promoters during pollen development with constructs that were used for other approaches in this study, that are the constructs pUBQ10::ATeam and pM32::mt-GFP (see sections 2.3.3 and 2.4.2 respectively), in Cvi-0. The ATeam sensor is detectable from the late binucleate to the trinucleate stages when it is expressed under the pUBQ10 promoter (figure 2.7). It is also constitutively expressed in vegetative tissues and in the tapetum. The GFP is detectable from the uninucleate microspore to the trinucleate pollen grain stages when it is expressed under the pM32 promoter (figure 2.8). This promoter is specifically expressed in pollen.
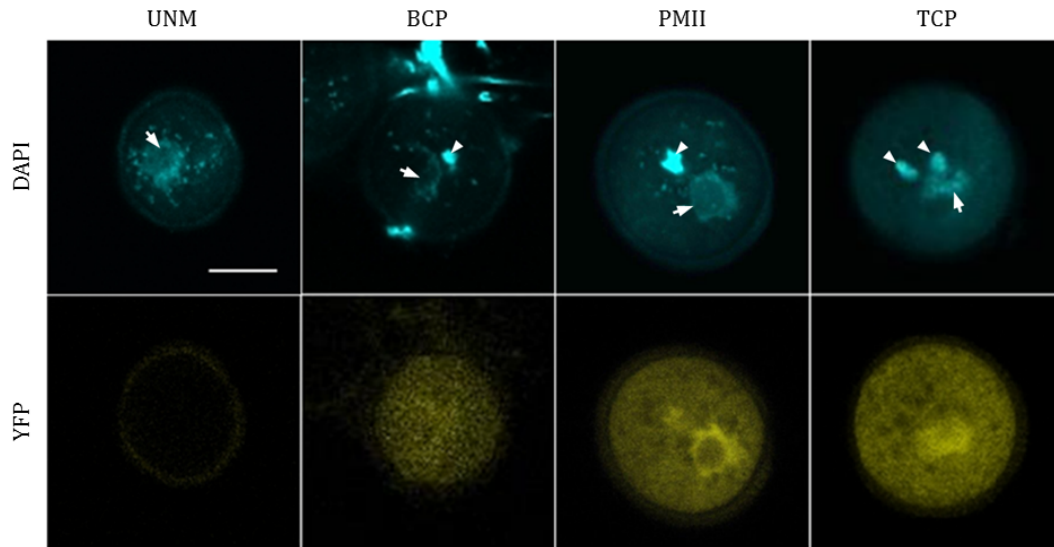
Figure 2.7: Expression profile of the pUBQ10 promoter during pollen development
Transformed Cvi-0 plants with the construct pUBQ10::ATeam were used to check the promoter expression profile during the development of pollen. Pollen grains were stained with DAPI to determine the developmental stage. UNM: uninucleate microspore, arrow: microspore nucleus; BCP: binucleate pollen grain, arrow: vegetative nucleus, arrowhead: generative nucleus; PMII: pollen mitosis II, arrow: vegetative nucleus, arrowhead: dividing generative nucleus; TCP: trinucleate pollen grain, arrow: vegetative nucleus, arrowheads: spermatic nuclei. Scale bar: 10 μm.
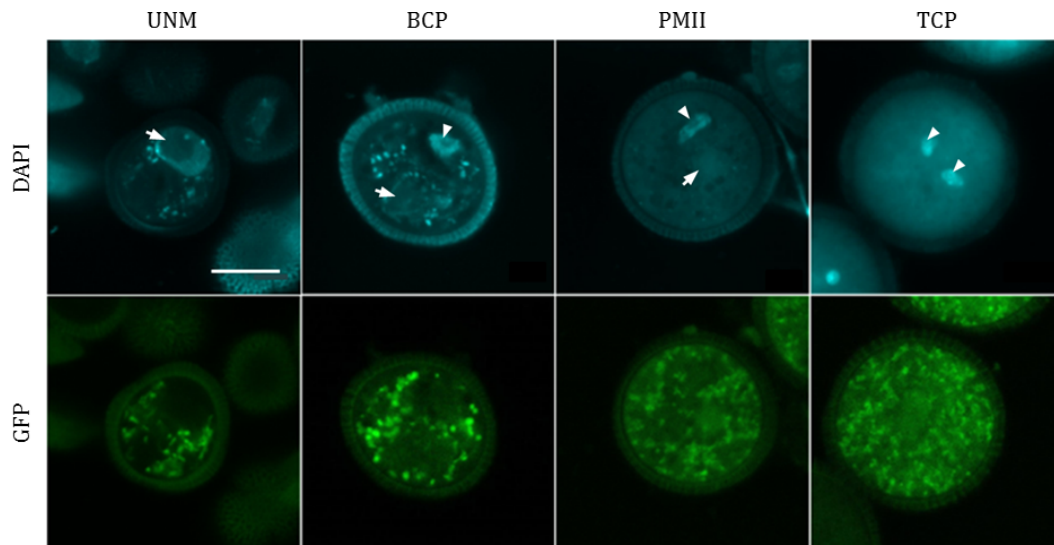
Figure 2.8: Expression profile of the pM32 promoter during pollen development.
Transformed Cvi-0 plants with the construct pM32::mt-GFP were used to check the promoter expression profile. Pollen grains were stained with DAPI to determine the developmental stage. UNM: uninucleate microspore, arrow: microspore nucleus; BCP: binucleate pollen grain, arrow: vegetative nucleus, arrowhead: generative nucleus; PMII: pollen mitosis II, arrow: vegetative nucleus, arrowhead: dividing generative nucleus; TCP: trinucleate pollen grain, arrowheads: spermatic nuclei, the vegetative nucleus is not visible because in another focal plane. Scale bar: 10 μm.

2.2.2 Production and characterization of transgenic plants

I transformed Cvi-0 lines with the different constructs. After *in vitro* selection, I transferred positive plants on soil, genotyped them for the insert, and grown them to flowering. As Sha CMS is gametophytic (see part 1.3.2.1), a successful phenocopy of the CMS should lead to a sterilizing effect of the transgene in the male gametophyte: only the pollen grains carrying the transgene would die, that is 50 % in T1 (hemizygous) plants, and this should impair the transmission of the transgene to the next generation by the pollen. If the CMS was sporophytic, male sterile plants with 100 % of dead pollen would be expected even in heterozygous plants, provided that the sterilizing gene is expressed in the right sporophytic tissue. Hence, I performed Alexander's staining on T1 plants in order to look for dead pollen. After harvesting the self-progenies from the plants carrying the transgene, I analyzed the T2 segregation of the T-DNA *in vitro* with the appropriate selection, or by genotyping, in order to look for a bias in the transgene transmission.

I first obtained transformants expressing the transgenes under the control of the pUBQ10 promoter. Only very few plants could be selected per construct, and even less presented dead pollen: 1 plant out of 2 with the construct pUBQ10::ORF117 presented dead pollen, 2 out of 5 with pUBQ10::mt-ORF117, 1 out of 3 with pUBQ10::ORF108 and 0 out of 2 with pUBQ10::mt-ORF108. These results are summarized in table 2.1. The T1 plants presenting pollen abortion had approximately half of dead pollen in the observed anthers. Examples of Alexander staining of anthers from fully fertile or partially sterile T1 individuals are presented in figure 2.9. All alive pollen grains are red-colored, whereas the dead ones are blue-colored.

These T1 plants were selfed and I analyzed the segregation of the T-DNA in the T2 generation by *in vitro* selection on 100 plants, and by genotyping on 100 other plants. A chi square test was used to test if there was a segregation bias in the T-DNA transmission, considering one or two insertion sites. All the plants that did not present dead pollen transmitted the transgene in expected Mendelian proportions. Among plants presenting dead pollen, only the two plants expressing the ORF117SHA addressed to the mitochondria under the pUBQ10 promoter presented a segregation bias: almost no offspring carried the resistance gene or the *orf117Sha* gene, suggesting an induced lethality in the male but also in the female gametophytes. From these two T1 plants, only one T2 individual carried the transgene but it was unfortunately lost because used for DNA extraction and genotyping. Repeated attempts to get transgenic T2 plants from these families failed. Therefore, as these T1 did not transmit the insert to offspring, the transformation events were lost and I could not analyze them further. RT-PCR on the transgene was performed on transgenic T2 plants from pUBQ10::mt-ORF117SHA T1s not presenting dead pollen

and the expression of transgene was detected in all families. The very low number of selected plants carrying either gene under the pUBQ10 promoter could be explained by a deleterious effect of the ORF117SHA or ORF108 proteins on early stages of development whether or not they are targeted to mitochondria.

In parallel, I used the pollen-specific promoter pM32, and focused on the pM32::mt-ORF117 construct. I obtained 20 T1 plants, among which 6 presented dead pollen in varying amounts, as indicated in table 2.2. When testing T2 segregation, no segregation bias was found. Moreover, the transgenic T2 plants did not present dead pollen anymore. The pollen mortality that was detectable in the T1 generation was therefore not due to the presence of the transgene, but most probably to environmental factors. Here again, *orf117Sha* RT-PCR analysis was performed on the T2 plants. Amplification was observed for all plants, indicating that the transgene was properly transcribed.

I reasoned that the sterilizing activity of ORF117SHA could depend on the presence of a partner present in the Sha, or a very closely related, cytoplasm but absent from the Cvi-0 cytoplasm. I assumed that if such a partner is present in Sha's cytoplasm, it would likely be present in Kz-9 cytoplasm as well. Therefore, in order to test this hypothesis, we crossed [Kz-9]Cvi-0 cytoline as the female parent with four transgenic T2 carrying the pM32::mt-ORF117SHA construct as the male parent. The F1 progenies were genotyped for the presence of the *orf117Sha*, and Alexander's staining was performed on positive plants. Half of the pollen grains should abort in the case where a partner mandatory for the expression of the sterility phenotype was encoded in the Kz-9 cytoplasmic genome. None of the plants presented dead pollen, ruling out this hypothesis.

In this part, I attempted to phenocopy the CMS in transgenic plants in order to bring functional evidence of the involvement of the *orf117Sha* in the CMS, and eventually provide a tool for its structure-function analysis. However, in the rare cases where the mt-OF117SHA construct induced pollen death and has the expected effect on the transgene transmission through pollen, it was not transmitted to the progeny at all. Maybe this is due to an effect of the mt-OF117SHA construct in ovaries, where the pUBQ10 promoter is active [203]. The absence of induced gametophytic sterility when the mt-OF117SHA production is driven by the pollen specific pM32 promoter will be discussed in section 3.1.2.
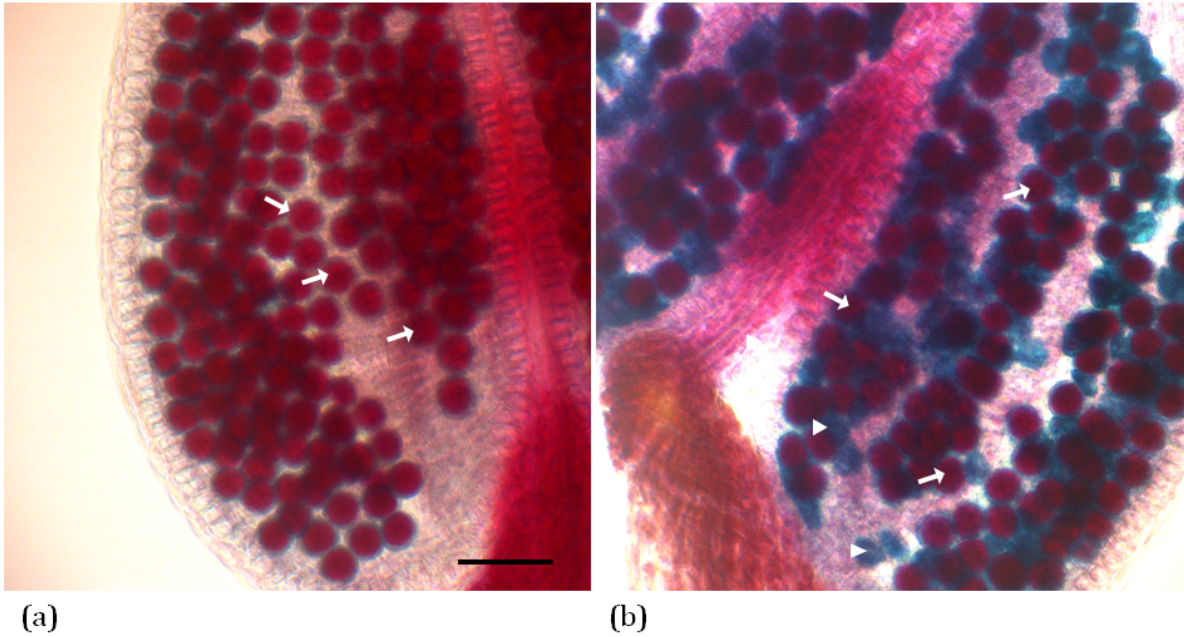
Figure 2.9: Alexander staining of anthers from T1 plants. Flowers from T1 plants were fixed in ethanol and stained with Alexander's stain. (a) T1 individual presenting only viable pollen (red-colored, arrows); (b) T1 individual presenting approximately half of dead pollen (blue-colored, arrowheads). Scale bar: 50 μm.

Table 2.1: Results of transgenesis with pUBQ10 constructs.

Promoter	pUBQ10			
Coding sequence	ORF117	mt-ORF117	ORF108	mt-ORF108
Number of plants selected	2	5	3	2
Number of plants with dead pollen	1	2	1	0
Number of plant with dead pollen and segregation bias	0	2	0	0

Table 2.2: Results of transgenesis with pM32 construct.

Promoter	pM32
Coding sequence	mt-ORF117
Number of plants selected	20
Number of plants with dead pollen	6
Number of plant with dead pollen and segregation bias	0

The two previous sections focused on the *orf117Sha* gene: its expression, the effect of fertility restoration on it, and the effect on pollen viability of its ectopic expression from the nucleus in transgenic plants. The next sections present approaches that are completely independent from the role of this gene in the sterility. Firstly, I described pollen abortion in sterile plants with cytological approaches, and then I investigated mitochondrial functions in pollen in the sterile and fertile lines.

2.3   Analysis of cytological events during abortion

As the CMS phenotype is specifically restricted to pollen grain, I wanted to investigate the events taking place specifically in this tissue prior to abortion. The determination of pollen developmental stage at which abortion occurs was a prerequisite for sterility description, as I wanted to analyze the events prior to it. Then, I verified if pollen mitoses occur properly. Finally, as CMS are likely caused by a mitochondrial defect, I characterized the mitochondria morphology in the pollen grain during male gametophyte development.

2.3.1   Identification of the developmental stage at which the abortion starts

In order to determine the developmental stage in which the abortion occurs, I performed propidium iodide staining of the pollen nuclei in whole anthers. Total inflorescences were collected and fixed. After fixation, floral buds were stained with propidium iodide, and whole anthers were mounted between a slide and a cover-slip. These slides were observed on a confocal microscope, in order to count the living and the dead pollen grains during development. Three individuals per genotype were analyzed, and at least three anthers per stage and per individual were imaged and counted. I took Z-stack accumulations in order to look to pollen grains deeply in the anthers.

In figure 2.10, examples of images used to count the pollen grains in the sterile cytoline [Sha]Cvi-0 and the fertile control [Kz-9]Cvi-0 are presented, at the expected trinucleate stage. In the sterile cytoline, two pollen grains are round-shaped and full, presenting three nuclei (not visible for both of them in this image as it is an optical slice of a Z-stack accumulation), whereas all the other pollen grains are empty and shrunken (figure 2.10a). In the fertile cytoline, it is the opposite: a few pollen grains are shrunken and empty whereas the vast majority are round-shaped and harbor three nuclei (figure 2.10b). The round-shaped pollen grains were counted as alive, whereas the shrunken and collapsed ones were counted as dead.
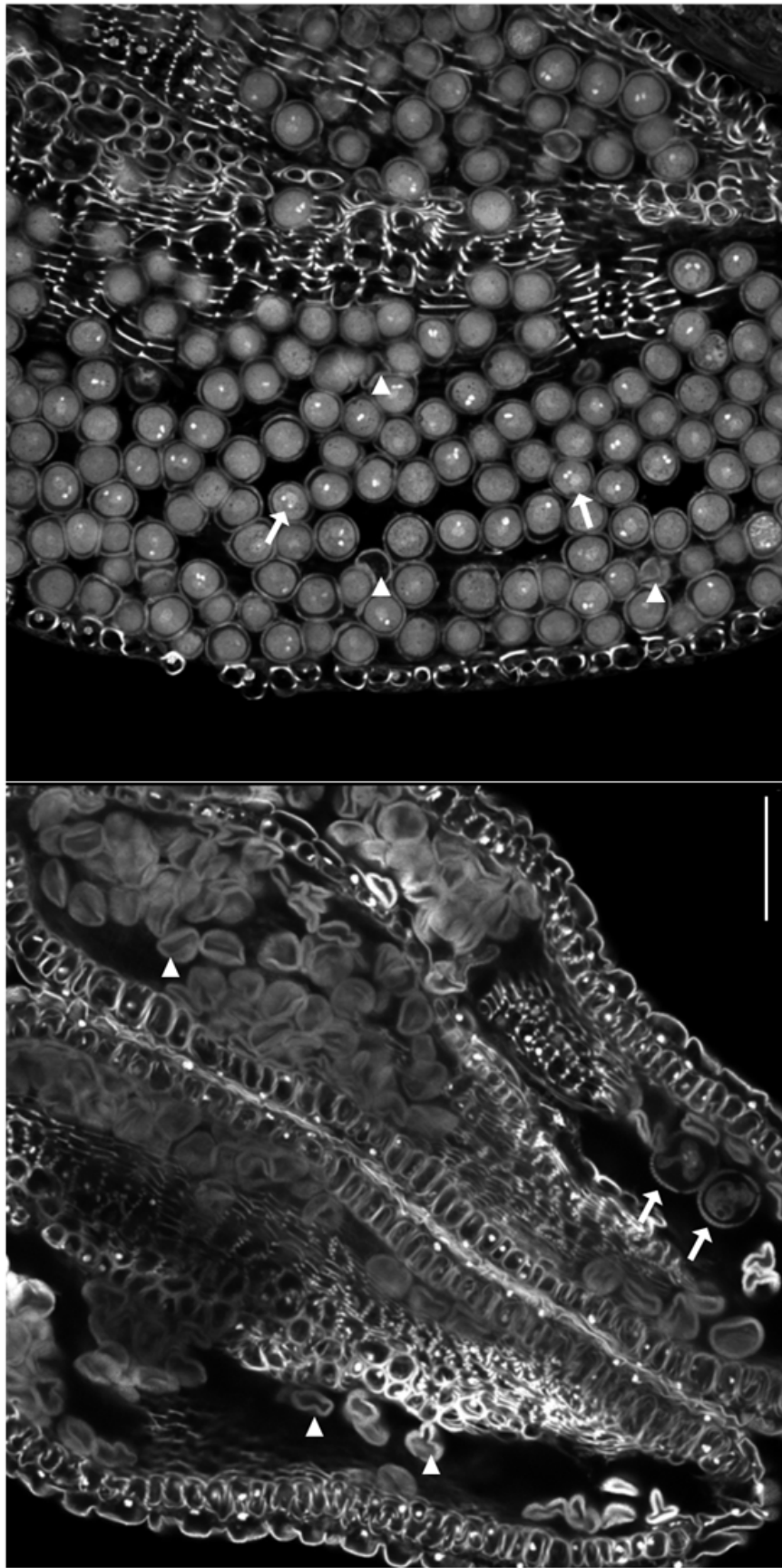
(a)

(b)

Figure 2.10: Image of an anther section at the trinucleate stage in fertile and sterile lines. Typical images obtained after propidium staining of whole anthers of the sterile [Sha]Cvi-0 (a) and the fertile [Kz-9]Cvi-0 (b) cytolines. (a) In the sterile line, two pollen grains are still alive (arrows), while all the others are shrunken and dead (arrowheads). (b) In the fertile line, some of the pollen grains are dead (arrowheads) but most of them are alive, with clearly stained nuclei (arrows). The absence of visible nuclei in living pollen grains is due to their position out of the focal plan. Scale bar: 50 μm.

53

The results for all stages and genotypes are synthesized in figure 2.11. In the fertile genotypes, I observed 100 % of pollen viability until the early trinucleate stage, with a light decrease at the late trinucleate stage. In the sterile line however, 100 % of pollen is viable at the microspore stage, and viability starts to decrease from the binucleate stage and dramatically drops at the late binucleate stage. At the trinucleate stage, almost all pollen grains are dead.

These results suggest that in the sterile plants pollen aborts after the first pollen mitosis, and that the abortion is a progressive process during development. Also, immediately after the first pollen mitosis, some of the pollen grains are dead already and the ones that are still alive present a different phenotype in the sterile cytoline [Sha]Cvi-0 compared with [Kz-9]Cvi-0 and Cvi-0: they contain unidentified black dots when propidium iodide-stained (see figure 2.12).

Then, I wanted to verify whether the majority of pollen grains could undergo first pollen mitosis with proper determination of the germinal lineage fate.
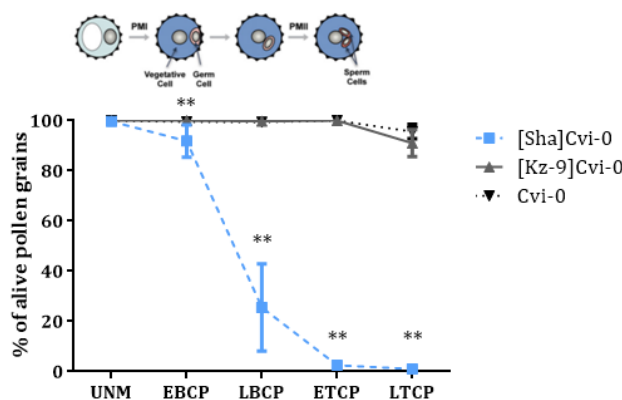
Figure 2.11: Time line of pollen viability from propidium iodide staining of pollen nuclei. Propidium iodide-stained whole anthers were observed in confocal microscopy. Living and dead pollen grains were counted in each Z-stack, and proportions were calculated. For each developmental stage, the average proportion of alive pollen grains and standard deviations were calculated. Total number of counted pollen grains per stage, genotype and biological replicate varied from 50 to 100. The error bars represent ±SD. Three independent biological replicates were performed ($n=3$). Mann & Whitney test between [Sha]Cvi-0 and [Kz-9]Cvi-0 showed that the genotype [Sha]Cvi-0 has significant different viability at stages EBCP, LBCP, ETCP and LTCP, whereas no significant difference was detected between [Kz-9]Cvi-0 and Cvi-0 at any developmental stage ($\alpha= 5$ %). UNM: uninucleate microspore; EBCP: early binucleate pollen grain; LBCP: late binucleate pollen grain; ETCP: early trinucleate pollen grain; LTCP: late trinucleate pollen grain. The pollen development schema above the graph is modified from M. Borg et al. (2009) [13].
**$P \leq 0.01$
***$P \leq 0.001$
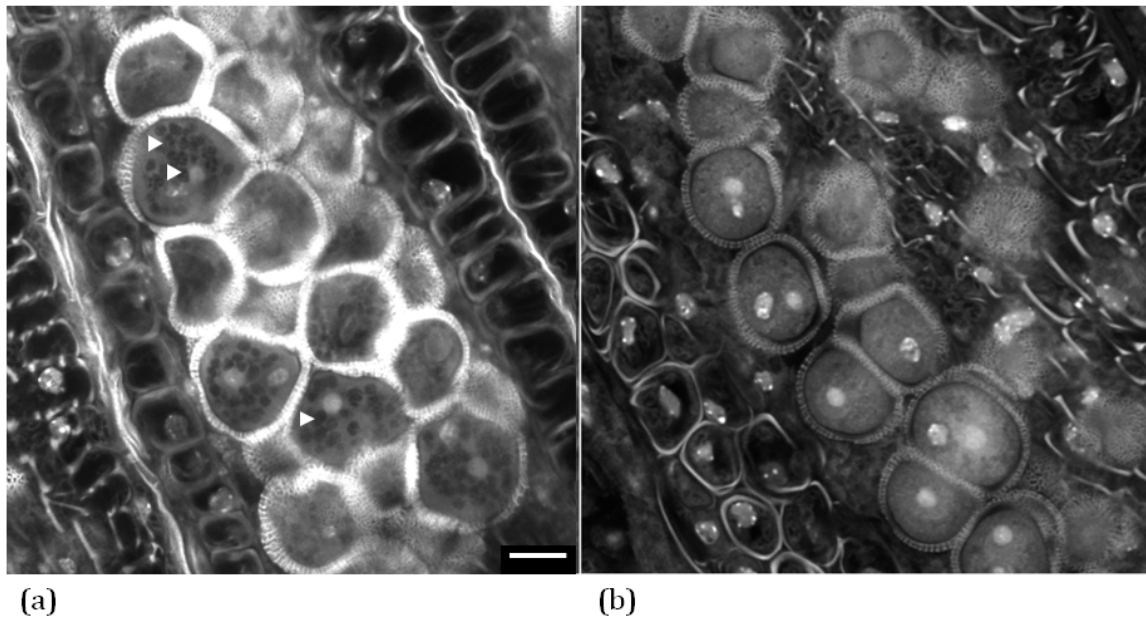
Figure 2.12: Image of binucleate pollen grains colored with propidium iodide in sterile and fertile lines. Propidium iodide staining of pollen grains nuclei in whole anthers of the sterile [Sha]Cvi-0 cytoline (a) and the fertile [Kz-9]Cvi-0 cytoline (b). (a) In the sterile line, pollen grains present black dots (arrowheads). (b) In the fertile line, pollen grains are fully grey. Scale bar: 10 μm.

2.3.2   Verification of the male germ lineage fate

In order to verify the proper fate of the generative lineage in the male gametophyte of sterile plants, I used the pTIP5;1::H2B-GFP construct, kindly provided by Pr David Twell (Leicester University). The pTIP5;1 promoter is specifically expressed in the generative lineage of the male gametophyte, that is in germ and sperm cells [204]. The promoter controls the production of a GFP fused to a histone, so this construct marks generative and spermatic nuclei with GFP.

The Cvi-0 accession was transformed with the pTIP5;1::H2B-GFP construct and the transgene was introduced into the cytolines by crossing, using the T1 plants as the fathers. Generative and spermatic nuclei were observed in developing pollen of the T2 (Cvi-0 genetic background) and F1 plants ([Sha]Cvi-0 and [Kz-9]Cvi-0 genetic backgrounds). Floral buds were collected and dissected in order to take out the anthers. Pistil size was measured to determine the expected developmental stage of pollen, as described in section 4.2.5.2, and samples were mounted in water and observed with the confocal microscope. Pollen grains presenting fluorescence in the germinal lineage were counted as positive, and the number of nuclei was checked. I focused on three developmental stages: the first pollen mitosis, the binucleate pollen grain stage and the second pollen mitosis. For each of these developmental stages, I looked at the four large anthers of one flower from three

different individuals.

In the Cvi-0 line, I observed individuals homozygous for the transgene. Almost 100 % of the pollen grains are positive from the first to the second pollen mitosis (figure 2.13), with the appropriate number of nuclei according to the developmental stage. The [Kz-9]Cvi-0 analyzed plants were heterozygous, and approximately 50 % of the pollen grains are positive at the three stages of pollen development, also with the proper number of nuclei according to the expected developmental stage. A higher variability during the first pollen mitosis (figure 2.13a) is likely due to the fact that not all pollen grains underwent the first pollen mitosis at the exact same time. The [Sha]Cvi-0 plants were heterozygous as well, but no more than 25 % of the pollen grains are positive at first pollen mitosis and binucleate pollen grain stages, suggesting that half of the pollen grains never undergo the first pollen mitosis and therefore do not produce a male germ lineage.

Also, in the sterile lines Cvi-0 and [Kz-9]Cvi-0, at second pollen mitosis and trinucleate stage the pollen grains harbor two fluorescent nuclei. In contrast, in [Sha]Cvi-0 only 3 % of the pollen grains presented two fluorescent nuclei at the second pollen mitosis stage, and around 17 % had only one fluorescent nucleus. This indicates that in the pollen grains alive at this stage, almost none had undergone the second pollen mitosis, and that pollen grains died during the binucleate stage (as the proportion of positive pollen grains decreased). The phenotype of pollen grains from the [Sha]Cvi-0 cytoline still presenting one marked nucleus at the second pollen mitosis and at the expected trinucleate stage is presented in figure 2.14. Such pollen grains are also observed at the late binucleate stage of pollen grains for which nuclei were colored with propidium iodide: the two nuclei are located against the cell wall and the cytoplasm started to collapse. These results suggest that, in the sterile plants, those pollen grains that can achieve the first pollen mitosis scarcely undergo the second pollen mitosis.
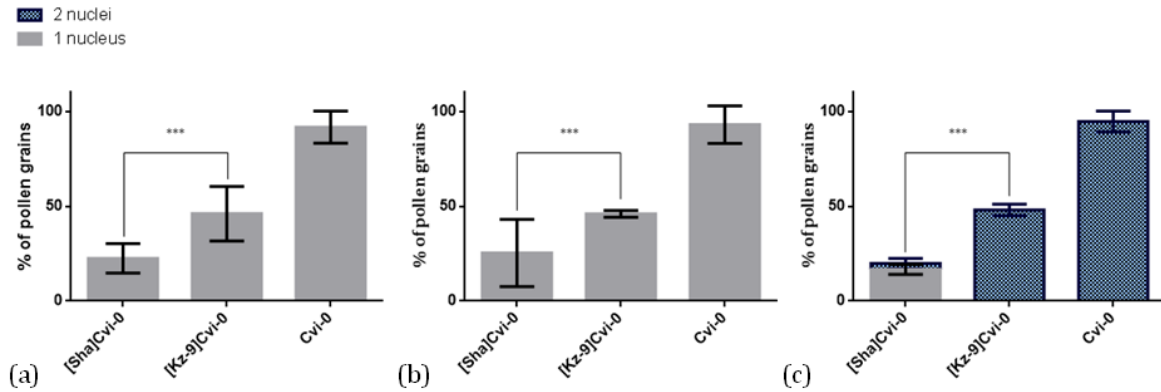
Figure 2.13: Counting of pollen grains presenting generative nuclei marked with GFP. Floral buds of sterile ([Sha]Cvi-0) and fertile ([Kz-9]Cvi-0 and Cvi-0) lines with the pTIP5;1::H2B-GFP were collected, dissected and the pistil size was measured in order to determine the expected developmental stage of the pollen. 25 to 75 pollen grains were counted per stage, genotype, and biological replicate. Three biological replicates were performed ($n=3$). The error bars represent ±SD. Mann & Whitney test detected significant difference between ranks of [Sha]Cvi-0 and [Kz-9]Cvi-0. [Sha]Cvi-0 and [Kz-9]Cvi-0 were hemizygous whereas Cvi-0 was homozygous for the *GFP* transgene (a) pollen mitosis I; (b) binucleate pollen; (c) pollen mitosis II.
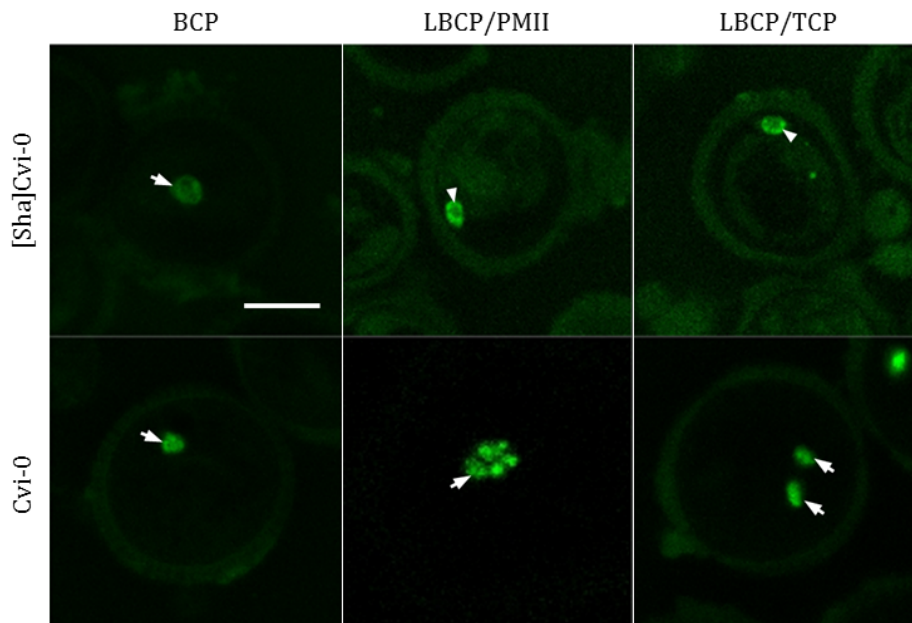
Figure 2.14: Confocal images of GFP-tagged generative and spermatic nuclei in CMS and fertile lines during pollen development. Floral buds of CMS and fertile lines were collected, dissected and the pistil size was measured in order to determine the expected developmental stage of the pollen grains. GFP-tagged generative and spermatic nuclei were observed at different pollen development stages. BCP: binucleate pollen, arrow: generative nucleus; LBCP: late binucleate pollen, arrowhead: generative like nucleus; PMII: pollen mitosis II, arrow: dividing generative nucleus; TCP: trinucleate pollen, arrows: spermatic nuclei. Scale bar: 10 μm.

57

2.3.3 Mitochondria morphology during pollen development

As a mitochondrial gene is responsible for CMS, and because mitochondria may fulfill a specific role in male gametophyte production, I analyzed mitochondria morphology during male gametophyte development. The Cvi-0 accession was transformed with the pM32::mt-GFP construct and the transgene was introduced into the [Sha]Cvi-0 and [Kz-9]Cvi-0 cytolines by crossing, using the T1 plants as the fathers. Mitochondria were observed in developing pollen of T2 and F1 plants. Floral buds were collected and dissected in order to take out the anthers. Anthers were then shredded in DAPI with Citifluor, and mounted between slide and cover-slip. The DAPI staining of nuclei was used to determine the developmental stage.

Typical observations of the mitochondria during pollen development in the three genotypes are presented in figure 2.15. In the Cvi-0 and [Kz-9]Cvi-0 lines, the mitochondria are round shaped and are stationary at the uninucleate and binucleate stages. During the second pollen mitosis they seem to form a network. At the trinucleate stage, the mitochondria are round shaped again, they look smaller and they are mobile. In the sterile [Sha]Cvi-0 cytoline, the observation of the GFP signal led to the grouping of pollen in three classes: (1) "normal" looking mitochondria, as those of Cvi-0 and [Kz-9]Cvi-0 at the corresponding developmental stage; (2) round shaped and "swollen" mitochondria; (3) "ruptured" mitochondria: the GFP is observable in the whole cytosol, indicating that mitochondria released their content into the cytosolic compartment. The number of pollen grains in each class was counted at different developmental stages, and results are synthesized in figure 2.16. For each developmental stage, pollen grains in the four big anthers of one flower from three different individuals were observed. Twenty to seventy pollen grains per stage per genotype per individual were observed.

In [Kz-9]Cvi-0 and Cvi-0, almost 100 % of pollen grains harbors normal looking mitochondria all along development. In [Sha]Cvi-0, half of the pollen grains has normal mitochondria at the uninucleate stage, and this proportion decreases during development down to 3 % of "normal" pollen grains at the late binucleate stage (corresponding to the normal trinucleate stage in fertiles, according to the pistil size as explained in part 2.3.2). In parallel, the class of pollen grains with swollen mitochondria is around 40 % at the uninucleate stage, and it decreases during pollen development while the proportion of pollen grains with mitochondria that released their content into the cytosol increases to finally represent the vast majority of pollen grains at the late binucleate stage. Mann and Withney test was performed at each developmental stage to compare proportions of "normal" pollen. Significant difference was detected between the sterile line and the controls, whereas no significant difference was detected between the two fertile lines.
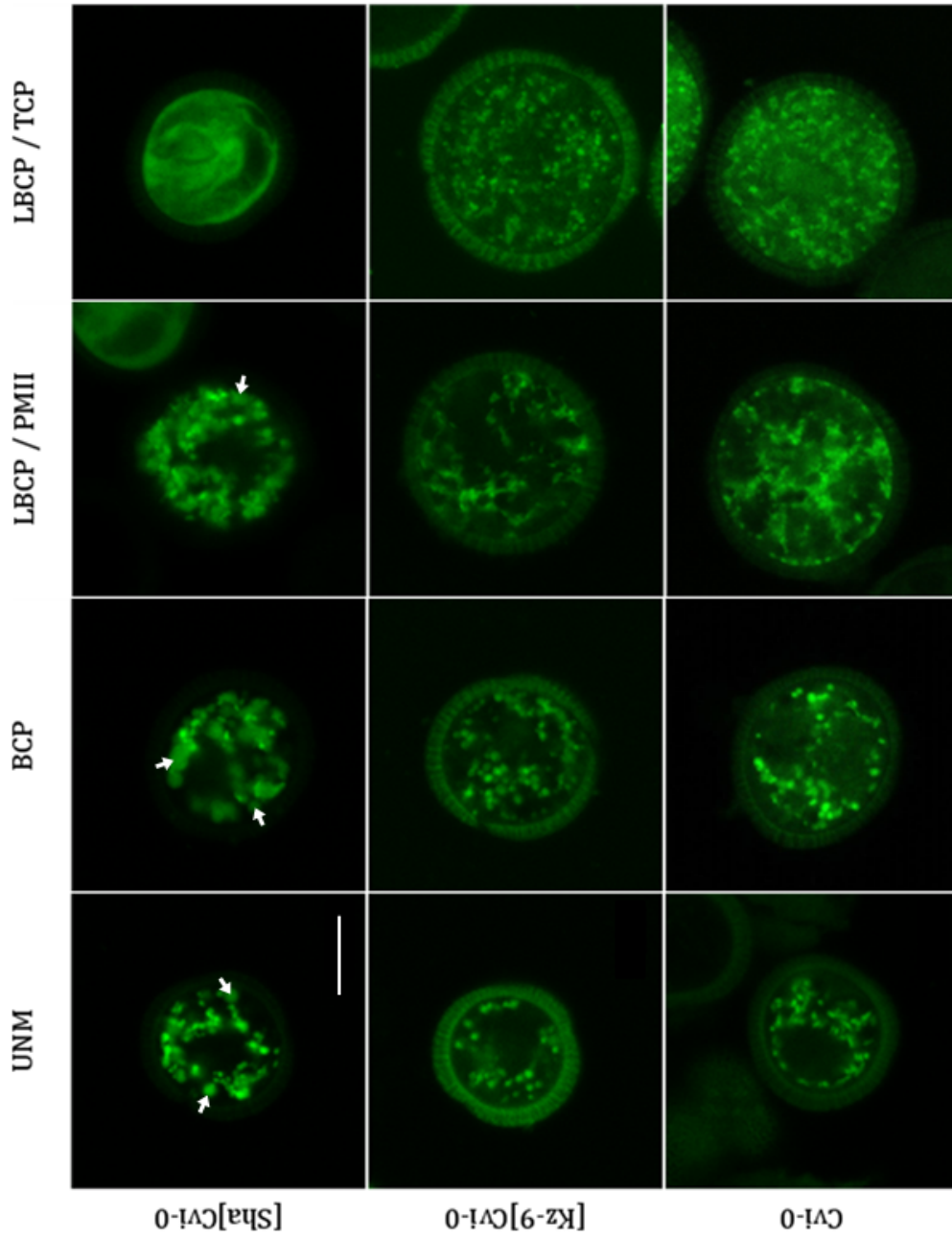
Figure 2.15: Confocal images of GFP-tagged mitochondria in CMS and fertile lines during male gametophyte development. Anthers of floral buds from CMS and fertile lines were dissected and mounted in Citifluor with DAPI. The pollen development stage was determined by observation of the nuclei. Three biological repetitions on different individuals were performed. In the sterile [Sha]Cvi-0 cytoline, swollen (arrows) and ruptured mitochondria (LBCP) were observed. UNM: uninucleate microspore; BCP: binucleate pollen; LBCP: late binucleate pollen; PMII: pollen mitosis II; LBCP: late binucleate pollen; TCP: trinucleate pollen. Scale bar: 10 μm.

These results indicate that prior to pollen abortion, the mitochondria of sterile plants swell and eventually break, releasing their content into the cytosol. This phenomenon is progressive during pollen development, as is the abortion. Mitochondrial swelling is the earliest abnormal event that I detected in male gametophyte development of sterile plants, as it concerned half of the pollen grains already at the uninucleate stage.
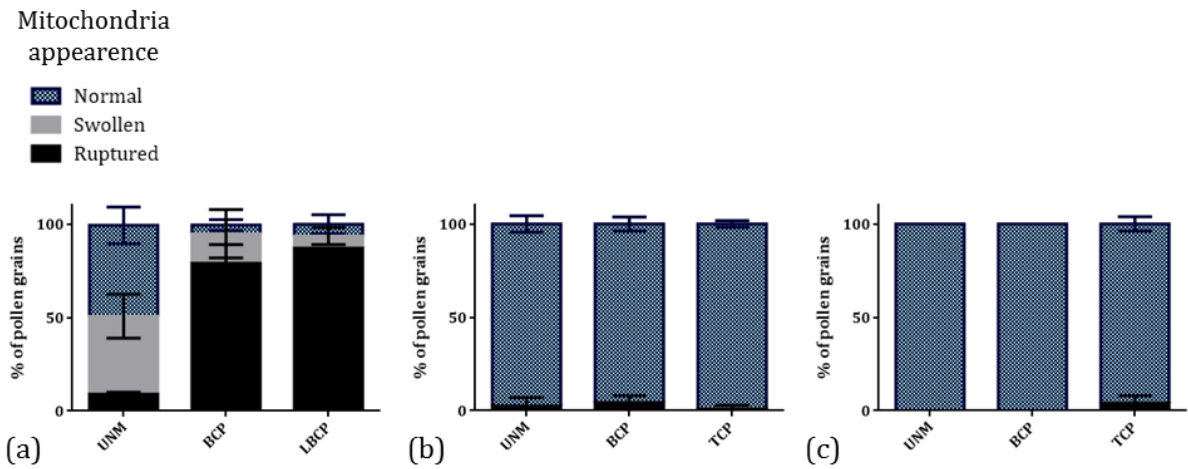
Figure 2.16: Proportions pollen grain classes according to mitochondria morphology in CMS and fertile lines during pollen development. The three classes of pollen grains defined according to the appearance of their GFP-tagged mitochondria - "normal", "swollen" or "ruptured" - were counted in the CMS line [Sha]Cvi-0 (a), and the fertile lines [Kz-9]Cvi-0 (b) and Cvi-0 (c) at different stages of development. Their proportion were calculated after observations of three anthers of a flower from three different individuals ($n=3$). The error bars represent ±SD. 20 to 70 pollen grains were observed per stage, genotype, and biological replicate. UNM: uninucleate microspore; BCP: binucleate pollen; LBCP: late binucleate pollen; TCP: trinucleate pollen.

2.4 Mitochondrial functions in sterile and fertile lines

As already mentioned above, a mitochondrial sterilizing gene induces CMS, and mito-chondria possibly fulfill a special role in pollen development. In addition, my cytological studies pointed a swelling of mitochondria as the first observable defect in the pollen of CMS plants (see section 2.3.3). For these reasons, investigations of the mitochondrial functions in CMS and fertile lines were of special interest. The main function of plant mitochondria is to produce ATP through the OXPHOS system (as explained in section 1.4.1), therefore I verified the proper function of the mitochondrial OXPHOS supercom-plexes with different approaches. Some of these approaches were not feasible specifically in pollen, because the amount of purified pollen that we are able to extract, especially from sterile plants, would not be sufficient for the analyses. Therefore, I performed these analyses on whole plants. I first checked the integrity of mitochondrial OXPHOS complexes with biochemical approaches. Then, I used approaches that allowed *in situ* evaluation of mitochondrial activity, giving access to the specific observation of pollen. I measured the ATP steady state in vegetative tissues and developing pollen in order to confront the commonly accepted but controversial "ATP hypothesis" [177]. Also, as ROS production is inherent to the mitochondrial function, and because an increase of ROS production might be deleterious to the cell (see part 1.4.2), I compared the redox state of mitochondria in CMS and fertile lines. Both last approaches were based on innovative tools: fluorescent sensors allowing the quantification of those two parameters in confo-cal microscopy. They were developed in collaboration with Markus Schwarzländer from Bonn University, and were performed in his Plant Energy Biology laboratory in Bonn. Finally, I measured expression of alternative oxidase (AOX) genes. In collaboration with D. Macherel (IRHS, Angers) we verified the respiration rate as an integrated mitochon-drial function, and examined the AOX capacity on plantlets. The two different types of approaches (on whole plant / specifically in different tissues) allowed the collection of complementary information on mitochondrial functions in the different genotypes.
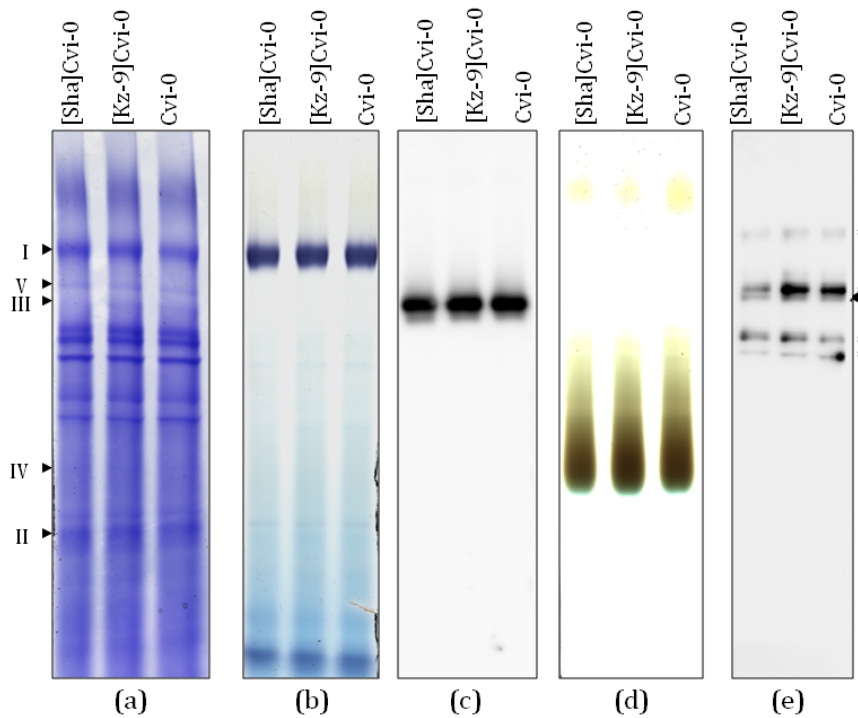
Figure 2.17: In gel determination of mitochondrial complexes integrity. Crude membrane proteins from sterile and fertile flower buds were solubilized in digitonin. After ultracentrifugation, the supernatant was loaded on BN-PAGE and the gel was Coomassie Blue stained (a), immunobloted (c and e) or activity stained (b and d). The position of respiratory complexes are indicated (arrowheads), (b) Complex I detection with NADH dehydrogenase assay, (c) complex III detection in immunoblot with a anti-RISP antibody, (d) complex IV detection with Cytochrome C oxidase assay and (e) complex V detection in immunoblot with anti-ATP-B antibody. The asteriks indicate aspecific bands from plastid proteins, whereas the expected complex V band is indicated by an arrowhead on the right side of the panel.

2.4.1 In gel analysis of respiratory complexes

In order to evaluate the integrity of mitochondrial respiratory complexes in [Sha]Cvi-0, [Kz-9]Cvi-0 and Cvi-0 lines, crude membrane proteins were extracted from unopened floral buds. These proteins were then solubilized in digitonin, and ultracentrifuged before being loaded on BN-PAGE. After migration, different assays were performed: one part of the gel was stained with Coomassie blue as a loading control, complexes I and IV were analyzed *via* in gel activity staining while complexes III and V were analyzed *via* immunoblot assays (with the antibodies against RISP and ATP-B respectively). The resulting gels and blots are presented in figure 2.17.

This experiment did not highlight any obvious discrepancy between the CMS and fertile lines. Therefore, there is no strong complex size or accumulation difference between

the whole plant extracts of the different genotypes. However, a subtle dysfunction of one complex would probably not be detectable by this approach. Then, because I wanted to investigate further a possible stress response induction in CMS line, I evaluated the AOX response.

2.4.2 ATP production in sterile and fertile lines

The ATP steady-state concentration in the cytosol was evaluated in hypocotyl epidermis cells and in developing pollen grains of CMS and fertile lines. To that end, Cvi-0 was transformed with the pUBQ10::ATeam and the pM32::ATeam constructs. I first attempted to determine the profile expression of the sensor with these different promoters. The pollen-specific promoter pM32 does not allow a bright-enough fluorescence of the sensor to quantify ATP in pollen grains. The pUBQ10 promoter allows ATP quantification from the binucleate pollen stage (see figure 2.7). Therefore, the pUBQ10::ATeam construct was introduced into the cytolines [Sha]Cvi-0 and [Kz-9]Cvi-0 by crossing with Cvi-0 T1.

The ATeam sensor is a FRET-based sensor for which the emission properties are changed when ATP binds to it. The higher the YFP/CFP emission ratio gets, the more the sensor is in the ATP-bound form, and thus the more ATP is present in direct proximity of the sensor. For detailed informations on the ATeam sensor, refer to section 4.2.5.5. Ten six-day old, *in vitro* grown, individuals per genotype were used to measure the YFP/CFP ratios in the hypocotyl epidermis, with three image acquisitions for each plant. Eight one month old plants were used to calculate YFP/CFP ratios in pollen grains, with three acquisitions on three big anthers from one individual for each developmental stage. As pUBQ10 promoter is not expressed during early male gametogenesis (see section 2.2.1), ATP content could not be investigated before the first pollen mitosis.

In hypocotyl epidermis, no difference is detected in YFP/CFP ratios between CMS and fertile lines (Figure 2.18a), which is not surprising as CMS plants did not present any growth retardation or any defect in the vegetative tissues. Also, no difference is detectable in the pollen neither at the binucleate stage (Figure 2.18b) between CMS and fertile lines, nor at the late binucleate stage in steriles compared with the corresponding normal trinucleate stage of fertiles (Figure 2.18c). At this latter stage the ratio softly decreases in the sterile line, but it is not significantly different from the ratio in the fertile lines. Thus, there is no evidence of ATP depletion in the pollen of sterile plants during abortion, compared to viable pollen of fertile plants.

2.4.3 Glutathione pool redox state in sterile and fertile lines

The redox state of the glutathione pool was measured in hypocotyl epidermis mitochondria and in developing pollen grains of CMS and fertile lines. To that end, the Cvi-0 line was transformed with the pUBQ10::SHMT-roGFP2-Grx1 construct, that was then introduced into the [Sha]Cvi-0 and [Kz-9]Cvi-0 cytolines by crossing. The roGFP2-Grx1 sensor can be in oxidized or reduced form, and the two forms do not have the same excitation properties. The ratio of the fluorescences emitted at both excitation wavelengths is used to calculate the oxidation state of the sensor. The higher the calculated ratio is, the more the compartment in which the sensor is located is oxidized. For detailed informations on the roGFP2-Grx1 sensor, refer to section 4.2.5.6.

Redox state of the glutathione pool was first investigated in mitochondria of the hypocotyl epidermis of sterile and fertile lines. Ten six-day old, *in vitro* grown, individuals per genotype were used to measure ratios in the hypocotyl epidermis, with three acquisitions per individual. The confocal images were then analyzed with the RRA software from M. Fricker (available on line), in order to quantify precisely the ratios. Regions of interest were determined inside the mitochondria, in order to avoid autofluorescence from cell wall. The average ratio of the different lines in hypocotyl epidermis cells is presented in figure 2.19. I measured a significantly higher ratio, indicating a higher oxidation of the glutathione pool, in the hypocotyl epidermis cells of the CMS line than in those of fertile lines.

The roGFP2-Grx1 sensor was hitherto never used to monitor the glutathione pool redox state in the pollen. In this regard, before the real measurements of redox states in pollen, I first calibrated the experiment and verified the dynamic range of the sensor in the pollen. Anthers were taken out from floral buds and treated either by DPS or DTT in order to bring the sensor to its completely oxidized or reduced forms, respectively. This experiment was performed with trinucleate pollen from Cvi-0. Examples of images taken in these conditions are presented in figure 2.20. When anthers are DTT-treated, the fluorescence intensity of the sensor is very low when excited at 405 nm (that is the oxidized form) and strong when excited at 488 nm. In the merged image, mitochondria are greenish, indicating that the sensor is more in reduced than oxidized form.
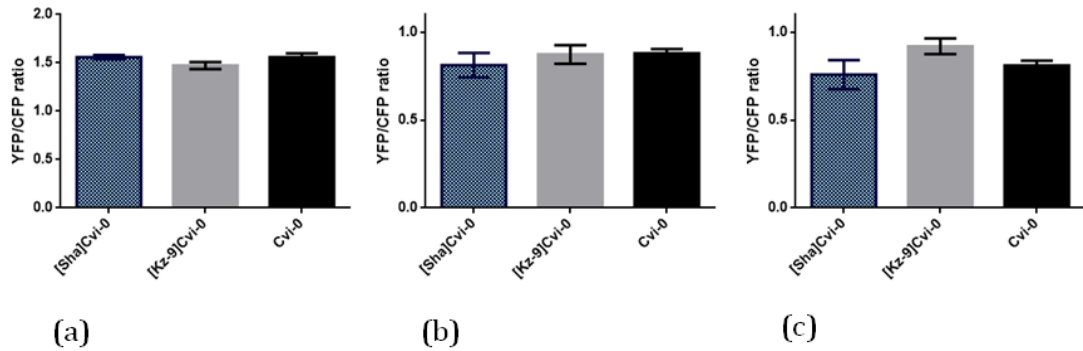
Figure 2.18: Fluorescence ratios of the ATeam sensor in CMS and fertile lines.
Fluorescence ratios of the ATeam sensor were calculated from confocal microscopy images acquired on (a) hypocotyl epidermis from 6-day old plants, (b) binucleate pollen grains or (c) late binucleate (CMS line) and trinucleate pollen grains (fertile lines). (a) Ten independent biological replicates were performed ($n=10$); (b) and (c) eight independent biological replicate were performed ($n=8$). Each bar represents the mean of the calculated ratios, and the error bars represent ±SEM. No significant differences were detected between the ratios in the different genotypes in the tissues and developmental stages considered (Mann and Whitney test, $\alpha= 5$ %). Ratios were calculated with the RRA software from M. Fricker.
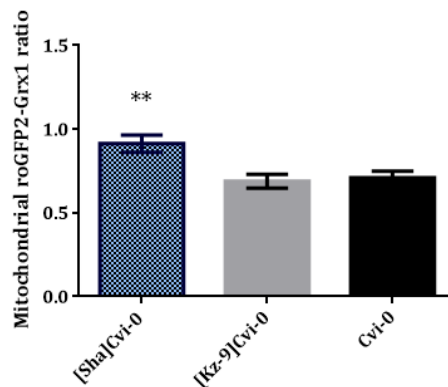
Figure 2.19: Mitochondrial redox state measurement in hypocotyl from CMS and fertile lines. Mitochondrial redox state was measured with the SHMT-roGFP2-Grx1 sensor in confocal microscopy on hypocotyl epidermis from 6-day old plants. Ten independent biological replicates were performed ($n=10$). Each bar represents the mean of the calculated ratios, and the error bars represent ±SEM. Significant difference was detected between the ratios of the sterile ([Sha]Cvi-0) and fertile ([Kz-9]Cvi-0 and Sha) lines (Mann and Whitney tests). Ratios were calculated with the RRA software from M. Fricker.
**$P \leq 0.01$

Oppositely, when anthers are DPS-treated, the fluorescence intensity of the sensor excited at 405 nm is much higher than the one of the sensor excited at 488 nm, resulting in yellowish mitochondria in the merged image. The anthers that are mock-treated (treated with water) present greenish mitochondria, suggesting a prevalence of the reduced form of the sensor in trinucleate pollen grains, as it is expected for mitochondria under non-stressed conditions [164].

Confocal images were analyzed with the RRA software to calculate the fluorescence ratios. As the mitochondrial-targeting of the SHMT-roGFP2-Grx1 construct leaks, leading to some accumulation of the sensor in the cytosol, I measured the ratios in the cytosol, the mitochondria, and the whole pollen grain, by determining appropriate regions of interest (ROI). The average ratios of the different ROI of the calibration experiment are presented in figure 2.21a. The average ratios of fully oxidized and fully reduced form are not significantly different in cytosol and in mitochondria. Moreover, the mock-treated pollen grains have similar ratios to those treated by DTT in these two compartments, supporting the idea that the glutathione pools are near to fully reduced form in normal trinucleate pollen.

Eight one month old plants were used to measure the redox state of the glutathione pool in pollen grains of the different genotypes. Measurements were performed at the late binucleate stage in the CMS line and trinucleate stage in the fertile lines, which corresponds to equivalent pistil size. Measures at earlier stages were technically impossible because when excited at 405 nm, the pollen exine showed higher autofluorescence intensity than the sensor. A silencing phenomenon was observed in pollen grains, so that less than the expected 50 % of pollen grains presented fluorescence. Together with the high proportion of dead pollen at the late binucleate stage in the CMS line, this contributed to the fact that three images could not be acquired for each sterile individual. I thus collected fourteen images from four different individuals in the CMS line. For the fertile lines, three images per individual on the eight individuals were acquired. Then, I calculated ratios in late binucleate pollen grains from the CMS line and trinucleate pollen grains from the fertile lines in cytosol, in mitochondria, and in the whole pollen grain. The average ratios for each compartment and genotype are presented in figure 2.21b. Ratios are significantly higher in the pollen from sterile lines than in the pollen of fertile lines in cytosol, mitochondria and whole pollen grain, despite the high variability observed for the measures from the sterile line. This variability might come from the fact that most of the pollen grains are dying at this late binucleate stage in sterile plants.
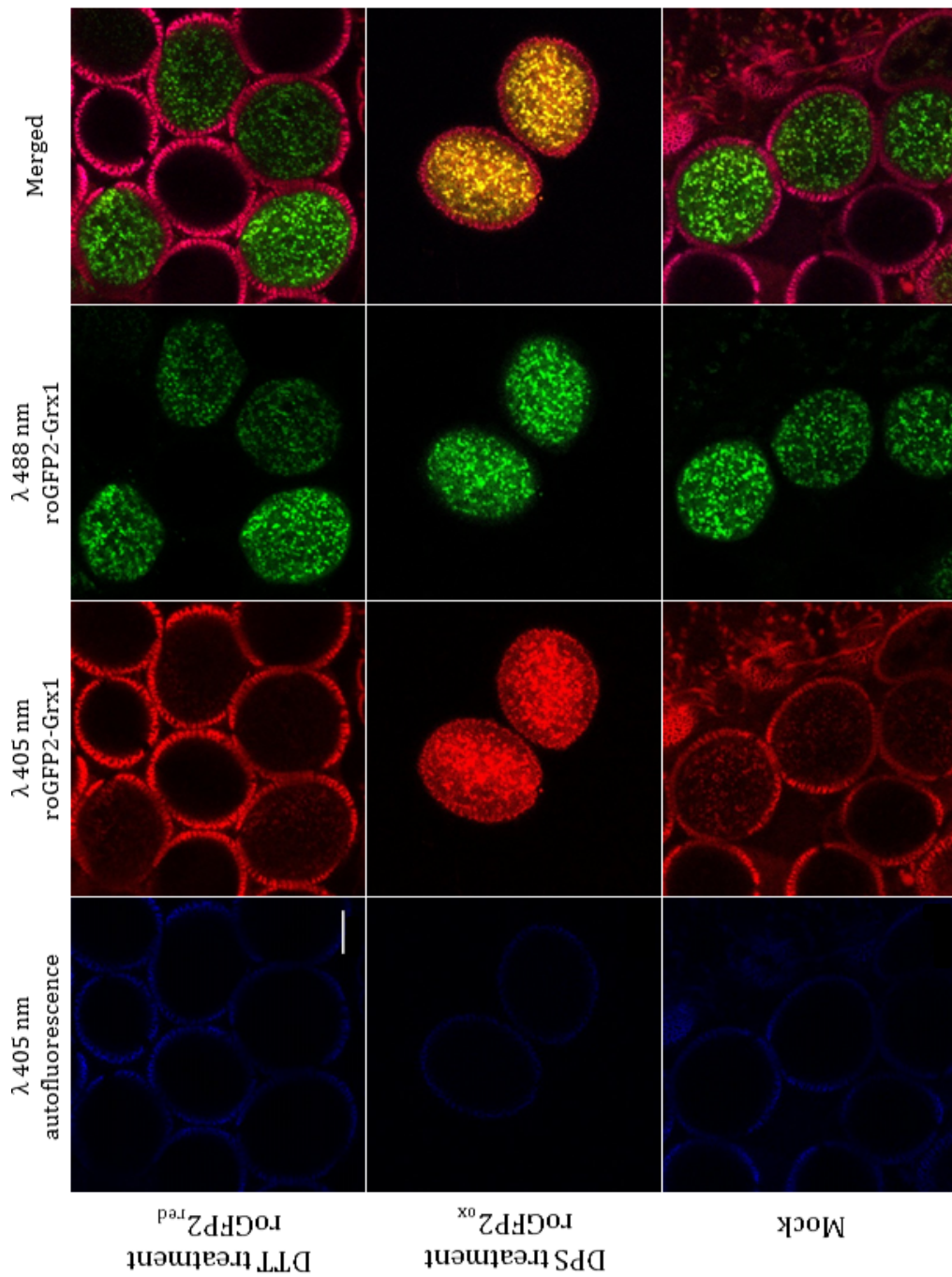
Figure 2.20: Imaging of SHMT-roGFP2-Grx1 in trinucleate pollen grains. Cvi-0 floral buds were collected and dissected in order to take out the anthers, and to mount them in water between a slide and a cover-slip. Calibration was performed by imaging the sensor of DTT-treated (sensor at the fully reduced form) or DPS-treated (sensor at the fully oxidized form) pollen grains. Control was performed with a mock-treatment. Autofluorescence channel was collected in order to take it into account in the analysis. Scale bar: 10 μm.

These results indicate that there is an over-oxidation of the mitochondrial glutathione pool in hypocotyl epidermis (which is a vegetative tissue) as well as of mitochondrial and cytosolic glutathione pools of late binucleate pollen in the CMS line compared with the trinucleate pollen in the fertile lines. In order to study the effect of fertility restoration on this over-oxidation and establish a possible correlation between the redox state and the sterility phenotype, we crossed Cvi-0, [Sha]Cvi-0 and [Kz-9]Cvi-0 plants expressing the sensor with Sha plants also expressing the sensor, independently obtained by transgenesis. The hybrids Sha x Cvi-0 and [Sha]Cvi-0 x Sha are genetically identical, and they possess the sterilizing cytoplasm in presence of all Sha restorer alleles, in the heterozygous state. Because the Sha genotype contains numerous restorer genes [195] we expected that nearby all pollen grains of the hybrid would be restored to fertility by at least one Sha restorer. The hybrid [Kz-9]Cvi-0 x Sha which possesses an identical nuclear background and a non sterilizing cytoplasm was used as a control. The calculated ratios are not significantly different between hybrids carrying the sterilizing cytoplasm in a fertility restoring background and hybrids not carrying the sterilizing cytoplasm, neither in hypocotyl epidermis (figure 2.22a) nor in trinucleate pollen grains (figure 2.22b). These results indicate that the mitochondria are not over-oxidized when fertility is genetically restored, suggesting that the over-oxidation phenotype is correlated to the CMS.
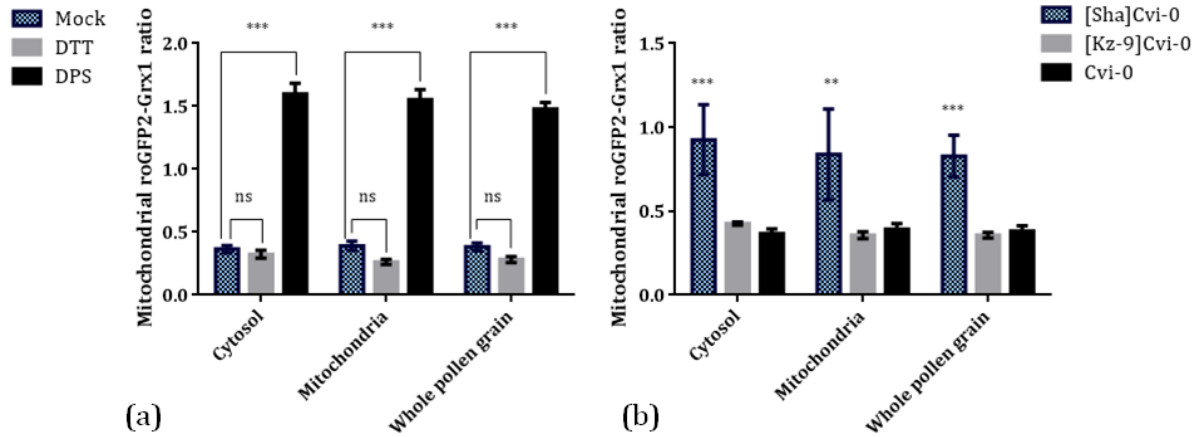
Figure 2.21: Redox state measurement in pollen from CMS and fertile lines. Mitochondrial redox state was measured with the SHMT-roGFP2-Grx1 sensor in confocal microscopy on (a) Cvi-0 trinucleate pollen grains DPS, DTT or mock-treated, and (b) late binucleate (CMS line) and trinucleate (fertile lines) pollen grains. Eight independent biological replicates were performed ($n=8$). Each bar represents the mean of the calculated ratios, and the error bars represent $\pm$SEM. No significant difference was detected between the ratios of the mock and the DTT-treated samples (Mann and Whitney test, $\alpha= 5$ %), while significant difference was detected between the ratios of the sterile ([Sha]Cvi-0) and fertile ([Kz-9]Cvi-0 and Sha) lines in cytosol, mitochondria and whole pollen grain at the trinucleate stage (Mann and Whitney test). Ratios were calculated with the RRA software from M. Fricker.
**$P \leq 0.01$
***$P \leq 0.001$
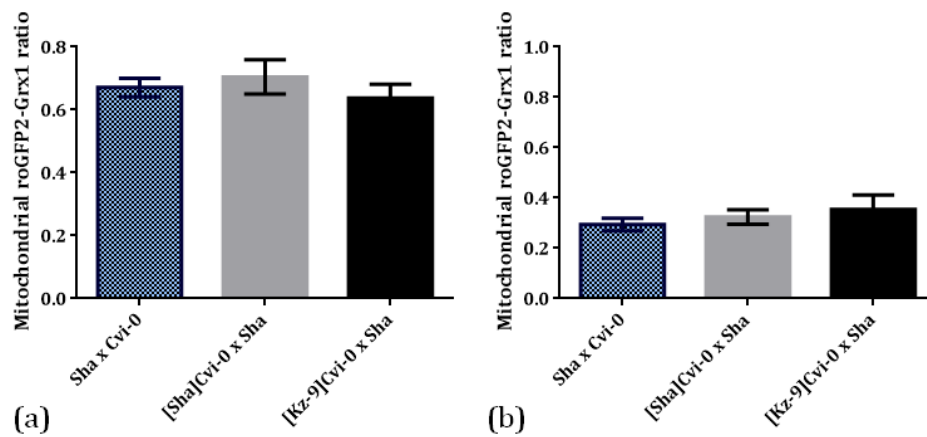
Figure 2.22: Mitochondrial redox state measurement in restored hybrids. Mitochondrial redox state was measured with the SHMT-roGFP2-Grx1 sensor in confocal microscopy on (a) hypocotyl epidermis from 6-day old plants, and (b) trinucleate pollen grains. (a) Ten independent biological replicates were performed ($n=10$); (b) eight independent biological replicate were performed ($n=8$). Each bar represents the mean of the calculated ratios, and the error bars represent $\pm$SEM. No significant difference was detected between the ratios (Mann and Whitney test, $\alpha = 5$ %). Ratios were calculated with the RRA software from M. Fricker. Ratios were calculated with the RRA software from M. Fricker.

2.4.4   AOX response in sterile and fertile lines

I investigated the AOX expression in the different genotypes, as an induction of AOX is known to participate in diverse stress response and in the control of ROS production in plant mitochondria [157]. First, I investigated the AOX response in 6-day old, *in vitro* grown, plantlets as over-oxidation of the mitochondrial glutathione pool was detected in hypocotyl epidermis of sterile plants. *AOX1a* mRNA accumulation was verified with qRT-PCR and normalization was performed on *APT1*, highlighting no mRNA accumulation differences between the genotypes (figure 2.23a.). An immunoblot experiment was realized on mitochondrial extracts from one month old *in vitro* grown plantlets on CMS line [Sha]Cvi-0, fertile maintainer lines [Kz-9]Cvi-0 and Cvi-0 and restored line Sha to check whether the AOX1 and AOX2 proteins were more accumulated in any of these lines (figure 2.23b.). No difference could be detected. On these six day old *in vitro* grown plantlets, the respiration rate of CMS, fertile and restored lines was measured as an indicator of global mitochondrial functioning (collaboration with D. Macherel, IRHS Angers). No significant difference in the respiration rate is detected between the lines. Moreover, the proportion of cyanide insensitive respiration of plantlets do not differ between the genotypes neither. Regarding these results, despite the over-oxidation measured in vegetative tissue and in pollen we could not highlighting an AOX response in the sterile plants.

Then, as over-oxidation of the mitochondrial and cytosolic glutathione pools was detected in pollen grains, I investigated the different *AOX* isoforms mRNAs accumulation. I performed qRT-PCR on total RNA from unopened floral buds in fertile Cvi-0 and [Kz-9]Cvi-0 and CMS [Sha]Cvi-0 lines to quantify mRNA accumulation of *AOX1a*, *AOX1b*, and *AOX1c*. *AOX1a* normalization was performed on *APT1*, because it is an isoform expressed constitutively with a lower expression in male gametophyte. The *AOX1b* and *AOX1c* normalization was performed on *ATSTP2* (*AT1G07340*), because they are preferentially accumulated in the male gametophyte at early stages of development and the *ATSTP2* mRNA is expressed specifically in the male gametophyte at the uninucleate and binucleate stages [15]. The results are presented in figure 2.24. I did not detect any difference in mRNA accumulation of any of these isoforms between extracts from sterile and fertile lines.

In the CMS line, the respiratory complexes are accumulated as in the fertile lines, and the ATP production seems to be equivalent. However, a mitochondrial dysfunction probably induces an increase in ROS production, leading to an over-oxidation of the glutathione pool, in vegetative tissues (hypocotyl epidermis) and in pollen, and is annihilated in restored hybrids. The AOX pathway is not induced in sterile line.

(a)   (b)
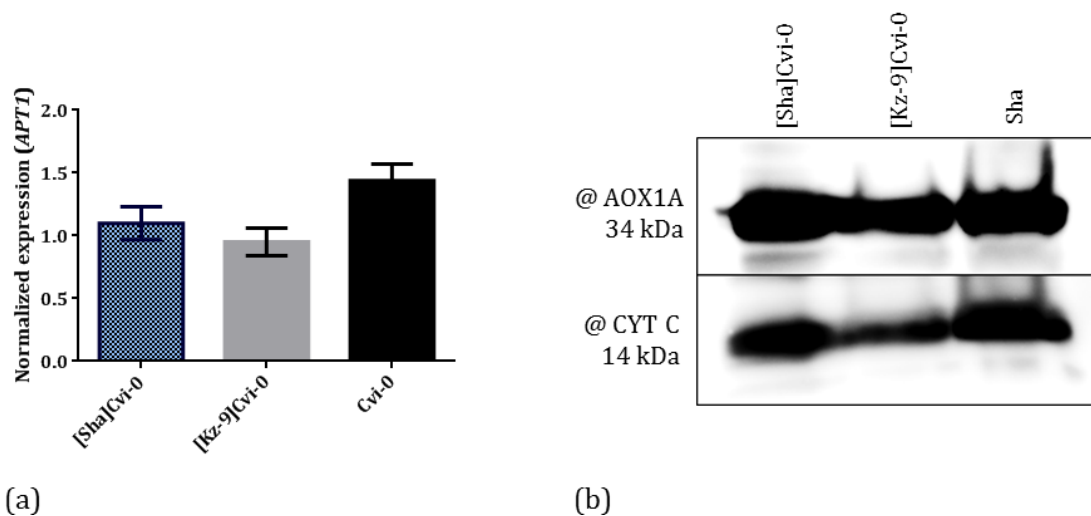
Figure 2.23: AOX response in *in vitro* grown plantlets. (a) qRT-PCR analysis. Total RNAs were extracted from sterile ([Sha]Cvi-0) and fertile ([Kz-9]Cvi-0 and Sha) *in vitro* grown plantlets, and DNase treated. The amount of *AOX1a* mRNA was normalized by the *APT1* mRNA level. The error bars represent ± SEM. Three independent biological replicates were performed ($n=3$). No significant difference was detected between the populations' distributions (Mann and Whitney, $\alpha=$ 5 %); (b) Immunoblot analysis. Mitochondrial proteins were isolated from one month-old *in vitro* grown plantlets and separated on 10-20 % SDS-PAGE. 20 μg of proteins were blotted onto a 0.20 μm PVDF membrane and probed with the AOX1/2 (top) or CYT *C* (bottom) primary antibodies.

(a)   (b)   (c)
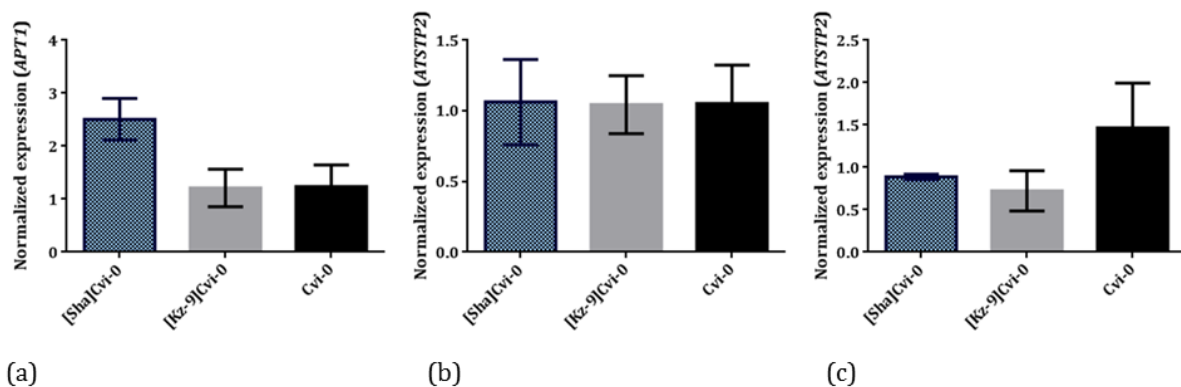
Figure 2.24: AOX response in floral buds. Total RNAs of unopened floral buds were extracted from sterile ([Sha]Cvi-0) and fertile ([Kz-9]Cvi-0 and Cvi-0) lines, and DNase treated. (a) *AOX1a* mRNA accumulation normalized on the *APT1* mRNA level, (b) *AOX1b* mRNA normalized on the *ATSTP2* mRNA level, (c) *AOX1c* mRNA accumulation normalized on the *ATSTP2* mRNA level. The error bars represent ± SEM. Three independent biological replicates were performed ($n=3$). No significant difference was detected between the populations' distributions (Mann and Whitney test, $\alpha=$ 5 %).

71

3 — Discussion

In the previous chapter, I presented the experiments that I realized to better understand the Sha CMS in *A. thaliana*. I first attempted to bring further evidence on the role of the candidate gene *orf117Sha* in this CMS, then I described phenomenons occurring during pollen development prior to and during abortion by comparing fertile and sterile lines, and finally I evaluated some mitochondrial functions in the sterile and fertile lines. The results I obtained will contribute to further explore two questions, puzzling in most CMS systems, that are (1) What criteria should be used to formally identify the sterilizing gene? and (2) How does a mitochondrial gene cause pollen abortion in CMS without having other deleterious effect on the plant fitness?

3.1   Is the *orf117Sha* the sterilizing gene?

As mentioned in section 1.5, no direct genetic evidence such as recombinant or fertile revertant lines are available for the unequivocal identification of the mitochondrial gene responsible of the Sha CMS in *A. thaliana*. Yet, the availability of the wide natural variability allowed an association genetic approach. Although the Kz-9 accession is not a fertile revertant line *stricto sensu*, its non-sterilizing cytoplasm is genetically highly similar to the Sha sterilizing cytoplasm. Polymorphism detection between Sha and Kz-9 chloroplastic and mitochondrial genomes highlighted the presence of *orf117Sha* specifically in Sha, and subsequently in all tested sterilizing cytoplasms [193]. Even though this evidence is not as strong as a recently diverged fertile revertant or a recombinant line, it greatly supports the hypothesis of *orf117Sha* being the CMS-associated gene. With the genetic markers that have been used, it has been calculated that approximately 280 kb, that is over three quarters of the size of the *A. thaliana*'s mitochondrial genome of reference, were covered by the RFLP analysis [193]. Moreover, the high similarity of ORF117SHA with ORF108 that has been proven to induce sterility in other Brassicaceae [69, 90, 91] supports the implication of *orf117Sha* in the CMS. Nevertheless, these findings are not sufficient to definitely eliminate the possibility that still undetected poly-

morphisms between Sha and Kz-9 cytoplasms cause CMS.

In order to strengthen the hypothesis of *orf117Sha* role in the CMS, I attempted to describe its expression, as a prerequisite for validation is to verify that the orf is indeed expressed in sterile lines. Also, as a wide range of identified restorers act on the expression products of the sterilizing gene in other CMS systems [87], I characterized the expression of the *orf117Sha* in maintainer (Cvi-0) and restorer (Sha) backgrounds, in order to look for any difference possibly linked to restoration of fertility. Finally, as the transgenically expressed ORF108 was found to induce pollen abortion in *A. thaliana* [90], I tried to transgenically express the ORF117SHA in order to phenocopy the CMS and provide tools to study it.

3.1.1 Expression of the *orf117Sha*

3.1.1.1 Expression profile of the *orf117Sha* in CMS line

The first observation is that *orf117Sha* mRNA as well as ORF117SHA protein could be detected in the CMS line, showing that it is actually expressed. The northern blot and cRT-PCR analyses of *orf117Sha* mRNA molecules showed a great diversity of mRNA molecules of different sizes. The high size variability detected in northern blot analysis could be partly explained by the presence of several possible promoters regulating the *orf117Sha* transcription initiation. Indeed, it has been shown that multiple mitochondrial promoters are common in *A. thaliana* [205]. Nevertheless, this cannot be the only reason: multiple mRNA sizes were also detected *via* the cRT-PCR approach. Indeed, the 3' end of the *orf117Sha* mRNA was found to be quite stable, but a wide range of different 5' ends were detected, which is a frequent feature for plant mitochondrial genes [196]. Yet, the circularization with T4 RNA ligase is not possible on primary transcripts. Therefore, the high number of transcript sizes is due, at least in part, to the presence of several processed 5' ends, leading to mRNA molecules of different sizes. It is generally assumed that 5' processing is a necessary process to stabilize plant mitochondrial mRNA molecules and generate the mature mRNAs [206].

Mitochondrial gene expression signal hijacking is a common feature in CMS; it is notably visible because a lot of described CMS associated genes are co-transcribed with essential mitochondrial genes and are thus using their mandatory neighbor's expression signals to drive their own expression [52]. F. Budar and G. Pelletier (2001) proposed that the localization of CMS-associated genes nearby essential mitochondrial genes allowed their opportunistic expression and lowered significantly their chances to be eliminated from the genome by recombination events that would lead to the deleterious loss of their

mandatory neighbor gene [68]. The *A. thaliana*'s Sha CMS does not follow this scheme, as no essential gene is co-transcribed with *orf117Sha*. As for not conserved intergenic orfs that were found to be partly transcribed (for example in rice, 36.9 % of orfs in intergenic regions are transcribed without association with any essential mitochondrial gene) [207], the origin of transcription signals used by *orf117Sha* is still elusive. The identification of the promoter(s) used to produce the *orf117Sha* primary transcript(s) would necessitate to determine the position of transcription start(s), for example by comparing the 5' ends identified by cRT-PCR of tobacco acid phosphatase treated RNAs with those of untreated RNAs. Although the *orf117Sha* promoter does not seem to be shared with any conserved mitochondrial gene, the candidate CMS-associated gene shares 1025 base pairs of its 5'UTR region with *cob*, and this putatively brings, immediately upstream of the start codon, a PPR target site that likely favors its translation (figure 3.1).

Indeed, an interesting result obtained by the team during my thesis provides an additional clue for the implication of *orf117Sha* in the CMS. A gene encoding a PPR protein named RFL19, that is predicted to be addressed to mitochondria, was identified by genetic mapping as an active maintainer of the Sha CMS: the [Sha]Cvi-0 plants carrying the EMS-mutated *rfl19* (KO) allele are fertile and the mutated *rfl19* allele co-segregates with pollen viability in this background (S. Durand, C. Camilleri et al., unpublished work). Interestingly, the target site predicted with the PPR code [208] for RFL19 is a region located upstream of the *cob* start codon, which is also present upstream of the *orf117Sha* start codon (see figure 3.1). This predicted target site is currently under investigation by gel shift analyses, as we suspect RFL19 to be involved in the translation of its target mRNAs. The experimental validation that the *orf117Sha* mRNA is one of RFL19's targets would further support the *orf117Sha* as the sterilizing gene. Immunoblots with the ORF117SHA antibody will also be performed on the [Sha]Cvi-0 cytoline, the Sha accession and the [Sha]Cvi-0 cytoline homozygous for the *rfl19* mutated allele (which is fertile).
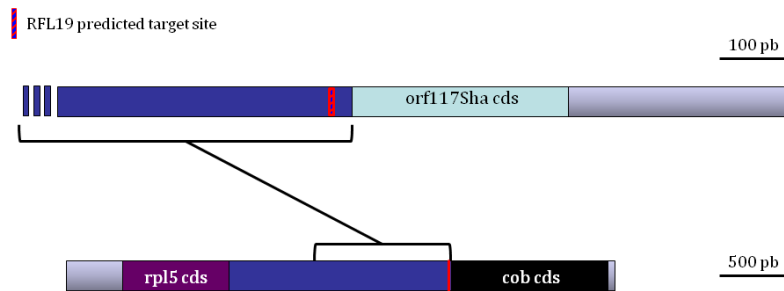
Figure 3.1: The *orf117Sha* probably hijacks the *cob* 5'UTR for its expression. The *orf117Sha* and *cob* genes share the same 5'UTR. The predicted target site of RFL19 is located on this sequence, and we suspect that it is important for the internal recruitment of ribosomes between *rpl5* and *cob* coding sequences, and necessary for the translation of ORF1117SHA.

3.1.1.2 The effect of restoration on the *orf117Sha* expression products

As I showed in section 2.1, qRT-PCR analysis highlighted that the *orf117Sha* mRNA accumulates equally in floral buds and in leaves, and in sterile and restored lines. Also, the different *orf117Sha* mRNA molecules do not notably differ between sterile and Sha restored lines when investigated with cRT-PCR and northern blot approaches. These results suggest that if the *orf117Sha* is really the sterilizing gene, none of the Sha restorer genes acts at the mRNA level on its expression, or alternatively if there is such a restorer, it acts only in specific cell types (the pollen grain at least), which were absent or diluted in the RNA samples studied. Indeed, restorers can have an effect on the whole plant or on a specific organ (for example, anthers or pollen grain) in the different CMS systems already known [78]. As the Sha restoration is multigenic [194, 195] and as identified restorers often act on the mRNA profile of sterilizing genes [209], the most likely hypothesis is the second one. In order to check whether at least one of the Sha's restorers has an effect on the *orf117Sha* mRNA level in the pollen, we are currently performing total RNA extraction from microspores that will be followed by *orf117Sha* mRNA quantification *via* qRT-PCR analysis in [Sha]Cvi-0 and Sha lines.

The detection of the ORF117SHA protein in the sterile but not in the restored line supports the hypothesis of its role in causing the sterility, and of at least one of the Sha's restorers acting at the translational or post-translational level. In order to identify which restorer(s) could act at these levels, immunoblot experiments should be performed on plants carrying individual Sha restorer alleles in the Cvi-0 nuclear background in presence of the Sha cytoplasm. The absence of ORF117SHA detection in any of these lines would indicate that the translation is blocked or the protein degraded by the corresponding restorer. Some of the possible lines meeting these criteria are already available in the team, and mitochondria isolation followed by immunoblot detection of the ORF117SHA

will be performed on them. In parallel, the *RFL19* expression in maintainer and restored backgrounds is under investigation, in order to determine whether a higher expression of RFL19 in the maintainer background could explain a higher accumulation of the ORF117SHA protein in the sterile line.

3.1.2   Functional evidence for the role of *orf117Sha* in CMS

A transgenic approach was used in order to bring functional evidence on the *orf117Sha*'s role in CMS. Because ORF108 and ORF117SHA are highly similar, I also attempted to induce a male sterility by transgenic expression of ORF108. As nowadays, it is technically not feasible to transform *A. thaliana*'s mitochondria, we transformed nuclei with *orf117Sha* and *orf108* fused downstream of a mitochondrial targeting sequence. We transformed Cvi-0, even though this accession presents weak transformation efficiency and its dormancy delays the results by one to three months, because the widely used Col-0 genetic background restores fertility. Therefore, if any of the Col-0's restorers acts on the ORF117SHA protein in the mitochondria, this would possibly interfere with the mitochondria-targeted transgenic sterilizing protein. I first attempted to phenocopy the sterility by using the pUBQ10 promoter, that is constitutive and expressed in the male gametophyte from the binucleate to the trinucleate pollen stages. Then, in order to avoid vegetative or female gametophyte effect of the transgene, I used a pollen-specific promoter that is expressed from the uninucleate microspore to the trinucleate pollen stages (see section 2.2.1): the pM32 [202].

3.1.2.1   Phenocopy attempt with a constitutive promoter

In the transgenic plants expressing the ORF117SHA with the constitutive promoter pUBQ10, very few transformed plants were selected. Only 5 plants were selected that carry the ORF117SHA addressed to the mitochondria. This low success in transformed plants obtention could be explained either by a low transformation efficiency, or by a lethality induction by the transgene when expressed under a constitutive promoter. Indeed, the pUBQ10 promoter is known to be expressed in the embryo [210]. Among these 5 pUBQ10::mt-ORF117SHA selected transformed plants, even though 3 did not produce dead pollen and transmitted the transgene in the expected Mendelian ratio, 2 presented half dead pollen and transmitted very poorly the inserted T-DNA at a ratio of 0 to 1 %, leading to the unfortunate loss of these transformation events. Thus, the insert probably does not only cause pollen lethality in these transgenic plants, but also female gametophyte lethality, which does not exclude an effect of the transgene, as the *UBQ10* gene was found to be transcribed in *A. thaliana*'s ovary [203]. The transgenic plants expressing the

ORF117SHA or ORF108 without mitochondrial targeting signal transmitted the inserted T-DNA in the expected Mendelian ratio, even though some of them presented dead pollen in various proportions, excluding in these cases a direct effect of the transgene on pollen viability. None of the 2 plants expressing the ORF108 with a mitochondrial targeting sequence that I obtained presented dead pollen, nor a bias in transgene transmission.

My results are somehow similar to those reported by Kumar et al. (2012) [90], who produced *A. thaliana* transgenic lines expressing the CMS-associated gene *orf108*. They also found both male and female gametophyte abortion in transgenic plants expressing the ORF108 [90]. However their results and mine also present some differences. Indeed, Kumar et al.'s results indicated that the ORF108 could induce sterility also when it was not targeted to mitochondria. In my experiments, none of the constructs with the *orf108* gene induced male sterility. I did not use the same promoters, nor transformed the same accession, as they performed all their experiments on the Col-0 genotype. They used an anther-specific promoter, which surprisingly turned out to be likely expressed in female gametophyte and embryo as well, highlighting the fact that there is no certainty concerning a promoter specificity as its expression is rarely investigated in all organs and developmental stages.

As it was shown in section 2.2.1, the pUBQ10 promoter is expressed starting from the binucleate stage in pollen. Yet, the abortion phenotype of *A. thaliana* Sha CMS is already visible at the uninucleate microspore stage (see part 2.3.1), suggesting that the sterilizing gene would have an effect at this stage or even earlier in the development. Thus, the absence of sterility in some plants might come from the late expression of the transgene. As some plants present the expected gametophytic sterility phenotype, this hypothesis is not the most likely. In the experiment performed by Y. Duroc et al. (2006) [199], transgenic expression of ORF138 in *A. thaliana* did not succeed in phenocopying the CMS likely because the hydrophobic ORF138 was stuck in the outer mitochondrial membrane of transgenic plants, whereas it is inserted in the inner mitochondrial membrane of CMS plants. Such a wrong sub-localization is unlikely to occur with the ORF117SHA and the ORF108, as (1) the proteins do not have predicted trans-membrane domains, and (2) some plants presented a gametophytic sterility with the ORF117SHA in our experiment and with the ORF108 in experiments from Kumar et al. (2012). Also, it is extremely unlikely, if not impossible, that the gametophyte lethality in both plants expressing the mitochondria-addressed ORF117SHA was linked to the T-DNA insertion by itself. Indeed, such gametophytic mutational effect of T-DNA insertion is not frequent, as it was highlighted by T-DNA insertion collection screening to isolate male gametophyte defective mutants. For example, Bonhomme et al. (1998) identified 8 putative male gametophyte mutants out of 15,861 transgenic lines, which represented 0.2 % of the screened

collection [211]. Thus, the gametophytic sterility phenotype observed in two transgenic plants likely resulted from the expression of the *orf117Sha* inserted gene. Finally, I observed that plants expressing the mitochondria-targeted redox sensor roGFP2-Grx1 under the pUBQ10 promoter (see section 2.4.3) often presented silencing phenomenon in the pollen grains, even though the sensor was properly expressed in vegetative tissues. Therefore, the same phenomenon could occur in plants expressing the mitochondria-targeted ORF117SHA or ORF108 with the pUBQ10 promoter, which could be an explanation for the low proportion of transgenic plants displaying the expected phenotype.

3.1.2.2 Phenocopy attempt with a pollen-specific promoter

The results that were obtained with the pM32 promoter did not bring more evidence about *orf117Sha*'s function in CMS, although the use of this promoter was expected to alleviate some of the drawbacks detailed in the previous section: it is active from the earliest stage of pollen development, and is not, from my experience, subjected to silencing. Transgenic plants presenting dead pollen in varying amounts transmitted the insert in the expected Mendelian ratio, ruling out the role of the transgene in pollen lethality for these plants. As it was detailed in section 2.4.2, the pM32 promoter did not allow enough expression of the ATeam sensor to perform quantification of fluorescence. I concluded that this promoter is somehow weaker that expected, and that the ORF117SHA might not be accumulated enough in pM32::mt-ORF117SHA lines to cause sterility. Expression profile of the pM32 promoter was previously investigated using a GUS reporter [202], which might have led to an overestimation of its activity. Indeed, GUS staining is perfectly suited for weak promoter activity detection because its enzymatic activity allows signal amplification [212].

3.1.2.3 Conclusions and perspectives of the transgenic approach

The transgenic approach does not allow us to investigate further the role of *orf117Sha* in sterility by structure-function analysis for the moment, as the selected T1 plants were scarce and the transformation events lost in the T2 generation. Moreover, the induced phenotype was not shared by all the positive selected T1 plants, which would impede structure-function analysis. If some studies succeeded in inducing a male sterility with transgenic expression of CMS-associated genes [90, 89, 116, 213], other failed even though the candidate gene was proven to be the sterilizing gene [199, 214]. Other studies obtained a semi-sterility, with only a part of T1 individuals having a sterility phenotype. For example, *A. thaliana* plants transformed with the mitochondria-targeted ORF456 from pepper presented 45 % of T1 plants with a sterility phenotype, which were those with

the highest *orf456* mRNA level [127]. Therefore, the results I obtained during this study do not exclude the *orf117Sha*, even though they bring only weak support to its role in CMS.

We are currently transforming Cvi-0 plants with a new construct carrying the protein ORF117SHA fused to a GFP and addressed to the mitochondria under the pUBQ10 promoter (named pUBQ10::mt-ORF117SHA-GFP). The GFP fusion will allow us to verify that the ORF117SHA is properly expressed and localized in mitochondria and whether its expression is silenced in the pollen of (some) transgenic lines. In addition, it will allow to check whether the presence of the ORF117SHA (fused to GFP) is associated to mitochondria swelling and rupture in transgenic lines (see section 2.3.3). Also, additional transformation experiments of Cvi-0 with the pUBQ10::mt-ORF117SHA construct should allow us to collect new plants presenting dead pollen associated with a segregation bias, which would further strengthen the causal effect of ORF117SHA in the induced phenotype.

Still, plants presenting a sufficient expression of the ORF117SHA addressed to mitochondria specifically in male gametophyte would be extremely interesting to collect transgenic plants inducing male but not female gametophyte lethality. Indeed, an effect on the female gametophyte impaired the study of transgenic plants with the pUBQ10 promoter as we could not collect any T2 plant carrying the transgene. Some characterized promoters showed to be expressed specifically in the developing pollen grain: it is the case for the *AtXYLP3* promoter [215], the MSP1 promoter [216], as well as the *At5G17340* gene promoter [217]. Furthermore, transcriptomic analyses showed that the three genes *AtXYLP3*, MSP1 and *At5G17340* are more transcribed than the UBQ10 gene at the uninucleate microspore and binucleate pollen stages [15]. The *AtXYLP3* is the gene for which expression was much higher than UBQ10 from the uninucleate microspore to the tricellular pollen stages [15]. After checking of their expression profile with a GFP reporter, these promoters could be used to drive expression of the ORF117SHA addressed to the mitochondria. If results show more reliable induction of gametophytic pollen abortion, accompanied with the cytological symptoms of the CMS described in this study, a structure-function study of the ORF117SHA would become feasible. This would also open up opportunities for the use of antigen-tagged ORF117SHA to compensate the poor quality of the anti-ORF117SHA antibody in biochemical studies.

3.1.3 Concluding remarks on the role of the *orf117Sha* in male sterility

In this part of my thesis work, I tried to bring further evidence to support the role of *orf117Sha* in CMS. The transgenic approach gave heterogeneous results with the pUBQ10 promoter and showed no sterility induced phenotype with the pM32 promoter, but these results could be explained without rejecting *orf117Sha*'s role in CMS. Therefore, it would be interesting to further explore this approach with new constructs using different promoters for which we would have checked a strong expression in the male gametophyte all along pollen development. The use of a chimeric *ORF117SHA-GFP* coding sequence would allow following protein expression in the different tissues. Should the phenotype induced by the chimeric protein be similar to that induced by ORF117SHA, it would constitute a valuable tool in structure function experiments. The *orf117Sha* is transcribed but no difference between restored and sterile lines could be detected in whole plant RNA expression profile. We are currently investigating a possible effect of restoration on *orf117Sha* mRNA specifically in the pollen. The *orf117Sha* is translated in the sterile line and the protein is not detected in the Sha restored line, supporting the hypothesis that at least one Sha restorer gene acts on ORF117SHA accumulation. The link between fertility restoration and ORF117SHA accumulation needs to be strengthened by analyzing [Sha]Cvi-0 plants homozygous for the *rfl19* mutated allele, and [Sha]Cvi-0 plants carrying individual Sha restorer alleles. Taken together with the association genetics experiments, the fact that the only detected polymorphism between Kz-9 and Sha mitochondria was the *orf117Sha*, and the high protein similarity with the ORF108, even though there is no formal evidence for the sterilizing gene definitive identification, still point towards the *orf117Sha*. The whole mitochondrial genome sequencing and assembly of the Kz-9 and Sha accessions is in progress in the team, and any other candidate gene that escaped previous analyses should be detected soon. Moreover, further analyses on *RFL19* function could provide further support for the *orf117Sha* as the sterilizing gene.

3.2 How does a mitochondrial gene cause pollen abortion in CMS?

As it was detailed in section 1.4.4, several, non mutually exclusive, hypotheses are proposed to explain pollen abortion in CMS systems. The "ATP hypothesis" proposes that an energy depletion, due to a deficiency in ATP production, causes pollen abortion. Under another hypothesis there could be an interaction of the sterilizing protein with a still unknown X-factor, specifically in the pollen grain and/or the tapetum, with deleterious consequences. Also, a specific role of mitochondria in pollen production could be defective in CMS lines. Finally, a ROS burst in mitochondria would induce PCD and pollen abortion.

The *A. thaliana*'s Sha CMS system is gametophytic: the primary events leading to pollen abortion take place in developing pollen. Most of the studied CMS are sporophytic, with primary events leading to pollen abortion taking place in the tapetum, whereas few gametophytic CMS have been studied. The rice gametophytic HL-CMS was deeply explored, and a model was proposed to link molecular interaction between the CMS protein with a component of the mitochondrial complex III and pollen abortion [176]. Briefly, the product of the sterilizing gene, ORFH79, interacts with a nuclear-encoded subunit of the mitochondrial complex III and decreases its activity. The proposed model postulates that a consequent decrease of ATP concentration and a ROS burst would act together as retrograde signals that inhibit cell-cycle related gene expression and eventually block the second pollen mitosis. Therefore in this model, the sterility protein ultimately triggers a signal that blocks pollen at a definite step of its development.

3.2.1 Chronology of pollen death

Male gametophyte development in angiosperms is a complex process, and many steps could be affected that would lead to pollen abortion. In this study, I described events taking place prior to pollen abortion with the aim to better understand the cause of pollen death. In the first place, I determined the pollen developmental stage at which pollen grains aborted, and then I described some events occurring before abortion with cytological approaches.

3.2.1.1 Developmental stage of pollen abortion

The developmental stage at which abortion occurs was identified in order to possibly determine a critical step that would be affected in this CMS. The staining of nuclei and

counting of pollen grains with different phenotypes in the anthers showed that pollen grains with abnormal phenotype are already present at the early binucleate microspore stage, and that a decrease in pollen viability occurs during the binucleate stage. At the expected trinucleate stage, almost all pollen grains are dead and the few survivors have collapsed cytoplasm as if they would die soon. Most of the pollen grains seem to arrest their development at the binucleate stage, and they degenerate until the late binucleate stage, at which pollen grains harbor two nuclei located against the pollen wall. Considering the pistil and floral bud size, the late binucleate stage in the CMS line corresponds to the trinucleate stage in the fertile lines, suggesting that pollen grains that are still alive at the stage when they should enter the second pollen mitosis do not divide their germ cell.

The abortion stage varies from one gametophytic CMS to another: pollen grains from Boro-II rice CMS abort at the trinucleate stage [116], whereas those from HL-type rice CMS abort at the binucleate stage [176], even though their CMS-related genes share 98 % homology [65]. In common bean CMS the abortion starts at the tetrad stage [218]. Therefore, there is no critical male gametophyte developmental stage that would be impaired in every gametophytic CMS. This might be due to different mechanisms being involved in each CMS system, or it might also come from differences in CMS gene expression profiles, or from the presence of a specific partner for each sterilizing gene at different developmental stages. Finally, there might be a physiological defect that would accumulate along male gametophyte development and eventually lead to pollen abortion. The accumulation of such a deleterious effect could be faster or slower in the different CMS systems or even in different nuclear backgrounds or environmental conditions. In this case, the critical level of the deleterious effect required for pollen abortion would be reached at different stages, leading to variability in the stages of pollen death in the different situations. The rice BT- and LD- type CMS support this hypothesis: the abortion stage of pollen grain in these two CMS is the trinucleate stage, but it is delayed in LD-CMS. Interestingly, both CMS systems are linked to the presence of the *orf79*, which has a lower expression in LD-type CMS [118]. In *A. thaliana*'s Sha CMS, as pollen grains start to undergo abortion at the binucleate stage, I assumed that defects leading to male sterility start at the first pollen mitosis or earlier. Indeed, using a GFP specifically tagging the nuclei of germ and spermatic cells, I found that about half of the microspores did not undertake the first pollen mitosis in CMS plants (see section 2.3.2)

3.2.1.2 Description of events occurring prior to pollen abortion

As we expect that CMS comes from a mitochondrial dysfunction, and because mitochondria are highly dynamic organelles with different shapes in distinct tissues and developmental stages, I investigated *in vivo* mitochondrial shape in developing pollen grains from CMS and fertile lines with transgenic plants expressing a GFP targeted to mitochondria [219], with the pM32::mt-GFP construct. In the CMS line there is a heterogeneity in mitochondria appearance all along pollen development: some pollen grains presented normal looking mitochondria, whereas others presented either swollen or ruptured mitochondria (see section 2.3.3). As pollen presenting swollen mitochondria proportion decreases while pollen with ruptured mitochondria increases, it seems logical to assume that mitochondria swell before rupture. At the binucleate and late binucleate stages, only few pollen grains presented normal mitochondria. Mitochondrial swelling prior to cell degeneration and pollen death was reported in tapetal cells from Ogura CMS in *B. napus* [184], from maize CMS-T [187], and from CMS found in an alloplasmic cross between *Glycine max* and *G. soja* [220]. In both last cases, the morphological change of mitochondria from normal to swollen is progressive during the development, similarly to what I observed in developing pollen grains from *A. thaliana*. Another case of mitochondrial swelling in pollen grain is the self incompatibility response in *Papaver rhoeas* [221]. Mitochondria morphology change from normal to swollen has been reported as an early indicator of cell death in plants [222], as it will be detailed in section 3.2.3.

Concomitantly to mitochondria swelling, an arrest in pollen development seems to occur. About half of the pollen grains in anthers of transgenic plants with the pM32::mt-GFP construct did not present normal looking mitochondria in the CMS line at the uninucleate microspore stage. Interestingly, this corresponds to the proportion of microspores that do not undertake the first pollen mitosis, after my results with transgenic plants specifically expressing a GFP targeted to the nuclei of germ and spermatic cells. Similarly, the proportion of pollen grains that could undergo the second pollen mitosis corresponds to that of pollen grains with normal mitochondria at the late binucleate stage. It seems therefore that the pollen grains that do have swollen or ruptured mitochondria stop their development. These results suggest that normal mitochondria are necessary for the pollen mitoses, and that the cells stop their development as soon as their mitochondria changed their morphology. In order to confirm this hypothesis, transgenic plants expressing two different fluorophores, one targeted to the germ lineage nuclei and the other one targeted to the mitochondria, would allow a simultaneous observation of these two events and strengthen the link between mitochondrial morphology change and cell cycle arrest.

Finally, I observed that propidium iodide stained pollen grains present black dots starting from the binucleate stage whereas none was observable in fertile lines. At the uninucleate microspore stage, the large vacuole is detected in all lines as a black region, as there is no propidium iodide stain in it. Therefore, the black dots that are detected in sterile line could correspond to vacuoles. The possible vacuolization of pollen grains from *A. thaliana* could be early signs of collapsing, as it was observed by cytological approaches in other CMS systems [127, 187, 220] and in the self incompatibility response in *P. rhoeas* [221].

The first detectable phenotype in the pollen of CMS plants is a change in mitochondria morphology, which starts at the uninucleate microspore stage, or earlier, and is progressive until the late binucleate stage at which almost all mitochondria ruptured. Moreover, the arrest of pollen development occurs at the uninucleate microspore stage for half of the pollen grains, and at the binucleate stage for the other half. Taken together, these results are compatible with a default in mitochondria physiology as the source of a deleterious effect that would accumulate in pollen grain. Its first observable consequences would be the swelling of mitochondria and arrest of pollen cell cycle, and it would proceed until the mitochondria rupture and pollen death.

3.2.2 Physiological modifications in sterilizing mitochondria

As it was detailed in sections 1.4.1 and 1.4.2, the main function of plant mitochondria is to produce energy *via* respiration. Moreover, the commonly accepted hypothesis to explain CMS is the "ATP hypothesis" (see section 1.4.4), which postulates that a deficiency in ATP production would lead to pollen abortion because male gametogenesis is highly energy demanding. For these reasons, I investigated the ATP steady state content in developing pollen grains and some vegetative tissues in sterile and fertile lines. Also, as the mitochondrial genome principally contains genes encoding subunits of the OXPHOS complexes, I investigated the integrity of these complexes in the sterile and fertile lines in order to seek for any defect in the CMS line. Finally, I checked different features relative to mitochondria functions such as ROS production, AOX response and respiration rate.

One challenging technical issue in addressing pollen mitochondria functioning is to collect enough material to analyze general mitochondrial functions on one hand, but also to collect information on mitochondrial functions specifically in the pollen grains on the other hand. As I have shown that the candidate sterilizing gene is expressed in reproductive and in vegetative tissues (see section 2.1), as in many other CMS systems, it was relevant to characterize mitochondria functions in vegetative tissues in CMS and fertile lines: a possible effect due to the expression of the sterilizing gene could be expected in

this accessible and abundant material. Therefore, I investigated general mitochondrial functions such as respiratory complexes integrity, respiration rate and the AOX response on whole plant mitochondria or young *in vitro* grown plantlets. Now, as CMS is characterized by the male specificity of the phenotype, comparison of mitochondrial function in the pollen grain and in vegetative tissue was interesting, in order to possibly highlight a difference that could explain this phenotype specificity. In this regard, the fluorescent sensors allowing *in vivo* and single cell imaging are innovative tools that gave us access to informations hitherto unattainable.

3.2.2.1 Challenging the ATP hypothesis

In order to experimentally confront the "ATP hypothesis" in *A. thaliana* Sha CMS, I quantified the ATP steady-state in the cytosol of pollen grains and hypocotyl epidermis in fertile and sterile lines with the FRET-based ATeam sensor. As this fluorescent sensor imaging is done with confocal microscopy, it allows *in vivo* and in single cell measurement [223]. For these reasons, this sensor was particularly suited for ATP steady-state measurement in cells from CMS and fertile lines. No significant difference in ATP level was detected in hypocotyl epidermis from the CMS and fertile lines, which is not surprising since the plant has no growth retardation. Most relevant, ATP levels in the pollen of sterile plants did not significantly differ from that of fertile plants, neither at early binucleate nor at late binucleate stages compared with the corresponding binucleate and trinucleate stages, even though the rare measurable pollen grains already have a dying phenotype and swollen or ruptured mitochondria at this latter stage in steriles (see section 2.3.3). These results strongly suggest that a decrease in ATP production leading to energy depletion is not likely to be the primary cause for pollen abortion in *A. thaliana* Sha CMS. Therefore, other mitochondrial (dys)functions should be involved in order to explain the CMS phenotype.

3.2.2.2 Mitochondrial dysfunctions in CMS

I first investigated mitochondria functions on whole plants. No clear difference in accumulation or size of mitochondrial respiratory complexes I, III, IV and V was detected by immunodetection or in gel assay on BN-PAGE between the CMS line and the fertile ones. Therefore, it seems that, should the sterilizing protein interact with any of the respiratory complexes, it does not markedly modify its accumulation or its apparent size. In rice HL-CMS, even though the ORFH79 was found to interact with one of the complex III subunit and to decrease its activity, no band shift of complex III could be detected in BN-PAGE [176]. Also, respiration rate was measured in CMS and fertile lines, and

was found to be not altered in the CMS line, indicating a normal global function of CMS mitochondria in plantlets. This is not surprising, as the vegetative phenotype of CMS plants was not distinguishable from that of fertiles in all growth conditions used since the discovery of this CMS. Nevertheless it had to be verified as, in some CMS systems, defects in mitochondrial functions or respiratory complexes could be highlighted on vegetative tissues of sterile plants without being deleterious to vegetative development [176, 175, 123].

The redox state of the glutathione pool was investigated in hypocotyl epidermis cells and pollen from sterile and fertile lines. Taking advantage on the fact that the mitochondrial targeting leaks in the SHMT-roGFP2-Grx1 construct, both mitochondrial and cytosolic redox states of the glutathione pool were measured separately in pollen grains. Over-oxidation of the glutathione pool was detected in the mitochondria and the cytosol in pollen grains of sterile plants at late developmental stages. Unfortunately, measurements could not be performed at earlier developmental stages due to the lower activity of the pUBQ10 promoter and higher pollen autofluorescence of the pollen wall excited at 405 nm. The fact that the glutathione pool was over-oxidized in both compartments of pollen grains at a late developmental stage could be due to the fact that pollen grains were already almost all dead and the survivors, most probably those that could be measured, would die soon. Nevertheless, this over-oxidation was also detected in mitochondria from hypocotyl epidermis cells of sterile plants. Moreover, it is the unique phenotypical difference that I could highlight in vegetative tissues between CMS and fertile plants. Therefore, over-oxidation is unlikely to be a consequence of the cell death process in action in the observed pollen grains. It rather seems that there is a general oxidative stress in the CMS line. Interestingly, in the restored hybrids, the mitochondrial glutathione pool is not over-oxidized in epidermis cells of the hypocotyl. Also, the calculated ratio in pollen grains was not significantly different in restored hybrids carrying the Sha cytoplasm compared with a hybrid with identical nuclear background carrying the Kz-9 non sterilizing cytoplasm, indicating that the effect of the sterilizing cytoplasm on the glutathione redox status was completely annihilated by the presence of Sha alleles. Thus, the over-oxidation of the glutathione pool seems to be related to the sterilizing effect of the cytoplasm. Now, it would be of particular interest to measure the redox status of the glutathione pool on genotypes for which we would be certain that only the sterility mechanism is studied and no other possible effect of the Sha nuclear background. To this purpose, crosses were performed between the [Sha]Cvi-0 cytoline carrying the *rfl19* mutated allele, or other genotypes with limited Sha introgressions carrying restorer genes in the Cvi-0 nuclear background, and Cvi-0 transgenic plants expressing the SHMT-roGFP2-Grx1. However the silencing of the sensor expression did

not allow fluorescence measurements in the hybrids. Nevertheless, over-oxidation of the glutathione pool is the only phenotype shared by vegetative and pollen cells of plants carrying the sterilizing cytoplasm, and it seems to be linked with the sterility phenotype, although this correlation needs to be further consolidated. Yet, in vegetative tissues, the sterilizing cytoplasm has no further deleterious consequence that I could detect, whereas in pollen both over-oxidation and abortion are observed. As restoration of fertility seems to "cure" over-oxidation both in vegetative tissues and pollen, it is tempting to relate this observation with the "male specificity paradox" of the CMS phenotype: why is the effect of the sterilizing gene on mitochondria limited in vegetative tissues, whereas in the pollen mitochondria swell until explosion and development stops?

Unfortunately, monitoring redox state at earlier developmental stages was not possible as autofluorescence was higher than the sensor fluorescence intensity. Constructs with stronger promoters in the male gametophyte could be built, in order to allow measurement of the physiological parameters earlier in pollen development. Moreover, a silencing phenomenon coupled with the high number of dead pollen at the late binucleate stage in the CMS line rendered difficult to collect a high number of fluorescent pollen grains in CMS line to perform substantial statistical analyses. We are currently realizing new constructs with the promoter from the FKP1 gene from *A. thaliana* (*At4g11820*) [224], reported to drive expression in tapetal cells and pollen from the microspore stage. Unfortunately, the expression profile of this promoter was analyzed *via* GUS staining. Therefore, we will first check the expression profile of the pFKP1::mt-mCherry construct recently obtained in our team, and introduced into Cvi-0 and Sha accessions by floral dipping. Also, the promoter that will be chosen in order to phenocopy the CMS (see section 3.1.2) could be used for this approach as well, as it should ensure a high level of expression in young developing pollen. These tools, combined with the use of appropriate restored genotypes, will allow to draw robust conclusions on the link between over-oxidation of the glutathione pool and the sterility phenotype.

Because *AOX* induction is known to constitute a frequent response to oxidative stress [157], and AOX activity reduces the effects of oxidative stress by preventing ROS accumulation in plant mitochondria [225], I investigated whether AOX response was triggered in the sterile plants. Five genes encode isoforms of alternative oxidases in *A. thaliana*: *AOX1a*, *AOX1b*, *AOX1c*, *AOX1d* and *AOX2*. Transcriptome analysis showed that *AOX1a* mRNA is found in all tissues, but in lower amount in developing pollen grains compared with vegetative tissues and embryo suspensor [15]. In parallel, the *AOX1b* and *AOX1c* are expressed almost only in the developing pollen [15]. Therefore, an induction of the AOX pathway in vegetative tissues with *AOX1a* up-regulation and not in reproductive tissues if *AOX1b* and *AOX1c* expression are not up-regulated could

have explained the different tolerance of the different tissues to oxidative stress. Yet, no difference in mRNA level of any isoform was detected neither in *in vitro* plantlets nor in floral buds. Moreover, the analysis of AOX accumulation with western blot, as well as the AOX capacity measured by cyanide insensitive repiration, did not highlight differences between the genotypes. Thus, it seems that there is no AOX induction or activation in the sterile line in response to over-oxidation of the glutathione pool neither in vegetative nor in reproductive tissues. Hence, the hypothetic differential tolerance of the tissues to oxidative stress cannot be linked to a differential stress response in these tissues, and so the "male specificity" paradox cannot be explained in this way.

3.2.3 Possible mechanisms causing the Sha cytoplasmic male sterility

One relevant discovery made in this study is the fact that the ATP steady-state in pollen grains does not seem to differ between CMS and fertile lines, even though pollen grains had an abnormal phenotype in sterile plants at the observed stages. This result has to be confirmed at earlier stages of development. Nevertheless, from my results an ATP depletion is unlikely to be the cause for pollen abortion. No significant difference was detected in the respiration rate, and in the integrity and accumulation of respiratory complexes, in the vegetative tissues of CMS and fertile lines. However, the over-oxidation of the mitochondrial glutathione pool of vegetative tissues and pollen grains from the sterile line compared with the fertiles is possibly related to the sterilizing effect of the Sha cytoplasm. This over-oxidation is certainly due to higher ROS production in the CMS line, considering the role of glutathione in ROS detoxification (see section 1.4.1). Higher ROS content was observed in mitochondria of vegetative cells of rice plants with the gametophytic HL-CMS. In cotton, it has been shown that the CMS line had increased ROS production, but ROS-scavenging enzymes activities were at lower level than in maintainer lines, while ROS could be eliminated in the anthers of restored lines by an increase of ROS-scavenging enzyme activities compared with the CMS line [226].

In the *A. thaliana* Sha CMS system, it seems that over-oxidation of the glutathione pool, or its primary cause, is well tolerated in vegetative tissues whereas it ultimately leads to pollen death. Therefore, the puzzling "male specific paradox" of CMS systems translates into the following question: if the oxidative effect of the Sha cytoplasm is indeed related to its sterilizing effect, how a mitochondrial dysfunction with the same over-oxidative effect in different cell types would have so different consequences on cell fate?

Several hypotheses can be proposed to attempt addressing this question. The first one

implies a signaling defect specifically in the pollen of CMS lines. Mitochondria are known to have a role in cell cycle [227]. Moreover, even though an excess of ROS is deleterious to the cell, they are also necessary for the control of many biological processes [228]. Recent reviews suggested that ROS would play a role in reproductive development [229, 172]. It is postulated that ROS, RNS and antioxidant proteins could allow the switch from mitosis to meiosis, and regulate different steps of gametogenesis. Thus, a ROS signaling could be necessary in the male gametophyte development, and any ROS imbalance could lead to the arrest of development and subsequent abortion. In *A. thaliana* Sha CMS, the over-oxidation of the glutathione pool probably reflects an imbalance between the ROS producing and scavenging capacities that could lead to a confused signaling pathway in male gametophyte development and subsequent development arrest. However, the above hypothesis is not completely satisfying. Indeed, the progressivity of mitochondrial morphology modification and of pollen development arrest, as both pollen mitoses can be canceled, suggests that a progressive physiological defect rather than a signaling defect at a precise developmental step is involved in the CMS.

Mitochondrial glutathione pool is over-oxidized in the CMS line, and not in the restored hybrids carrying Sha restorer alleles. This over-oxidation might be due to an interaction of the sterilizing protein with one mitochondrial complex subunit, as it has been shown for ORFH79 interacting with complex III in rice HL-CMS [176], and WA352 interacting with complex IV in rice WA-CMS [89]. However, no evidence of such interaction is available in *A. thaliana* Sha CMS yet. The swollen appearance of mitochondria resemble the phenotype induced by heat or oxidative stress [222]. Thus, the mitochondrial morphology change in pollen grains from the CMS lines could be related to an oxidative stress, highlighted by the over-oxidation of the glutathione pool. In a study of *A. thaliana* protoplasts treated with heat stress, it was shown that mitochondrial morphology change is an early indicator of cell death, and was linked to the opening of the mitochondrial permeability transition pore. The mitochondrial permeability transition (MPT) ultimately lead to rupture of the outer mitochondrial membrane and release of the proteins located in the intermembrane space (such as Cytochrome C) that are signals triggering cell death [222]. In *A. thaliana*, it would be interesting to treat anthers of the CMS line with CsA, that is an inhibitor of the permeability transition pore, in order to challenge this hypothesis.

Yet, as tempting as the hypothesis of an oxidative stress leading to pollen abortion in *A. thaliana* Sha CMS could be, it is still not clear why oxidative stress in vegetative cells would not induce mitochondria swelling and cell death, whereas it would be the case in the male gametophyte. The male gametophyte could be more sensitive to oxidative damage, as it is reflected by some studies. For example, triple mutant plants with

deletion of NADPH-dependent thioredoxin reductases *NTRA* and *NTRB* and cytosolic Glutathione reductase 1 *GR1* present *ntr1/gr1* pollen lethality after gametogenesis whereas the female gametophyte is not affected [168]. Authors proposed that the male gametophyte might depend on robust redox buffer system, and that pollen grains were over-oxidized in the absence of NTRA and GR1, whereas female gametophyte are better protected with the surrounding sporophytic tissues. Also, it has been proven that pollen presenting over-oxidation of the glutathione pool had germination defects [230], highlighting the importance of this molecule in pollen development. Moreover, proteomic studies on *A. thaliana* showed that mitochondria of reproductive organs seem to have a specialized role in metabolism, such as the maintenance of the mitochondrial redox state [181]. Also, mitochondrial defect leading to ROS accumulation might be more deleterious in the developing pollen grain and tapetum than in other tissues, because they contain a high number of mitochondria. Therefore, a mitochondrial ROS production increase might be much more important in these tissues than in others containing less mitochondria per cell.

3.3   General conclusions and perspectives

As it was already detailed, the only other gametophytic CMS on which the mechanism of pollen abortion was well studied so far is the rice HL-type CMS. In Sha and HL-type CMS systems, an oxidative stress seems to occur on male gametophyte during development. However, some differences were highlighted between these two systems: no modification in any mitochondrial complex activity could be observed in Sha CMS from *A. thaliana*, and no ATP decrease was detected neither. The ROS production likely occuring in Sha CMS might act as a retrograde signal to block the pollen mitoses as it was proposed for HL-CMS, but it seems more likely that a continuous oxidative stress leads to male gametophyte cell death induction. Reproductive organs need strong antioxidant buffer, as plant male reproductive organs seem to be extremely sensitive to oxidative stress. Interestingly, during heat stress male gametophyte development is one of the most affected process. Moreover, the Sha CMS in *A. thaliana* is environment-dependent, as well as many other CMS systems [9]. F. Müller and I. Rieu (2016) stressed some similarities between CMS and high temperature defects in microspore and tapetum development [231]. Male gametophyte and tapetum are highly sensitive to high temperature compared with vegetative tissues and female gametophyte. As ROS production is increased during heat stress, similar mechanisms might be involved in CMS and heat stress.

4 — Material and methods

4.1 Material

4.1.1 Plant material

CMS results from a cytonuclear incompatibiliy. We possessed two natural accessions from *A. thaliana* harboring a sterilizing cytoplasm, and two accessions with a maintainer nucleus. We constructed cytolines as described in Roux et al, 2016 [45]. Cytolines' nomenclature is as following: [X]Y refers to cytoline combining the cytoplasm from the accession X with the nucleus from the accession Y. The accessions that were used in this study are presented in Table 4.1, whereas the cytolines are presented in Table 4.2. The [Kz-9]Cvi-0 has been produced specifically for this study, whereas the cytolines [Sha]Cvi-0 [45] and [Sha]Mr-0 [195] were already available. The cytolines were sequenced on a HiSeq3000 at the Genotoul Platform in Toulouse, and no residual zone of heterozygosity was detected (analysis with the help of J. Jimenez-Gomez).

4.1.2 Bacteria

The bacteria strains that were used are referenced in Table 4.3. The complete genotype of *E. coli* strains is available at http://www.openwetware.org/wiki/E._coli_genotypes.

4.1.3 Vectors

Different constructs were used in cytological and molecular approaches. These constructs are detailed in Table 4.4

4.1.4 Antibodies

The list of the antibodies that were used in this study to reveal proteins in western blot analyses are presented in Table 4.5.

91

Table 4.1: List of *A. thaliana* accessions used in this study

Accession	Origin	Cytoplasmic type	Nuclear type	Dormancy	Flowering
Col-0	Poland	Non sterilizing	Restorer	No	Early
Cvi-0	Cap Verde	Non sterilizing	Maintainer	3 months	Early
Kz-9	Karagandy	Non sterilizing	Restorer	No	Early
Mr-0	Italy	Non Sterilizing	Maintainer	4 months	Late
Rak-2	Russia	Sterilizing	Restorer	No	Late
Shahdara (Sha)	Tajikistan	Sterilizing	Restorer	No	Early

Table 4.2: List of the cytolines used in this study

Name	Cytoplasm	Nucleus	Male sterile/fertile	Source and description cytoline
[Kz-9]Cvi-0	Kz-9	Cvi-0	Fertile	This study
[Sha]Cvi-0	Sha	Cvi-0	Male-sterile	[45]
[Sha]Mr-0	Sha	Mr-0	Male-sterile	[195]

Table 4.3: List of bacteria strains used in this study

Specie	Strain	Notable features	Source	Use
E. coli	DB3.1	ccdB resistant	Invitrogen (11782-018)	Multiplication of donor and destination vectors of the Gateway system
E. coli	DH10b	None	Invitrogen (18290-015)	Cloning, plasmid multiplication
A. tumefaciens	C58C1 pMP90	Rif^R, $Genta^R$		*A. thaliana* transformation
A. tumefaciens	Gv3101 pMP90RK	Rif^R, $Kana^R$		*A. thaliana* transformation

4.1.5 Oligonucleotides

The oligonucleotides used in this study are presented in table 4.6, except those used for Gateway cloning strategies that are presented in table 4.7.

Table 4.4: List of vectors used in this study

Construct name	Targeting sequence	Sub-localization	Resistance	Source	Use
pUBQ10::cATEAM	None	Cytosol	$Spec^R$	[223]	Cytosolic ATP measurement
pUBQ10::SHMT-roGFP2-Grx1	SHMT	Mitochondria	$Spec^R$	[232]	Measurement of mitochondrial redox state
pM32::cATEAM	None	Cytosol	$Kana^R$	[223]	Cytosolic ATP measurement
pM32::mt-GFP	β ATPase (*N. plumbagini-folia*) [39]	Mitochondria	$Kana^R$	This study	Mitochondria shape in developing pollen
pM32::mt-ORF108	β ATPase (*N. plumbagini-folia*)	Mitochondria	$Kana^R$	This study	Sterility phenocopy
pM32::mt-ORF117	β ATPase (*N. plumbagini-folia*)	Mitochondria	$Kana^R$	This study	Sterility phenocopy
pTIP5;1::H2B-GFP	H2B	Nuclei	$Spec^R$	[204]	Generative lineage fate
pUBQ10::mt-ORF108	β ATPase (*N. plumbagini-folia*)	Mitochondria	$Spec^R$	This study	Sterility phenocopy
pUBQ10::mt-ORF117	β ATPase (*N. plumbagini-folia*)	Mitochondria	$Spec^R$	This study	Sterility phenocopy
pUBQ10::ORF117	None	Cytosol	$Spec^R$	This study	Sterility phenocopy
pUBQ10::ORF108	None	Cytosol	$Spec^R$	This study	Sterility phenocopy

Table 4.5: List of antibodies used in this study

Name	Target	Host	Dilution	Source
anti AOX1A	AOX1, AOX2	Rabbit	1:1,000	Agrisera
anti ATPB	β subunit of ATP synthase	Chicken	1:5,000	Agrisera
anti CYT C	Cytochrome C	Rabbit	1:5,000	Agrisera
anti ORF117	ORF117Sha	Rabbit	1:500	This work
anti Porin	Mitochondrial aquaporin	Mouse	1:500	David Day (Western Australia University)
anti RISP	Rieske iron sulfur protein	Rabbit	1:5,000	Chris Carrie (Western Australia University) [233]
anti mouse IgG HRP	Mouse antibodies	Goat	1:2,000	Santa Cruz
anti rabbit IgG HRP	Rabbit antibodies	Goat	1:20,000	Santa Cruz
anti chicken IgY HRP	Chicken antibodies	Goat	1:5,000	Santa Cruz

Table 4.6: List of oligonucleotides used in this study

Name	Sequence 5' - 3'	Use
A-team-F	CGTGACCACCCTGACCTG	ATeam sensor genotyping
A-team-R	CATGAATTCGTTTGCCTTCC	ATeam sensor genotyping
apt-rt1	TCCCAGAATCGCTAAGATTGCC	Nuclear control qRT-PCR
apt-rt2	CCTTTCCCTTAAGCTCTG	Nuclear control qRT-PCR
STP2-F	GCTCTCCAGATGACCGCTAC	Microspore control qRT-PCR
STP2-R	CAATACAATCAGCGGCACGG	Microspore control qRT-PCR
CmR-Gen-R	TCGTCGTGGTATTCACTCCA	Genotyping in pMDC-32
GFPRTR	GCAGATTGTGTGGACAGGTAATGG	GFP genotyping
GRX-F	TGGCTCTTCGAAGGCTTTCTT	roGFP2-Grx1 genotyping
GRX-R	TCTCGTTGGGGTCTTTGCTC	roGFP2-Grx1 genotyping
M13-F	ACTGGCCGTCGTTTTACA	Genotyping and sequencing in $pTOPO$
M13-R	CAGGAAACAGCTATGACCATG	Genotyping and sequencing in $pTOPO$
M32-F	GGCCGAACACTAAAATCACGTT	M32 promoter genotyping
ORF108-Gen-R	GCAACATTTCCCAAGGTCAT	ORF108 genotyping
ORF117-Gen-R	GCTGGCTAGTCCCAACTGAG	ORF117SHA genotyping
promTIP5;1-F	AAGCCTTCAGGTCCCACATC	TIP5;1 promoter genotyping
pUBDEST-R	TGTGATGGGCCCTTAGAGGAT	Genotyping in pUB-DEST
pUBI-F	TGCTTCACCGCCTTAGCTTT	Genotyping in pUB-DEST
QMR26SF	GACGAGACTTTCGCCTTTTG	Mitochondrial control qRT-PCR
QMR26SR	CTTGGAGCGAATTGGATGAT	Mitochondrial control qRT-PCR
Shamt6	GGGACTAGCCAGCGATGAGTT	cRT-PCR
Shamt7	TGAAACCCGAAAACCAATTGA	cRT-PCR
Shamt23	CATCGCTGGCTAGTCCCAAC	qRT-PCR ORF117SHA
Shamt24	TTGGACCCACGAGCAGATAC	qRT-PCR ORF117SHA
NdeI-ORF117SHA	CATATGAAACCCGAAAACCAATTGG TGCCTCGAGGATCAAGTGGTCATACA	Antibody anti-ORF117SHA production
BamHI-ORF117SHA	GGATCCTTAATTAAACCCCCCCCACC	Antibody anti-ORF117SHA production

Table 4.7: List of oligonucleotides used in this study for Gateway cloning strategies

Name	Sequence 5' - 3'	Features
ATPase-ORF108-F	GATGAGTTCACCGGCGGCGCTGGTAATACTATCAAATCACTTTCCC	Fusion targeting sequence - ORF108
ATPase-ORF108-R	GGGAAAGTGATTTGATAGTATTACCAGCGCCGCCGGTGAACTCATC	Fusion targeting sequence - ORF108
ATPase-ORF117-F	GATGAGTTCACCGGCGGCGCTGGTAAACCCGAAAAACCAATTGAT	Fusion targeting sequence - ORF117SHA
ATPase-ORF117-R	ATCAATTGGTTTTCGGGTTTACCAGCGCCGCCGGTGAACTCATC	Fusion targeting sequence - ORF117SHA
GTW-ORF108-F	GGGGACAAGTTTGTACAAAAAAGCAGGCTTCATGAATACTATCAAATCACTTTCCCAA	ORF108 Gateway cloning
GTW-ORF108-STOP-R	GGGGACCACTTTGTACAAGAAAGCTGGGTCCTAAACCCCCCCGCCCGTT	ORF108 Gateway cloning + Stop codon
GTW-ORF117-F	GGGGACAAGTTTGTACAAAAAAGCAGGCTTCATGAAACCCGAAAACCAATTGATATTA	ORF117SHA Gateway cloning
GTW-ORF117-STOP-R	GGGGACCACTTTGTACAAGAAAGCTGGGTCTTAATTAAAACCCCCCCAC	ORF117SHA Gateway cloning + Stop codon
GTW-preBATPase-F	GGGGACAAGTTTGTACAAAAAAGCAGGCTTCACCATGGCTTCTCGGAGGCTT	Targeting sequence Gateway cloning
pDNR-1	GCGTTCACCGACAAACAACA	Genotyping in pDNR207
pDNR-2	AGATTTTGAGACACGGGCCA	Genotyping in pDNR207
pM32-HindIII-F	CTCAAGCTTCGCTCAATTCAATTTAATTTTAAA	Cloning pM32 promoter in pMDC32 vector
pM32-KpnI-R	CGGGTACCCAGCAACTGTTTGTGATAATAATT	Cloning pM32 promoter in pMDC32 vector

97

4.2   Methods

4.2.1   Biological material culture

4.2.1.1   *A. thaliana* culture and breeding

Growth conditions, breeding and transformation of *A. thaliana* plants are detailed thereafter.

a. *In vitro* germination and early growth

Seeds were sterilized in sterilizing solution (45 mL of 95% EtOH and 5 mL of a first solution composed of one bleach pill and 5 to 6 drops of Teepol in 40 mL water), and then rinsed twice in pure ethanol. They were dried overnight under a sterile air flux, and subsequently sown on 3.1 g.L^{-1} Gamborg B5 medium supplemented with 0.08 % BCP, 1 % saccharose, 0.7 % agar, iron salt solution to a final concentration of 1 M, and adjusted to pH 6. The medium contained the proper selective agent in the cases where a selection was needed (hygromycin, Basta®or kanamycin) at 50 mg.L^{-1}. Seeds were stratified at 4°C for four days, before being placed in a growth chamber under long day conditions (16-h day, 8-h night) and at 20 °C.

b. Greenhouse culture

Dormant seeds were stratified for four days at 4 °C in 0.1 % agarose supplemented with 7 mM KNO3 and then sown on soil, whereas non dormant seeds were directly sown on soil. They were then grown under long-day conditions (16-h day, 8-h night) with additional artificial light (105 mE/m²/sec) when necessary.

c. Crosses and seed production

For crossing experiments, buds with immature anthers were emasculated, and hand pollination from the male parent was performed under the binocular. The siliques were harvested after they dried on the plant. Seeds from selfing were harvested when the plant was completely dried. After threshing, seeds were then stored at room temperature.

d. Transformation of *A. thaliana*, and selection of transformants

One-month-old plants from *A. thaliana* were dipped in an *A. tumefaciens* suspension containing 5 % sucrose (w/v) and 0.02 % Silwett L-77 (v/v) for 2 minutes. The obtention of the suspension is detailed in part 4.2.1.2. Plants were then watered

and placed in greenhouse for maturation. Seeds from fully matured plants were harvested and stored for 1 (*in vitro* selection) to 3 months (basta selection on sand) at least in the case in which the accession is dormant (Cvi-0 and Mr-0). *In vitro* selection was performed with appropriate selective antibiotic in a concentration of 50 μg.mL^{-1}, whereas seeds were sown on sand in the greenhouse and watered with a basta solution at 0.01 % (v/v) when the selection marker was the resistance to this herbicide. Resistant plants were transferred to soil and genotyped by PCR.

4.2.1.2 Bacteria culture conditions

a. Solid Culture

Cells were cultivated on agar LB-media (Duchefa) supplemented with the appropriate antibiotics. *E. coli* cells were cultivated 24 hours at 37 °C, and *A. tumefaciens* cells 48 hours at 28 °C.

b. Liquid culture

- Preparation of competent bacteria

  One isolated colony from *E. coli* DH10b or *A. tumefaciens* C58C1 was resuspended in 10 mL liquid LB, and incubated overnight. This pre-culture was used to inoculate 1 L of LB. When the culture reached $0.5 < \mathrm{OD}_{600} < 1$, it was transferred into large centrifuge bottles and incubated 30 minutes on ice. Samples were centrifuged at 4,000 g and 4 °C during 15 minutes. Pellets were washed in sterile water first separately, and then pooled. Pellets were then resuspended in 20 mL 10 % glycerol, centrifuged again in the same conditions and finally resuspended in 1 mL sterile 10 % glycerol. 50 μL aliquots were frozen in liquid nitrogen, and stored at -80 °C.

- Bacteria transformation and multiplication

  50 μL of bacteria were mixed with the appropriate plasmid at a concentration of about 150 ng.μL^{-1} and electroporated (Pulse: 2.5 kV for *E. coli* and 1.8 kV for *A. tumefaciens*). 1 mL of LB was added, and bacteria were then incubated 1 hour at the optimal growth temperature (*E. coli* 37 °C, *A. tumefaciens* 28 °C). Bacteria were then selected on solid LB containing the appropriate antibiotics.

- *A. tumefaciens* culture for *A. thaliana* transformation

  One isolated colony from *A. tumefaciens* was resuspended in 10 mL liquid LB containing the appropriate antibiotics, and incubated at 28 °C overnight.

The next day, 1 mL of this pre-culture was used to inoculate 400 mL of LB containing the appropriate antibiotics and incubated at 28 °C overnight. The culture should have a $0.8 < OD_{600} < 1$ to perform *A. thaliana* transformation. *A. tumefaciens* cells were pelleted by centrifugation at 5,000 *g* for 20 minutes, and resuspended in 400 mL of 5 % sucrose (w/v) and 0.02 % Silwett L-77 (v/v) solution.

4.2.2 Nucleic acids analyses

4.2.2.1 Nucleic acids isolation

a. Genomic DNA isolation from *A. thaliana*

Depending on the expected use of the genomic DNA, two alternative protocols were applied: CTAB extraction when high quality DNA was needed, and quick DNA extraction otherwise.

- CTAB DNA extraction

  Leaves from *A. thaliana* were harvested and placed in a pre-warmed (60 °C) lysis buffer composed of 100 mM Tris-HCl pH 8.20 mM EDTA, 1.4 M NaCl, 2 % CTAB (w/v) and 0.2 % 2-Mercaptoethanol (v/v). Material was ground at 30 Hz for 5 min, using a Mixer Mill (Qiagen), and subsequently incubated 30 minutes at 60 °C. DNA was extracted by adding 1 volume of chloroform-isoamylalcohol solution (48:2), and centrifuging 15 minutes at 15,000 *g* and 4 °C. The upper phase was recovered and DNA precipitated with the addition of 300 µL isopropanol followed by a centrifugation step 30 min at 15,000 *g*. The pellet was washed with 70 % ethanol, and DNA was resuspended in Tris-EDTA buffer (10 mM Tris, 1 mM EDTA, pH 8.0).

- Quick DNA extraction for genotyping

  Leaves from *A. thaliana* were harvested and placed in a lysis buffer containing 200 mL Tris-HCl pH 7.5, 250 mM EDTA, and 0.5 % SDS (v/v), with two metal balls. Plant material was then ground using a Mixer Mill (Qiagen). Crushed material was centrifuged, and the resulting supernatant transferred into isopropanol to precipitate the DNA. After a new centrifugation step, pellet was recovered and washed with cold ethanol 70 %. Precipitated DNA was dried at 37 °C and resuspended in sterile water.

b. Plasmidic DNA isolation from *E. coli*

pDNA was isolated with the NucleoSpin® Plasmid (Macherey-Nagel) kit according to manufacturer's instructions.

c. RNA isolation from *A.thaliana*

Fresh plant tissue was harvested on *A. thaliana* and immediately frozen in liquid nitrogen. Tissue was ground with liquid nitrogen-cold mortar and pestle, and RNA was extracted with the RNeasy Plant Mini Kit from Qiagen, according to manufacturer's protocol. When DNase treatment was needed, it was performed using the RTS-DNase™ (Ozyme) according to manufacturer's protocol, with minor modifications: nuclease treatment was extended up to 30 minutes, and treatment was stopped with phenol-chloroform-isoamylalcohol (pH 4.5) extraction, and RNA precipitation (1.5 vol Ethanol, 0.1 vol sodium acetate pH 4.8) at -20 °C overnight. The next day, RNA was pelleted with a centrifugation at 20,000 *g* for 20 minutes, air dried and resuspended in sterile water.

4.2.2.2   Agarose gel electrophoresis

Nucleic acids were analyzed on 1 % to 3 % agarose (Sigma-Aldrich) gels in 1 x TAE buffer (40 mM Tris-acetate, 1 mM EDTA, pH 8). 500 bp and 1 kb ladders DNA size standards (ThermoFisher Scientific) were used according to the needs.

4.2.2.3   PCR amplifications

Home-made Taq polymerase was used to amplify DNA fragments with PCR methods, using the following reaction mixture:

10X buffer	4 μL
MgCl$_2$ (25 mM)	4.8 μL
dNTP (25 mM each)	0.2 μL
Forward Primer (10 μM)	1 μL
Reverse Primer (10 μM)	1 μL
Taq-Polymerase	0.5 μL
DNA	5 to 50 ng
H$_2$O	Qsp 20 μL

10X buffer: 750 mM Tris-HCl, 200 mM $(NH_4)_2SO_4$, 0.1 % (v/v) triton, pH 8.8.

In a PCR thermocycler (Ependorf), the DNA was denatured for 2 min at 94 °C, followed by 35 cycles of 30 s denaturation at 94 °C, 30 s hybridization of oligonucleotides at (Tm-3) °C and 1 min elongation per kb of expected PCR product at 72 °C. The run was completed after another 2 min at 72 °C.

4.2.2.4   Sequencing

Purified PCR products and plasmids were sent to Beckman Coulter Genomics for Sanger sequencing (http://www.beckmangenomics.com).

4.2.2.5   Gene expression analysis

a. Northern blot analysis

RNA Electrophoresis in denaturing conditions :
20 μg of total RNA were denatured 5 min at 70 °C in denaturing loading buffer (50 % (v/v) formamide, 16 % (v/v) formaldehyde (39 % w /v), 0,5 x MOPS buffer) and placed on ice. After addition of 1/3 vol of bromophenol blue 0,25 % (w/v) in glycerol 20 % and 1 μL of ethidium bromide 10mg/mL, they were loaded on a 1.5 % agarose gel in 1x MOPS buffer with 8 % formaldehyde. Commercial RNA ladders (0.1-2kb and 0.5-10kb RNA ladders Invitrogen) were treated similarly before loading. Electrophoresis was conducted at 100V for approximately 7 hours.

Northern blotting of RNA:
After visualization and snap shop under UV light, the gel was rinsed three times 5 minutes in distilled water and transferred onto a nylon membrane (Genescreen) in 10 X SSPE buffer overnight. After a quick wash in 2 X SSPE buffer, the membrane was colored in 0.04 % (w/v) methylene blue, 0.5 M Na acetate pH 5.2 for 10 minutes and bleached in ethanol 20 % until the RNA bands clearly appeared, to check for correct transfer, and mark the ladder bands. The membrane was further bleached in 0.2 X SSPE 1 % SDS. It was kept at 4 °C between two Whatman papers or directly prehybridized.

Hybridization of Northern blots:
A nylon membrane was placed in a hybridization tube with 10 mL of PerfectHybTM buffer from Sigma at 68 °C for 2 hours. Hybridization was conducted at 68 °C overnight in 10 mL of new PerfectHybTM buffer containing the probe that had just been denatured at 100 °C for 5 minutes. After removal of the probe, the membrane

was rinsed at 68 °C in 2 X SSPE 0.1 % SDS 0.2 % $Na_4P_2O_7.10H_2O$ and 0.2 X SSPE 0.1 % SDS 0.2 % $Na_4P_2O_7.10H_2O$.

Labeling of DNA probes:
20 to 40 ng of DNA were denatured at 100 °C for 5 minutes and immediately placed on ice. Labeling was realized in a final volume of 50 μL in labeling buffer x1 (50 mM Tris-HCl pH 8, 5 mM MgCl2, 2 mM DTT, 200 mM HEPES pH 6.6) with random hexadeoxyribonucleotides (5 A260/ mL), dATP, dGTP, dTTP 20 μM each, 400 μg/mL BSA, 50 μCie of alpha ^{32}P dCTP (3000 Cie/mmol), and 5 units of Klenow DNA polymerase, at 37 °C for one hour. Non incorporated nucleotides were removed by purification on a G50 micro-column (Biorad). The eluate was denatured at 100 °C for 5 minutes and immediately placed on ice before addition to the hybridization buffer.

MOPS 10 X: 0.2 M MOPS, 0.05 M Na acetate, 0.01 M Na_2 EDTA, pH 7.
SSPE 20 X: 3 M NaCl, 0.2 M $NaH_2PO_4.2H_2O$, 0.02 M EDTA, pH 7.4.

b. RT-PCR

1 μg of RTS-DNase^{TM} treated RNA sample and random hexamer primers were heated up 5 minutes at 70 °C in order to minimize secondary RNA structures prior to RT-PCR. Denatured RNA was shortly spun and directly put on ice. cDNA synthesis was performed with M-MLV Reverse Transcriptase (Thermo Fisher Scientific) with the following reaction mixture:

RNA	1 μg
Random hexamers (100 μM)	1 μL
RNase-free dNTPs (25 mM each)	0.5 μL
M-MLV RT buffer (5X)	5 μL
M-MLV RT (200 U/μL)	1 μL
RiboLock RNase inhibitor (40 U/μL)	0.625 μL
RNase-free H_2O	Qsp 25 μL

For genes without introns, a negative control was performed by running in parallel the same reaction without the M-MLV RT. cDNA was synthesized in a thermocycler, at 37°C for 1 hour, and reaction was inactivated by heating up at 70 °C for 15 minutes. The obtained cDNA was diluted by adding 175 μL of sterile water and aliquots were stored at -20 °C for subsequent analysis. For regular RT-PCR, 5 μL of cDNA was used as PCR template.

c. cRT-PCR

5 μg of RTS-DNase treated RNA sample from floral buds were circularized with T4-RNA ligase (ThermoFisher Scientific) with the following reaction mixture:

RNA	5 μg
T4 RNA buffer 10X	5 μL
BSA (1 mg/mL)	5 μL
ATP (10 mM)	5 μL
T4 RNA ligase (10 U/μL)	4 μL
RiboLock RNase inhibitor (40 U/μL)	1 μL
RNase-free H$_2$O	Qsp 50 μL

Ligation was performed by incubating the samples 2 hours at 37 °C in a thermocycler. After ligation, RNA was extracted with phenol-chloroform-isoamylalcohol (pH 4.5), and precipitated (1.5 vol Ethanol, 0.1 vol sodium acetate pH 4.8) at -20 °C overnight. The next day, RNA was pelleted with centrifugation at 20,000 g for 20 minutes, air dried and resuspended in 10 μL sterile water. RT-PCR was performed on circularized RNA as described in part b with minor modifications: reverse transcriptase reaction was extended to 3 hours at 40 °C . PCR was performed on 5 μL cDNA with divergent oligonucleotides.

d. qRT-PCR

PCR amplification on genomic DNA sample was performed using primers designed for qRT-PCR (product size around 100 bp, Tm close to 55 °C), and qRT-PCR reaction was performed with the corresponding oligonucleotides and with a dilution array of the resulting PCR products as matrix. Oligonucleotides couples with an efficiency from 95 to 105 % were selected for subsequent analysis.

For sample analysis, 5 μg of RTS-DNase treated RNA samples were used to perform cDNA synthesis as described in part b. The SsoAdvanced™ SYBR® Green supermix kit from Biorad (Hercules, USA) was used. The reaction mix was the following:

cDNA	5 μL
Biorad 2X buffer	7.5 μL
Forward primer (100 μM)	0.1 μL
Reverse primer (100 μL)	0.1 μL
H$_2$O	2.3 μL

qRT-PCR was performed and analyzed by using the CFX96$^{\text{TM}}$ Real-Time PCR Detection System (Biorad). Significant differences were tested with Mann and Whitney statistical test.

4.2.3 Cloning and vector constructions

4.2.3.1 Cloning in *pTOPO*

Purified PCR products were cloned in *pTOPO* according to the manufacturer's instructions.

4.2.3.2 Construction of destination vector with pM32 promoter for the Gateway system

pM32 promoter was amplified from CTAB extracted DNA from rapeseed (Brutor cultivar), with the oligonucleotides pM32-*Hind*III-F and pM32-*Kpn*I-R, containing sequences specific to the pM32 promoter and additional *Hind*III and *Kpn*I restriction sites respectively (table 4.7). The resulting PCR products and the pMDC32 vector were firstly digested *Kpn*I restriction enzyme (Fermentas, Thermo Fisher Scientific) at 37 °C overnight. Digestion buffer was then supplemented with NaCl to reach a final concentration of 50 mM NaCl, and the second digestion was performed with *Hind*III for 8 more hours. Digestion was inactivated 10 min at 80 °C, and the digestion products were separated in agarose gel and purified with the Macherey-Nagel$^{\text{TM}}$NucleoSpin$^{\text{TM}}$Gel and PCR Clean up according to manufacturer's protocol. Ligation of the digested vector and PCR products was performed with T4 DNA ligase at 4 °C overnight. Then, the ligation products were introduced into *E. coli* DB3.1 strain. Colonies were then genotyped by PCR with the M32-F and CmR-Gen-R oligonucleotides (see table 4.6) in order to select colonies containing the new vector.

4.2.3.3 Gateway cloning

Sequences that needed to be inserted into Gateway vectors were amplified with the oligonucleotides referenced in table 4.7. Cloning reactions were performed with BP clonase II and LR clonase II according to the manufacturer's instructions.

4.2.4 Biochemistry: proteins analysis

4.2.4.1 Organelle isolation

a. Mitochondria isolation

Fresh material from around 400 whole plants were harvested, and each 10 g of material was ground with a blender in 40 mL of grinding medium composed of 300 mM sucrose, 25 mM $Na_4P_2O_7$, 10 mM KH_2PO_4, 0.8% (w/v) polyvinylpyrrolidone-40, 0.3 % (w/v) BSA, and 20 mM ascorbate, pH 7.5. Cell debris were removed by filtering through 2 layers of a Miracloth membrane (Calbiochem). After a low speed centrifugation (3,000 g for 10 min), the supernatant was recovered and centrifuged at 20,000 g for 20 min. Then, pellet was resuspended in washing buffer (0.3 M sucrose and 10 mM HEPES-KOH, pH 7.5), and a new round of low speed and high speed centrifugations was performed.

The last pellet was resuspended in washing buffer and organelles were loaded on Percoll density step gradients of 2 vol., 10 vol., and 2 vol. containing respectively 50, 30 and 16% (v/v) of Percoll diluted in washing buffer supplemented with 0.2% BSA. After 45 min of centrifugation at 40,000 g at 4 °C and no brake, mitochondria were collected from the 50/25% interface, diluted at least 10 times in washing buffer and pelleted at 20,000 g for 20 minutes. Three washing steps were performed by diluting the pellet in 10 vol. of washing buffer and centrifugation. After the last centrifugation, mitochondria pellets were stored at -80 °C or kept on ice for immediate analysis.

b. Crude membrane extracts

Crude membrane extraction was performed on 800 mg of unopened floral buds as described in [234].

4.2.4.2 Protein quantification with RC DC protein assay

Mitochondrial pellets were resuspended in 50 μL 30 mM Hepes, 10 mM KCl, 5 mM $MgCl_2$, 0.5% CHAPS (w/v), 10 % glycerol (v/v), and 1 mM DTT, pH 7.5. Samples were incubated for 30 min at 4 °C. 5μL of the protein solution were diluted in 20 μL resuspension buffer, and quantified with RC DC assay kit (Biorad) according to manufacturer's protocol.

4.2.4.3 Polyacrylamide gel Electrophoresis in denaturing conditions (SDS-PAGE)

Quantified protein extracts (see previous part) were diluted in Laemli loading buffer (300 mM Tris-Hcl, 12% SDS (v/v), 50 % glycerol (v/v), 1 M DTT, and 0.05% (w/v) bromophenol blue, pH 6.8) and heated up at 95 °C for 10 min. Proteins were then separated according to their molecular weight on precast 4-20 % polyacrylamide-SDS gel. Electrophoresis was performed in Tris-Glycine-SDS buffer at 120 Volts. A pre-stained molecular mass marker (Fermentas) was used to determine protein size.

4.2.4.4 Polyacrylamide gel Electrophoresis in native conditions (BN-PAGE)

The equivalent of 500 μg of proteins of crude membrane extracts were lysed in buffer containing 50 mM bis-Tris-HCl, 750 mM 6-aminohexanoic acid, 0.5 mM EDTA, 20% digitonin (w/w proteins), pH 7 for 30 min at 4 °C. Membranes and non-solubilized proteins were removed by centrifuging the samples at 100,000 g and 4 °C for 15 min. Supernatant was diluted and supplemented with Coomassie G-250. Samples were loaded on NativePage 4-16% Bis-Tris protein gel (Thermofisher Scientist) and migration was performed at 70 V and 4 °C overnight.

4.2.4.5 Immunoblot

Proteins or complexes separated respectively by SDS-PAGE or BN-PAGE were transferred on PVDF membranes. Gel was placed in contact with the PVDF membrane and sandwiched between 4 layers of Whatman 3MM paper soaked with transfer buffer (10% (v/v) EtOH, 2 mM Tris, 15 mM Glycine).

Denatured proteins were transferred using the Trans-Blot Turbo Transfer System (Biorad) according to manufacturer's protocol.

Native proteins were transferred in liquid conditions at 30 V and 4 °C overnight.

After transfer, the membrane was placed in a blocking solution containing 5 % of skimmed milk in TBS-T buffer (10 mM Tris-HCl, 1.5 M NaCl, and 0.1% Tween (v/v), pH 7.5) for 45 min at room temperature, before being incubated overnight at 4 °C in a solution containing 5 % of skimmed milk and the primary antibody diluted at the appropriate dilution (see Table 4.5) in TBS-T buffer. The membrane was then washed 3 times 10 min in TBS-T buffer and incubated with the appropriate secondary antibody (see Table 4.5) for 1 hour at room temperature. After 3 washing steps, proteins that were recognized by the primary antibody were revealed with the Clarity ECL Western

Blotting substrate (Biorad) and visualized with the LAS4000 chemiluminescence analyzer (Fujifilm).

4.2.4.6 Integrity of mitochondrial supercomplexes by in gel activity assay

Activities of complexes I and IV were revealed on proteins separated with BN-PAGE, as described in Sabar et al. (2005) [235].

4.2.4.7 Development of the anti-ORF117SHA antibody

The anti-ORF117SHA antibody was raised in collaboration with Nathalie Vrielynck. A 363-bp DNA fragment was amplified from ORF117SHA-CDS cloned in pTOPO using primers *Nde*I-ORF117SHA and *BamH*I-ORF117SHA and inserted into the pET15b plasmid digested with *Nde*I and *BamH*I (Novagen). The resulting construct was transferred to *E. coli* BL21 cells (Novagen) and protein expression was induced in liquid culture by addition of 1 mM IPTG for 3 h at 37 °C. Cells were harvested by centrifugation and resuspended in $1/100^{th}$ of culture volume with lysis buffer (50 mM Tris pH 8, 150 mM NaCl) supplemented with protease inhibitor (AEBSF 1 mM, E-64 1 mM, Pepstatin 10 μg/mL, Aprotin 10 μg/mL and Leupeptin 10 μg/mL). Cells were ruptured by a single pass through a French pressure cell (SLM Aminco) at 1000 psi. The recombinant protein mainly accumulated in the soluble fraction and was recovered by centrifugation at 40,000 g for 20 min. The protein was then purified and finally eluted 5 times in 0,5 mL of 100 mM Glycine pH 2, 0.5 M NaCl, 0.1 % (v/v) Tween 20 and 0.1 % (v/v) Triton X-100 and acidity was immediately neutralized with 100 ml of 1 M Tris pH 9.5.

4.2.5 Cytological approaches

4.2.5.1 Pollen viability analysis: Alexander staining

The viability of pollen grains was evaluated after Alexander staining [236]. Briefly, newly opened flowers were collected and fixed in 10 % EtOH for up to 1 week. Fixed samples were dissected under the binocular and anthers were mounted in Alexander's stain. After at least 24 h they were observed by transmitted light microscopy with a Leica Diaplan DIC microscope.

4.2.5.2 Pollen developmental stage determination

According to the experiments, the developmental stage of pollen was either determined by pollen nuclei coloration (see hereafter), or by measuring pistil size. Indeed, Daniel

Table 4.8: Correspondence of pollen developmental stage with pistil size.

Pollen developmental stage	Pistil size (mm)
Tetrad	0.75
Uninucleate microspore	1
First pollen mitosis	1.25
Second pollen mitosis	1.5
Early trinucleate	1.75
Late trinucleate	2

Vezon (IJPB, Versailles), established a correspondence between pollen developmental stage and the pistil size in Col-0 accession. I verified that the pistil sizes could be correlated to the same pollen developmental stages in Cvi-0, [Sha]Cvi-0 and [Kz-9]Cvi-0 by measuring the pistil and staining pollen grains nuclei with DAPI. This experiment validated the correlation of these two factors. The correspondence of pollen developmental stage with pistil size is presented in table 4.8.

4.2.5.3 Staining of pollen grain nuclei

a. DAPI staining

Floral buds were dissected under a binocular magnifier, and anthers were shredded with needles in Citifluor/DAPI 20 μg.mL^{-1}. Pollen grains were imaged using a Leica SP8 confocal microscope using a 405 nm diode laser line exciting DAPI. Fluorescence emission was detected between 410 and 480 nm.

b. Propidium iodide staining

Floral buds were fixed in 0.5 vol propionic acid, 1 vol 37 % formaldehyde and 7 vol ethanol for 2 h at room temperature. Such fixed samples could be stored up to several month in 70 % ethanol at 4 °C. In order to perform propidium iodide staining, samples were rehydrated in decreasing ethanol concentration solutions, and rinsed in pure water. Small buds were opened with a needle to allow the chemicals to penetrate the tissues. As propidium iodide stains DNA and RNA, RNA was removed with an RNase treatment in a 0.5 M Nacl, 10 mM Tris, 1 mM EDTA buffer and for 30 min at 37 °C. Samples were rinsed in this same buffer, and stained with 50 μg.mL^{-1} propidium iodide diluted in 0.1 M Arginine pH 12.4 for 5 days at 4 °C. After coloration, samples were washed 2 times for 1 hour in 0.1 M Arginine

pH 8. Buds were then dissected in order to collect the whole anthers that were mounted in Citifluor. Whole anthers were observed in confocal microscopy with the Leica SP5 tandem microscope, by doing Z-stack images acquisition. Propidium iodide-colored nuclei were excited with the Argon 488 nm laser line, and fluorescence emission was detected between 570 and 670 nm. For each genotype, 3 individuals were observed, and at least one bud per developmental stage and individual was analyzed. Alive and dead pollen grains were then counted on Z-stack series with ImageJ software.

c. Genetic fluorescent marker

The generative lineage nuclei were labeled with the construct pTIP5;1-H2B:GFP, kindly provided by David Twell, from Leicester University. This construct is composed of a GFP fused to a histone that locates the fusion protein in the nucleus, under the control of the generative lineage specific promoter of TIP5;1 (At3g47440) [204] (See Table 4.4). Buds of transgenic plants were dissected in order to take out the anthers, and those were shredded with needles in Citifluor. Pollen grains were imaged using a Leica SP8 confocal microscope. The 488 nm Argon laser line excites GFP and emission was detected between 510 and 530 nm. For each genotype, 3 individuals were observed, and at least one bud per developmental stage and individual was analyzed.

4.2.5.4 Observation of mitochondria in developing pollen grains

Mitochondria were observed in developing pollen grains with a GFP addressed to mitochondria and expressed under the control of the pM32 promoter [202] (see Table 4.4). Buds of transgenic plants were dissected in order to take out the anthers, and those were shredded with needles in Citifluor/DAPI 20 μg.mL^{-1}. Pollen grains were imaged using a Leica SP8 confocal microscope and a sequential acquisition. The 405 nm diode laser line excites DAPI and the 488 nm Argon laser line excites GFP. DAPI fluorescence emission was detected between 410 and 480 nm, and GFP between 510 and 530 nm. For each genotype, 3 individuals were observed, and at least one bud per developmental stage and individual was analyzed.

4.2.5.5 Quantification of the cytosolic ATP concentration (ATeam sensor)

The ATP steady state level is measured with the fluorescent resonance energy transfer (FRET) based sensor ATeam 1.03 nD/nA [223]. I used the pUBQ10::ATeam construct (see table 4.4), as I constructed by Gateway the pM32::ATeam construct that was not

expressed enough to allow quantification in pollen. It is composed of the msECFP and the circularly permutated (cp)-mVenus, linked by the ϵ subunit of the F_0F_1-ATP synthase from *B. subtilis*, as represented in figure 4.1. ATP binds to the ϵ subunit without being hydrolyzed, therefore cell homeostasis is not affected. In the ATP-free form of the sensor, the two fluorophores do not perform FRET efficiently, resulting in a high emission from the msECFP (noted CFP) and low emission from the cp-mVenus (noted YFP). By contrast, in the ATP-bound form of the sensor there is an increase in FRET efficiency resulting in higher emission from cp-mVenus and lower emission from msECFP. Therefore, the higher the YFP/CFP emission ratio, the more ATP-bound form, compared with unbound form, and thus the more ATP present in direct proximity of the sensor.

Plants expressing the sensor were *in vitro* sown, and grown for 6 days in culture chamber. The plants were then observed under binocular with a GFP-fluorescence filter, and the individuals presenting the brighter fluorescence were selected for further analysis: 10 individuals per genotype were used to measure YFP/CFP ratios in the hypocotyl epidermis, and others were transferred into soil and grown to flowering in order to measure the ratios in pollen grains.

Samples were mounted in sterile water and tissues were imaged using a Zeiss 780 confocal microscope, as described in [237]. It was verified with carbonylcyanide-m-chlorophenylhydrazone treated pollen grains that a depletion in ATP could be detected with lower ratios.

4.2.5.6 Quantification of the mitochondrial redox state (SHMT-roGFP2-Grx1 sensor)

Mitochondria redox state was analyzed in hypocotyl epidermis and pollen with the mt-roGFP2-Grx1 sensor (see Table 4.4). I used the pUBQ10::SHMT-roGFP2-Grx1 construct, as I constructed by Gateway the pM32::SHMT-roGFP2-Grx1 construct that was not expressed enough to allow quantification in pollen. The roGFP2-Grx1 sensor is a GFP for which sequence was modified to add two cystein residues. These two cystein residues can form a di-sulfure bound, changing the protein configuration. The oxidized and the reduced forms do not have the same excitation properties. Indeed, the oxidized form has two excitation peaks at 405 nm and 488 nm, whereas the reduced form has a unique excitation peak at 488 nm (figure 4.2). Therefore the ratio of fluorescence emission intensity at 405 nm to the fluorescence emission intensity at 488 nm indicates the redox state of the compartment where the sensor is expressed. The higher the ratio, the more oxidized the compartment. The roGFP2-Grx1 sensor allows the measurement of the glutathione pool redox state. The roGFP2 protein was genetically fused to the human

redox enzyme Grx1 because it facilitates real-time equilibration between the roGFP2 and the GSH:GSSG couple [238].

Samples were mounted in sterile water and tissues were imaged using a Zeiss 780 confocal microscope, as described in [239]. 6 day-old *in vitro* plantlets were used in order to image hypocotyl epidermis, and 6 week-old plants to image pollen grains. Calibration was performed by perfusion with 10 mM DTT and 10 mM DPS to drive the roGFP2 to the reduced and oxidized forms respectively. Fluorescence emission intensity was measured when the sensor was excited at 405 and 488 nm, and autofluorescence signal was collected in order to subtract it in the analysis, as a lot of autofluorescent compounds are excited at 405 nm.

4.2.5.7 Ratiometric analysis

Quantification of ATP level and mitochondria redox state was done with the Redox Ratio Analyser software, a custom MatLab (The MathWorks, Nantick, MA) analysis suite (available on https://markfricker.org/77-2/software/redox-ratio-analysis/) developed by Mark Fricker. Regions of interest were determined and ratio images were calculated on a pixel by pixel basis.

Significant differences of measurements between the genotypes were tested with Mann and Whitney test.
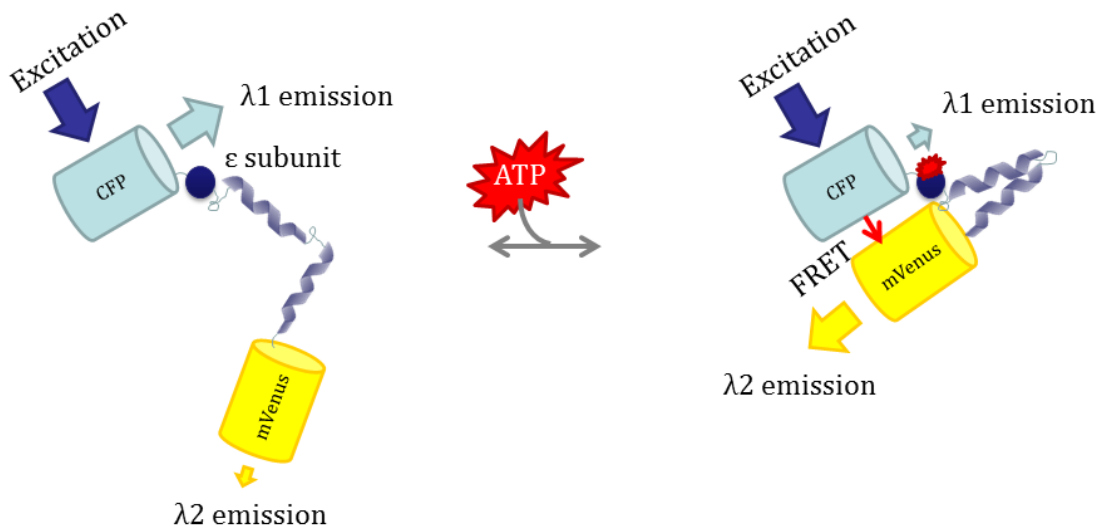
Figure 4.1: Quantification of ATP steady-state with the ATeam sensor. The sensor is made of a CFP fluorophore linked to a mVenus fluorophore (YFP), with the ϵ subunit of *B. subtilis* F_0F_1-ATP synthase in between. In the ATP-free form (on the left), the configuration of the sensor results in low FRET efficiency. When ATP binds to the ϵ subunit, a configuration change increases FRET efficiency. Measurement of YFP/CFP emission ratio will indicate the proportion of ATP-bound form and ATP-free form, and therefore the steady-state of ATP in presence of the sensor.
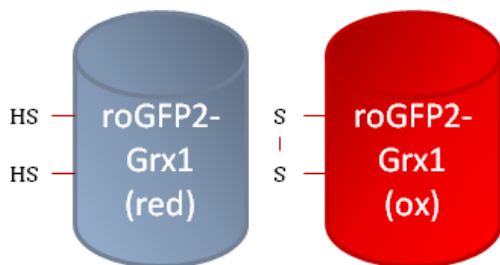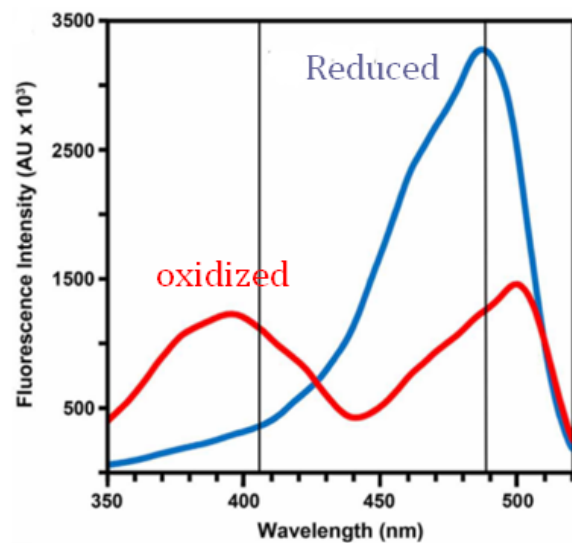
Figure 4.2: Measurement of the glutathione pool redox state with the roGFP2-Grx1 probe. (a) The sensor is a GFP with modified sequence to add two cystein residues, that can form a di-sulfure bound in the oxidized form. The reduced and oxidized form do not share the same excitation spectra. (b) From [240] Excitation spectra of roGFP2 in fully oxidized (red curve) and fully reduced (blue curve) states.

113

Bibliography

[1] R. Porter, *The Cambridge History of Science: Volume 4, Eighteenth-Century Science*, vol. 4. Cambridge University Press, 2003.

[2] S. S. Renner, "The relative and absolute frequencies of angiosperm sexual systems: Dioecy, monoecy, gynodioecy, and an updated online database," *American Journal of Botany*, vol. 101, no. 10, pp. 1588–1596, 2014.

[3] C. Darwin, *The different forms of flowers on plants of the same species*. John Murray, 1877.

[4] M. Dufaÿ, P. Champelovier, J. Käfer, J.-P. Henry, S. Mousset, and G. Marais, "An angiosperm-wide analysis of the gynodioecy–dioecy pathway," *Annals of botany*, vol. 114, no. 3, pp. 539–548, 2014.

[5] S. C. Barrett, "The evolution of plant sexual diversity," *Nature reviews. Genetics*, vol. 3, no. 4, pp. 274–284, 2002.

[6] R. Chittenden and C. Pellew, "A suggested interpretation of certain cases of anisogeny," *Nature*, vol. 119, no. 10, 1927.

[7] M. M. Rhoades, "Cytoplasmic inheritance of male sterility in zea mays," *Science*, vol. 73, no. 1891, pp. 340–341, 1931.

[8] M. M. Rhoades, "The cytoplasmic inheritance of male sterility in zea mays," *Journal of Genetics*, vol. 27, no. 1, pp. 71–93, 1933.

[9] M. L. H. Kaul, *Gynodioecy*, pp. 268–277. Berlin, Heidelberg: Springer Berlin Heidelberg, 1988.

[10] M. Tester and P. Langridge, "Breeding technologies to increase crop production in a changing world," *Science*, vol. 327, no. 5967, pp. 818–822, 2010.

[11] L. Chen and Y.-G. Liu, "Male sterility and fertility restoration in crops.," *Annu. Rev. Plant Biol.*, vol. 65, pp. 579–606, 2014.

[12] N. Li, D.-S. Zhang, H.-S. Liu, C.-S. Yin, X.-x. Li, W.-q. Liang, Z. Yuan, B. Xu, H.-W. Chu, J. Wang, *et al.*, "The rice tapetum degeneration retardation gene is required for tapetum degradation and anther development," *The Plant Cell*, vol. 18, no. 11, pp. 2999–3014, 2006.

[13] M. Borg, L. Brownfield, and D. Twell, "Male gametophyte development: a molecular perspective," *J. Exp. Bot.*, vol. 60, no. 5, pp. 1465–1478, 2009.

[14] D. Honys, D. Reák, and D. Twell, "Male Gametophyte Development and Function," *Plant Biotechnology*, vol. 1, pp. 209–224, 2006.

[15] D. Honys and D. Twell, "Transcriptome analysis of haploid male gametophyte development in Arabidopsis.," *Genome Biol.*, vol. 5, no. 11, p. R85, 2004.

[16] R. Tilney-Bassett, "Genetics of variegated plants," *Genetics and biogenesis of mitochondria and chloroplasts*, pp. 268–308, 1975.

[17] W.-L. Chiu, W. Stubbe, and B. B. Sears, "Plastid inheritance in oenothera: organelle genome modifies the extent of biparental plastid transmission," *Current genetics*, vol. 13, no. 2, pp. 181–189, 1988.

[18] C. Schumann and J. Hancock, "Paternal inheritance of plastids in medicago sativa," *Theoretical and Applied Genetics*, vol. 78, no. 6, pp. 863–866, 1989.

[19] M. J. Havey, J. W. Lilly, B. Bohanec, G. Bartoszewski, and S. Malepszy, "Cucumber: a model angiosperm for mitochondrial transformation?," *Journal of applied genetics*, vol. 43, no. 1, pp. 1–18, 2002.

[20] C. Mereschkowsky, "Über natur und ursprung der chromatophoren im pflanzenreiche," *Biol Centralbl*, vol. 25, pp. 593–604, 1905.

[21] L. Margulis, *Origin of eukaryotic cells: Evidence and research implications for a theory of the origin and evolution of microbial, plant and animal cells on the precambrian Earth*. Yale University Press, 1970.

[22] E. V. Koonin, "Origin of eukaryotes from within archaea, archaeal eukaryome and bursts of gene gain: eukaryogenesis just made easier?," *Phil. Trans. R. Soc. B*, vol. 370, no. 1678, p. 20140333, 2015.

[23] M. W. Gray and W. F. Doolittle, "Has the endosymbiont hypothesis been proven?," *Microbiological Reviews*, vol. 46, no. 1, pp. 1–42, 1982.

[24] J. N. Timmis, M. a. Ayliffe, C. Y. Huang, and W. Martin, "Endosymbiotic gene transfer: organelle genomes forge eukaryotic chromosomes.," *Nat. Rev. Genet.*, vol. 5, no. 2, pp. 123–135, 2004.

[25] A. Gibor and S. Granick, "Plastids and mitochondria: Inheritable systems," *Science*, vol. 145, no. 3635, pp. 890–897, 1964.

[26] J. F. Allen, "Why chloroplasts and mitochondria retain their own genomes and genetic systems: colocation for redox regulation of gene expression," *Proceedings of the National Academy of Sciences*, vol. 112, no. 33, pp. 10231–10238, 2015.

[27] A. H. Millar, J. Whelan, and I. Small, "Recent surprises in protein targeting to mitochondria and plastids," *Current Opinion in Plant Biology*, vol. 9, no. 6, pp. 610 – 615, 2006. Cell Biology / Edited by Laurie G Smith and Ulrike Mayer.

[28] S. Sato, Y. Nakamura, T. Kaneko, E. Asamizu, and S. Tabata, "Complete structure of the chloroplast genome of arabidopsis thaliana," *DNA research*, vol. 6, no. 5, pp. 283–290, 1999.

[29] M. Unseld, J. R. Marienfeld, P. Brandt, and A. Brennicke, "The mitochondrial genome of Arabidopsis thaliana contains 57 genes in 366,924 nucleotides," *Nat Genet*, vol. 15, no. 1, pp. 57–61, 1997.

[30] W. Sakamoto, S.-y. Miyagishima, and P. Jarvis, "Chloroplast biogenesis: control of plastid development, protein import, division and inheritance," *The Arabidopsis Book*, p. e0110, 2008.

[31] J.-D. Rochaix, "The role of nucleus-and chloroplast-encoded factors in the synthesis of the photosynthetic apparatus," in *The structure and function of plastids*, pp. 145– 165, Springer, 2007.

[32] N. Haïli, N. Arnal, M. Quadrado, S. Amiar, G. Tcherkez, J. Dahan, P. Briozzo, C. Colas des Francs-Small, N. Vrielynck, and H. Mireau, "The pentatricopeptide repeat mtsf1 protein stabilizes the nad4 mrna in arabidopsis mitochondria," *Nucleic acids research*, vol. 41, no. 13, pp. 6650–6663, 2013.

[33] S. Mackenzie and L. McIntosh, "Higher plant mitochondria," *The Plant Cell*, vol. 11, no. 4, pp. 571–585, 1999.

[34] M. Balsera, J. Soll, and B. Bölter, "Protein import machineries in endosymbiotic organelles," *Cellular and molecular life sciences*, vol. 66, no. 11, pp. 1903–1923, 2009.

[35] K. J. van Wijk, "Protein maturation and proteolysis in plant plastids, mitochondria, and peroxisomes," *Annual review of plant biology*, vol. 66, pp. 75–111, 2015.

[36] E. Glaser, A. Eriksson, and S. Sjöling, "Bifunctional role of the bc1 complex in plants mitochondrial bc1 complex catalyses both electron transport and protein processing," *FEBS letters*, vol. 346, no. 1, pp. 83–87, 1994.

[37] M. Boutry, F. Nagy, C. Poulsen, K. Aoyagi, and N.-H. Chua, "Targeting of bacterial chloramphenicol acetyltransferase to mitochondria in transgenic plants," *Nature*, vol. 328, no. 6128, pp. 340–342, 1987.

[38] F. Chaumont, M. de Castro Silva Filho, D. Thomas, S. Leterme, and M. Boutry, "Truncated presequences of mitochondrial f1-atpase β subunit from nicotiana plumbaginifolia transport cat and gus proteins into mitochondria of transgenic tobacco," *Plant molecular biology*, vol. 24, no. 4, pp. 631–641, 1994.

[39] F. Chaumont, B. Bernier, R. Buxant, M. E. Williams, C. S. Levings, and M. Boutry, "Targeting the maize t-urf13 product into tobacco mitochondria confers methomyl sensitivity to mitochondrial respiration," *Proceedings of the National Academy of Sciences*, vol. 92, no. 4, pp. 1167–1171, 1995.

[40] M.-H. Chen, L.-F. Huang, H.-m. Li, Y.-R. Chen, and S.-M. Yu, "Signal peptide-dependent targeting of a rice α-amylase and cargo proteins to plastids and extracellular compartments of plant cells," *Plant physiology*, vol. 135, no. 3, pp. 1367–1377, 2004.

[41] A. Nott, H.-S. Jung, S. Koussevitzky, and J. Chory, "Plastid-to-nucleus retrograde signaling," *Annu. Rev. Plant Biol.*, vol. 57, pp. 739–759, 2006.

[42] D. M. Rhoads and C. C. Subbaiah, "Mitochondrial retrograde regulation in plants," *Mitochondrion*, vol. 7, no. 3, pp. 177–194, 2007.

[43] S. Ng, I. De Clercq, O. Van Aken, S. R. Law, A. Ivanova, P. Willems, E. Giraud, F. Van Breusegem, and J. Whelan, "Anterograde and retrograde regulation of nuclear genes encoding mitochondrial proteins during growth, development, and stress," *Molecular Plant*, vol. 7, no. 7, pp. 1075–1093, 2014.

[44] S. Greiner and R. Bock, "Tuning a ménage à trois: Co-evolution and co-adaptation of nuclear and organellar genomes in plants," *BioEssays*, vol. 35, no. 4, pp. 354–365, 2013.

[45] F. Roux, T. Mary-Huard, E. Barillot, E. Wenes, L. Botran, S. Durand, R. Vill-outreix, M.-L. Martin-Magniette, C. Camilleri, and F. Budar, "Cytonuclear interactions affect adaptive traits of the annual plant Arabidopsis thaliana in the field," *Proc. Natl. Acad. Sci. U. S. A.*, vol. 113, no. 13, pp. 3687–3692, 2016.

[46] V. S. Bogdanova, E. R. Galieva, and O. E. Kosterin, "Genetic analysis of nuclear-cytoplasmic incompatibility in pea associated with cytoplasm of an accession of wild subspecies pisum sativum subsp. elatius (bieb.) schmahl.," *Theoretical and applied genetics*, vol. 118, no. 4, pp. 801–809, 2009.

[47] L. M. Cosmides and J. Tooby, "Cytoplasmic inheritance and intragenomic conflict," *Journal of Theoretical Biology*, vol. 89, no. 1, pp. 83 – 129, 1981.

[48] D. Lewis, "Male sterility in natural populations of hermaphrodite plants. the equilibrium between females and hermaphrodites to be expected with different types of inheritance," *New Phytologist*, vol. 40, pp. 56–63, 1941.

[49] P. Touzet and F. Budar, "Unveiling the molecular arms race between two conflicting genomes in cytoplasmic male sterility?," *Trends Plant Sci.*, vol. 9, no. 12, pp. 568–570, 2004.

[50] J. D. Thompson and M. Tarayre, "Exploring the genetic basis and proximate causes of female fertility advantage in gynodioecious thymus vulgaris," *Evolution*, vol. 54, no. 5, pp. 1510–1520, 2000.

[51] M. Dufay and E. Billard, "How much better are females? the occurrence of female advantage, its proximal causes and its variation within and among gynodioecious species," *Ann. Bot.*, vol. 109, no. 3, pp. 505–519, 2012.

[52] M. R. Hanson and S. Bentolila, "Interactions of Mitochondrial and Nuclear Genes That Affect Male Gametophyte Development," *Plant Cell*, vol. 16, no. no suppl 1, pp. S154–S169, 2004.

[53] F. Budar, P. Touzet, and R. De Paepe, "The nucleo-mitochondrial conflict in cytoplasmic male sterilities revisited," *Genetica*, vol. 117, no. 1, pp. 3–16, 2003.

[54] L. F. Delph, P. Touzet, and M. F. Bailey, "Merging theory and mechanism in studies of gynodioecy," *Trends in Ecology & Evolution*, vol. 22, no. 1, pp. 17–24, 2007.

[55] K. D. Laser and N. R. Lersten, "Anatomy and cytology of microsporogenesis in cytoplasmic male sterile angiosperms," *The Botanical Review*, vol. 38, no. 3, pp. 425–454, 1972.

[56] P. Touzet, "Mitochondrial genome evolution and gynodioecy," *Advances in botanical research*, vol. 63, pp. 71–98, 2012.

[57] M. Landgren, M. Zetterstrand, E. Sundberg, and K. Glimelius, "Alloplasmic male-sterile brassica lines containing b. tournefortii mitochondria express an orf 3 of the atp6 gene and a 32 kda protein," *Plant molecular biology*, vol. 32, no. 5, pp. 879–890, 1996.

[58] R. Whitford, D. Fleury, J. C. Reif, M. Garcia, T. Okada, V. Korzun, and P. Langridge, "Hybrid breeding in wheat: technologies to improve hybrid wheat seed production," *Journal of experimental botany*, vol. 64, no. 18, pp. 5411–5428, 2013.

[59] L. Fishman and J. H. Willis, "A cytonuclear incompatibility causes anther sterility in mimulus hybrids," *Evolution*, vol. 60, no. 7, pp. 1372–1381, 2006.

[60] J. Leppälä and O. Savolainen, "Nuclear-cytoplasmic interactions reduce male fertility in hybrids of arabidopsis lyrata subspecies.," *Evolution; international journal of organic evolution*, vol. 65, no. 10, pp. 2959–2972, 2011.

[61] M. Rhoades, "Gene induced mutation of a heritable cytoplasmic factor producing male sterility in maize," *Proceedings of the National Academy of Sciences*, vol. 36, no. 11, pp. 634–635, 1950.

[62] C. W. Birky, "Transmission Genetics of Mitochondria and Chloroplasts," *Annu. Rev. Genet.*, vol. 12, no. 1, pp. 471–512, 1978.

[63] T. Kubo and K. J. Newton, "Angiosperm mitochondrial genomes and mutations," *Mitochondrion*, vol. 8, pp. 5–14, 2008.

[64] H. Tang, X. Zheng, C. Li, X. Xie, Y. Chen, L. Chen, X. Zhao, H. Zheng, J. Zhou, S. Ye, *et al.*, "Multi-step formation, evolution, and functionalization of new cytoplasmic male sterility genes in the plant mitochondrial genomes," *Cell research*, pp. 1–17, 2016.

[65] X. Peng, K. Wang, C. Hu, Y. Zhu, T. Wang, J. Yang, J. Tong, S. Li, and Y. Zhu, "The mitochondrial gene orfH79 plays a critical role in impairing both male gametophyte development and root growth in CMS-Honglian rice," *BMC Plant Biol.*, vol. 10, no. 1, p. 125, 2010.

[66] H. V. Tang, D. R. Pring, L. C. Shaw, R. A. Salazar, F. R. Muza, B. Yan, and K. F. Schertz, "Transcript processing internal to a mitochondrial open reading frame is

correlated with fertility restoration in male-sterile sorghum," *The Plant Journal*, vol. 10, no. 1, pp. 123–133, 1996.

[67] Y. L'Homme, R. J. Stahl, X.-Q. Li, A. Hameed, and G. G. Brown, "Brassica nap cytoplasmic male sterility is associated with expression of a mtdna region containing a chimeric gene similar to the pol cms-associated orf224 gene," *Current genetics*, vol. 31, no. 4, pp. 325–335, 1997.

[68] F. Budar and G. Pelletier, "Male sterility in plants: occurrence, determinism, significance and use," *Comptes Rendus de l'Acadmie des Sciences - Series III - Sciences de la Vie*, vol. 324, no. 6, pp. 543 – 550, 2001.

[69] Ashutosh, P. Kumar, V. Dinesh Kumar, P. C. Sharma, S. Prakash, and S. R. Bhat, "A Novel orf108 Co-Transcribed with the atpA Gene is Associated with Cytoplasmic Male Sterility in Brassica juncea Carrying Moricandia arvensis Cytoplasm," *Plant Cell Physiol.*, vol. 49, no. 2, pp. 284–289, 2008.

[70] S. Bonhomme, F. Budar, D. Lancelin, I. Small, M.-C. Defrance, and G. Pelletier, "Sequence and transcript analysis of the nco2.5 ogura-specific fragment correlated with cytoplasmic male sterility in brassica cybrids," *Molecular and General Genetics MGG*, vol. 235, no. 2, pp. 340–348, 1992.

[71] J. Heazlewood, J. Whelan, and A. Millar, "The products of the mitochondrial orf25 and orfb genes are fo components in the plant f1fo atp synthase," *Febs Letters*, vol. 540, no. 1-3, pp. 201–205, 2003.

[72] P. Yi, L. Wang, Q. Sun, and Y. Zhu, "Discovery of mitochondrial chimeric-gene associated with cytoplasmic male sterility of hl-rice," *Chinese Science Bulletin*, vol. 47, no. 9, pp. 744–747, 2002.

[73] C. Johns, M. Lu, a. Lyznik, and S. Mackenzie, "A mitochondrial DNA sequence is associated with abnormal pollen development in cytoplasmic male sterile bean plants.," *Plant Cell*, vol. 4, no. April, pp. 435–449, 1992.

[74] J. Rasmussen and M. R. Hanson, "A nadh dehydrogenase subunit gene is co-transcribed with the abnormal petunia mitochondrial gene associated with cytoplasmic male sterility," *Molecular and General Genetics MGG*, vol. 215, no. 2, pp. 332–336, 1989.

[75] E. G. Young and M. R. Hanson, "A fused mitochondrial gene associated with cytoplasmic male sterility is developmentally regulated," *Cell*, vol. 50, no. 1, pp. 41–49, 1987.

[76] P. S. Schnable and R. P. Wise, "The molecular basis of cytoplasmic male sterility and fertility restoration," *Trends Plant Sci.*, vol. 3, no. 5, pp. 175–180, 1998.

[77] C. D. Chase, "Cytoplasmic male sterility: a window to the world of plant mitochondrialnuclear interactions," *Trends Genet.*, vol. 23, no. 2, pp. 81–90, 2007.

[78] T. Kubo, K. Kitazaki, M. Matsunaga, H. Kagami, and T. Mikami, "Male Sterility-Inducing Mitochondrial Genomes: How Do They Differ?," *CRC. Crit. Rev. Plant Sci.*, vol. 30, no. 4, pp. 378–400, 2011.

[79] R. E. Dewey, C. S. Levings, and D. H. Timothy, "Novel recombinations in the maize mitochondrial genome produce a unique transcriptional unit in the texas male-sterile cytoplasm," *Cell*, vol. 44, no. 3, pp. 439–449, 1986.

[80] R. E. Dewey, D. H. Timothy, and C. S. Levings, "A mitochondrial protein associated with cytoplasmic male sterility in the t cytoplasm of maize," *Proceedings of the National Academy of Sciences*, vol. 84, no. 15, pp. 5374–5378, 1987.

[81] G. Zabala, S. Gabay-Laughnan, and J. R. Laughnan, "The nuclear gene rf3 affects the expression of the mitochondrial chimeric sequence r implicated in s-type male sterility in maize," *Genetics*, vol. 147, no. 2, pp. 847–860, 1997.

[82] S. Bonhomme, F. Budar, M. Férault, and G. Pelletier, "A 2.5 kb ncoi fragment of ogura radish mitochondrial dna is correlated with cytoplasmic male-sterility in brassica cybrids," *Current Genetics*, vol. 19, no. 2, pp. 121–127, 1991.

[83] M. Grelon, F. Budar, S. Bonhomme, and G. Pelletier, "Ogura cytoplasmic male-sterility (CMS)-associated orf138 is translated into a mitochondrial membrane polypeptide in male-sterile Brassica cybrids," *Mol. Gen. Genet.*, vol. 243, pp. 540–547, 1994.

[84] K. Kitazaki and T. Kubo, "Cost of having the largest mitochondrial genome: evolutionary mechanism of plant mitochondrial genome," *Journal of Botany*, vol. 2010, 2010.

[85] A. Darracq, J.-S. Varré, L. Maréchal-Drouard, A. Courseaux, V. Castric, P. Saumitou-Laprade, S. Oztas, P. Lenoble, B. Vacherie, V. Barbe, *et al.*, "Structural and content diversity of mitochondrial genome in beet: a comparative genomic analysis," *Genome Biology and Evolution*, vol. 3, pp. 723–736, 2011.

[86] Y. D. Jo, Y. Choi, D.-H. Kim, B.-D. Kim, and B.-C. Kang, "Extensive structural variations between mitochondrial genomes of cms and normal peppers (capsicum

annuum l.) revealed by complete nucleotide sequencing," *BMC genomics*, vol. 15, no. 1, pp. 561–575, 2014.

[87] L. Gaborieau, G. G. Brown, and H. Mireau, "The propensity of pentatricopeptide repeat genes to evolve into restorers of cytoplasmic male sterility," *Frontiers in Plant Science*, vol. 7, p. 1816, 2016.

[88] M. Singh, N. Hamel, R. Menasaa, X.-Q. Li, B. Young, M. Jean, B. S. Landry, and G. G. Brown, "Nuclear genes associated with a single brassica cms restorer locws influence transcripts of three different mitochondrial gene regions," *Genetics*, vol. 143, no. 1, pp. 505–516, 1996.

[89] D. Luo, H. Xu, Z. Liu, J. Guo, H. Li, L. Chen, C. Fang, Q. Zhang, M. Bai, N. Yao, H. Wu, H. Wu, C. Ji, H. Zheng, Y. Chen, S. Ye, X. Li, X. Zhao, R. Li, and Y.-G. Liu, "A detrimental mitochondrial-nuclear interaction causes cytoplasmic male sterility in rice," *Nat Genet*, vol. 45, no. 5, pp. 573–577, 2013.

[90] P. Kumar, N. Vasupalli, R. Srinivasan, and S. R. Bhat, "An evolutionarily conserved mitochondrial orf108 is associated with cytoplasmic male sterility in different allo-plasmic lines of Brassica juncea and induces male sterility in transgenic Arabidopsis thaliana," *J. Exp. Bot.*, vol. 63, no. 8, pp. 2921–2932, 2012.

[91] V. Naresh, S. K. Singh, A. Watts, P. Kumar, V. Kumar, K. R. S. S. Rao, and S. R. Bhat, "Mutations in the mitochondrial orf108 render Moricandia arvensis restorer ineffective in restoring male fertility to Brassica oxyrrhina-based cytoplasmic male sterile line of B. juncea," *Molecular Breeding*, vol. 36, no. 6, pp. 36–37, 2016.

[92] Z. Wang, Y. Zou, X. Li, Q. Zhang, L. Chen, H. Wu, D. Su, Y. Chen, J. Guo, D. Luo, Y. Long, Y. Zhong, Y.-G. Liu, W. Zhonghua, Z. Yanjiao, L. Xiaoyu, Z. Qunyu, C. Letian, W. Hao, S. Dihua, C. Yuanling, G. Jingxin, L. Da, L. Yunming, Z. Yang, and L. Yao-Guang, "Cytoplasmic Male Sterility of Rice with Boro II Cytoplasm Is Caused by a Cytotoxic Peptide and Is Restored by Two Related PPR Motif Genes via Distinct Modes of mRNA Silencing," *Plant Cell Online*, vol. 18, no. 3, pp. 676–687, 2006.

[93] M. Singh and G. G. Brown, "Suppression of cytoplasmic male sterility by nuclear genes alters expression of a novel mitochondrial gene region.," *The Plant Cell*, vol. 3, no. 12, pp. 1349–1362, 1991.

[94] K. D. Pruitt and M. R. Hanson, "Transcription of the petunia mitochondrial cms-associated pcf locus in male sterile and fertility-restored lines," *Molecular and General Genetics MGG*, vol. 227, no. 3, pp. 348–355, 1991.

[95] A. R. Abad, B. J. Mehrtens, and S. A. Mackenzie, "Specific expression in reproductive tissues and fate of a mitochondrial sterility-associated protein in cytoplasmic male-sterile bean," *Plant Cell*, vol. 7, no. 3, pp. 271–285, 1995.

[96] F. Moneger, C. Smart, and C. Leaver, "Nuclear restoration of cytoplasmic male sterility in sunflower is associated with the tissue-specific regulation of a novel mitochondrial gene.," *The EMBO journal*, vol. 13, no. 1, p. 8, 1994.

[97] R. Geddy, L. Mahé, and G. G. Brown, "Cell-specific regulation of a Brassica napus CMS-associated gene by a nuclear restorer with related effects on a floral homeotic gene promoter," *Plant J.*, vol. 41, no. 3, pp. 333–345, 2004.

[98] S. Bentolila, A. A. Alfonso, and M. R. Hanson, "A pentatricopeptide repeat-containing gene restores fertility to cytoplasmic male-sterile plants," *Proceedings of the National Academy of Sciences*, vol. 99, no. 16, pp. 10887–10892, 2002.

[99] I. D. Small and N. Peeters, "The ppr motif–a tpr-related motif prevalent in plant organellar proteins," *Trends in biochemical sciences*, vol. 25, no. 2, pp. 45–47, 2000.

[100] M. Uyttewaal, N. Arnal, M. Quadrado, A. Martin-Canadell, N. Vrielynck, S. Hiard, H. Gherbi, A. Bendahmane, F. Budar, and H. Mireau, "Characterization of Raphanus sativus Pentatricopeptide Repeat Proteins Encoded by the Fertility Restorer Locus for Ogura Cytoplasmic Male Sterility," *Plant Cell Online*, vol. 20, no. 12, pp. 3331–3345, 2008.

[101] E. Itabashi, N. Iwata, S. Fujii, T. Kazama, and K. Toriyama, "The fertility restorer gene, rf2, for lead rice-type cytoplasmic male sterility of rice encodes a mitochondrial glycine-rich protein," *The plant journal*, vol. 65, no. 3, pp. 359–367, 2011.

[102] H. Janska, R. Sarria, M. Woloszynska, M. Arrieta-Montiel, and S. A. Mackenzie, "Stoichiometric shifts in the common bean mitochondrial genome leading to male sterility and spontaneous reversion to fertility," *The Plant Cell*, vol. 10, no. 7, pp. 1163–1180, 1998.

[103] S. Fujii and K. Toriyama, "Suppressed expression of Retrograde-Regulated Male Sterility restores pollen fertility in cytoplasmic male sterile rice plants.," *Proc. Natl. Acad. Sci. U. S. A.*, vol. 106, pp. 9513–9518, 2009.

[104] L. Wen, K. L. Ruesch, V. M. Ortega, T. L. Kamps, S. Gabay-Laughnan, and C. D. Chase, "A nuclear restorer-of-fertility mutation disrupts accumulation of mitochondrial atp synthase subunit α in developing pollen of s male-sterile maize," *Genetics*, vol. 165, no. 2, pp. 771–779, 2003.

[105] X. Cui, R. P. Wise, and P. S. Schnable, "The rf2 nuclear restorer gene of male-sterile t-cytoplasm maize," *Science*, vol. 272, no. 5266, p. 1334, 1996.

[106] F. Liu, X. Cui, H. T. Horner, H. Weiner, and P. S. Schnable, "Mitochondrial aldehyde dehydrogenase activity is required for male fertility in maize," *The Plant Cell*, vol. 13, no. 5, pp. 1063–1078, 2001.

[107] R. Wise, A. Fliss, D. Pring, and B. Gengenbach, "urf13-t of t cytoplasm maize mitochondria encodes a 13 kd polypeptide," *Plant molecular biology*, vol. 9, no. 2, pp. 121–126, 1987.

[108] J. Kennell, R. Wise, and D. Pring, "Influence of nuclear background on transcription of a maize mitochondrial region associated with texas male sterile cytoplasm," *Molecular and General Genetics MGG*, vol. 210, no. 3, pp. 399–406, 1987.

[109] J. C. Kennell and D. R. Pring, "Initiation and processing of atp6, t-urf13 and orf221 transcripts from mitochondria of t cytoplasm maize," *Molecular and General Genetics MGG*, vol. 216, no. 1, pp. 16–24, 1989.

[110] R. Dewey, D. Timothy, and C. Levings, "Chimeric mitochondrial genes expressed in the c male-sterile cytoplasm of maize," *Current genetics*, vol. 20, no. 6, pp. 475–482, 1991.

[111] J. Hu, K. Wang, W. Huang, G. Liu, Y. Gao, J. Wang, Q. Huang, Y. Ji, X. Qin, L. Wan, *et al.*, "The rice pentatricopeptide repeat protein rf5 restores fertility in hong-lian cytoplasmic male-sterile lines via a complex with the glycine-rich protein grp162," *The Plant Cell*, vol. 24, no. 1, pp. 109–122, 2012.

[112] H. Akagi, M. Sakamoto, C. Shinjyo, H. Shimada, and T. Fujimura, "A unique sequence located downstream from the rice mitochondrialatp6 may cause male sterility," *Current genetics*, vol. 25, no. 1, pp. 52–58, 1994.

[113] M. Iwabuchi, J. Kyozuka, and K. Shimamoto, "Processing followed by complete editing of an altered mitochondrial atp6 rna restores fertility of cytoplasmic male sterile rice.," *The EMBO Journal*, vol. 12, no. 4, p. 1437, 1993.

[114] K.-i. Kadowaki, T. Suzuki, and S. Kazama, "A chimeric gene containing the 5 portion of atp6 is associated with cytoplasmic male-sterility of rice," *Molecular and General Genetics MGG*, vol. 224, no. 1, pp. 10–16, 1990.

[115] T. Kazama, Y. Yagi, K. Toriyama, and T. Nakamura, "Heterogeneity of the 5-end in plant mRNA may be involved in mitochondrial translation," *Front. Plant Sci.*, vol. 4, 2013.

[116] Z. Wang, Y. Zou, X. Li, Q. Zhang, L. Chen, H. Wu, D. Su, Y. Chen, J. Guo, D. Luo, Y. Long, Y. Zhong, and Y.-G. Liu, "Cytoplasmic male sterility of rice with boro ii cytoplasm is caused by a cytotoxic peptide and is restored by two related ppr motif genes via distinct modes of mrna silencing," *The Plant Cell Online*, vol. 18, no. 3, pp. 676–687, 2006.

[117] E. Itabashi, T. Kazama, and K. Toriyama, "Characterization of cytoplasmic male sterility of rice with Lead Rice cytoplasm in comparison with that with Chinsurah Boro II cytoplasm," *Plant Cell Rep.*, vol. 28, no. 2, pp. 233–239, 2009.

[118] T. Kazama, E. Itabashi, S. Fujii, T. Nakamura, and K. Toriyama, "Mitochondrial orf79 levels determine pollen abortion in cytoplasmic male sterile rice," *The Plant Journal*, vol. 85, no. 6, pp. 707–716, 2016.

[119] S. Fujii and K. Toriyama, "Suppressed expression of retrograde-regulated male sterility restores pollen fertility in cytoplasmic male sterile rice plants," *Proceedings of the National Academy of Sciences*, vol. 106, no. 23, pp. 9513–9518, 2009.

[120] S. Fujii, T. Kazama, M. Yamada, and K. Toriyama, "Discovery of global genomic re-organization based on comparison of two newly sequenced rice mitochondrial genomes with cytoplasmic male sterility-related genes," *Bmc Genomics*, vol. 11, no. 1, p. 209, 2010.

[121] Z.-L. Liu, H. Xu, J.-X. Guo, and Y.-G. Liu, "Structural and expressional variations of the mitochondrial genome conferring the wild abortive type of cytoplasmic male sterility in rice," *Journal of Integrative Plant Biology*, vol. 49, no. 6, pp. 908–914, 2007.

[122] R. Menassa, Y. LHomme, and G. G. Brown, "Post-transcriptional and developmental regulation of a cms-associated mitochondrial gene region by a nuclear restorer gene," *The Plant Journal*, vol. 17, no. 5, pp. 491–499, 1999.

[123] E. Ducos, P. Touzet, and M. Boutry, "The male sterile G cytoplasm of wild beet displays modified mitochondrial respiratory complexes," *Plant J.*, vol. 26, pp. 171–180, 2001.

[124] R. Horn, R. H. Köhler, and K. Zetsche, "A mitochondrial 16 kDa protein is associated with cytoplasmic male sterility in sunflower," *Plant Mol. Biol.*, vol. 17, pp. 29–36, 1991.

[125] H. Laver, S. Reynolds, F. Moneger, and C. Leaver, "Mitochondrial genome organization and expression associated with cytoplasmic male sterility in sunflower (helianthus annuus)," *The Plant Journal*, vol. 1, no. 2, pp. 185–193, 1991.

[126] R. Horn, B. Kusterer, E. Lazarescu, M. Prüfe, and W. Friedt, "Molecular mapping of the rf1 gene restoring pollen fertility in pet1-based f 1 hybrids in sunflower (helianthus annuus l.)," *TAG Theoretical and Applied Genetics*, vol. 106, no. 4, pp. 599–606, 2003.

[127] D. H. Kim, J. G. Kang, and B.-D. Kim, "Isolation and characterization of the cytoplasmic male sterility-associated orf456 gene of chili pepper (capsicum annuum l.)," *Plant Molecular Biology*, vol. 63, no. 4, pp. 519–532, 2007.

[128] S. Kim, H. Lim, S. Park, K.-H. Cho, S.-K. Sung, D.-G. Oh, and K.-T. Kim, "Identification of a novel mitochondrial genome type and development of molecular markers for cytoplasm classification in radish (raphanus sativus l.)," *Theoretical and applied genetics*, vol. 115, no. 8, pp. 1137–1145, 2007.

[129] G. Gulyas, Y. Shin, H. Kim, J.-S. Lee, and Y. Hirata, "Altered transcript reveals an orf507 sterility-related gene in chili pepper (capsicum annuum l.)," *Plant molecular biology reporter*, vol. 28, no. 4, pp. 605–612, 2010.

[130] Y. D. Jo, Y. Ha, J.-H. Lee, M. Park, A. C. Bergsma, H.-I. Choi, S. Goritschnig, B. Kloosterman, P. J. van Dijk, D. Choi, *et al.*, "Fine mapping of restorer-of-fertility in pepper (capsicum annuum l.) identified a candidate gene encoding a pentatricopeptide repeat (ppr)-containing protein," *Theoretical and applied genetics*, vol. 129, no. 10, pp. 2003–2017, 2016.

[131] H. T. Nivison and M. R. Hanson, "Identification of a mitochondrial protein associated with cytoplasmic male sterility in petunia.," *Plant Cell*, vol. 1, no. November, pp. 1121–1130, 1989.

[132] J. D. Gillman, S. Bentolila, and M. R. Hanson, "The petunia restorer of fertility protein is part of a large mitochondrial complex that interacts with transcripts of the CMS-associated locus," *Plant J.*, vol. 49, no. 2, pp. 217–227, 2007.

[133] R. Klein, P. Klein, J. Mullet, P. Minx, W. Rooney, and K. Schertz, "Fertility restorer locus rf1 of sorghum (sorghum bicolor l.) encodes a pentatricopeptide repeat protein not present in the colinear region of rice chromosome 12," *Theoretical and Applied Genetics*, vol. 111, no. 6, pp. 994–1012, 2005.

[134] A. L. Case and J. H. Willis, "Hybrid male sterility in mimulus (phrymaceae) is associated with a geographically restricted mitochondrial rearrangement," *Evolution*, vol. 62, no. 5, pp. 1026–1039, 2008.

[135] C. M. Barr and L. Fishman, "The nuclear component of a cytonuclear hybrid incompatibility in mimulus maps to a cluster of pentatricopeptide repeat genes," *Genetics*, vol. 184, no. 2, pp. 455–465, 2010.

[136] A. H. Millar, I. D. Small, D. A. Day, and J. Whelan, "Mitochondrial biogenesis and function in arabidopsis," *The Arabidopsis Book*, p. e0111, 2008.

[137] D. C. Logan, "The dynamic plant chondriome," *Semin. Cell Dev. Biol.*, vol. 21, no. 6, pp. 550–557, 2010.

[138] R. P. Jacoby, L. Li, S. Huang, C. Pong Lee, a. H. Millar, and N. L. Taylor, "Mitochondrial Composition, Function and Stress Response in Plants," *J. Integr. Plant Biol.*, vol. 54, no. 11, pp. 887–906, 2012.

[139] P. Giegé, J. L. Heazlewood, U. Roessner-Tunali, A. H. Millar, A. R. Fernie, C. J. Leaver, and L. J. Sweetlove, "Enzymes of glycolysis are functionally associated with the mitochondrion in arabidopsis cells," *The Plant Cell*, vol. 15, no. 9, pp. 2140–2151, 2003.

[140] A. G. Rasmusson, V. Heiser, E. Zabaleta, A. Brennicke, and L. Grohmann, "Physiological, biochemical and molecular aspects of mitochondrial complex i in plants," *Biochimica et Biophysica Acta (BBA)-Bioenergetics*, vol. 1364, no. 2, pp. 101–111, 1998.

[141] N. Dudkina, S. Sunderhaus, E. Boekema, and H.-P. Braun, "The higher level of organization of the oxidative phosphorylation system: mitochondrial supercomplexes," *J. Bioenerg. Biomembr.*, vol. 40, no. 5, pp. 419–424, 2008.

[142] M. L. Genova and G. Lenaz, "Functional role of mitochondrial respiratory supercomplexes," *Biochimica et Biophysica Acta (BBA)-Bioenergetics*, vol. 1837, no. 4, pp. 427–443, 2014.

[143] O. Van Aken, E. Giraud, R. Clifton, and J. Whelan, "Alternative oxidase: a target and regulator of stress responses," *Physiologia plantarum*, vol. 137, no. 4, pp. 354–361, 2009.

[144] M. P. Murphy, "How mitochondria produce reactive oxygen species," *Biochemical Journal*, vol. 417, no. 1, pp. 1–13, 2009.

[145] M. Ott, V. Gogvadze, S. Orrenius, and B. Zhivotovsky, "Mitochondria, oxidative stress and cell death," *Apoptosis*, vol. 12, no. 5, pp. 913–922, 2007.

[146] S. W. Tait and D. R. Green, "Mitochondria and cell death: outer membrane permeabilization and beyond," *Nature reviews. Molecular cell biology*, vol. 11, no. 9, p. 621, 2010.

[147] O. Van Aken and F. Van Breusegem, "Licensed to Kill: Mitochondria, Chloroplasts, and Cell Death," *Trends Plant Sci.*, vol. 20, no. 11, pp. 754–766, 2015.

[148] R. Mittler, S. Vanderauwera, M. Gollery, and F. Van Breusegem, "Reactive oxygen gene network of plants," *Trends in Plant Science*, vol. 9, no. 10, pp. 490–498, 2004.

[149] M. Schwarzländer and I. Finkemeier, "Mitochondrial Energy and Redox Signaling in Plants," *Antioxid. Redox Signal.*, vol. 18, no. 16, pp. 2122–2144, 2012.

[150] R. Mittler, "Ros are good," *Trends in plant science*, vol. 22, no. 1, pp. 11–19, 2017.

[151] K.-J. Dietz, R. Mittler, and G. Noctor, "Recent progress in understanding the role of reactive oxygen species in plant cell signaling," *Plant physiology*, vol. 171, no. 3, pp. 1535–1539, 2016.

[152] S. Mangano, S. P. D. Juárez, and J. M. Estevez, "Ros regulation of polar growth in plant cells," *Plant physiology*, vol. 171, no. 3, pp. 1593–1605, 2016.

[153] C. Gapper and L. Dolan, "Control of plant development by reactive oxygen species," *Plant physiology*, vol. 141, no. 2, pp. 341–345, 2006.

[154] C. H. Foyer and G. Noctor, "Stress-triggered redox signalling: what's in prospect?," *Plant, cell & environment*, vol. 39, no. 5, pp. 951–964, 2016.

[155] L.-J. Quan, B. Zhang, W.-W. Shi, and H.-Y. Li, "Hydrogen peroxide in plants: a versatile molecule of the reactive oxygen species network," *Journal of Integrative Plant Biology*, vol. 50, no. 1, pp. 2–18, 2008.

[156] S. Huang, O. Van Aken, M. Schwarzländer, K. Belt, and A. H. Millar, "The roles of mitochondrial reactive oxygen species in cellular signaling and stress response in plants," *Plant physiology*, vol. 171, no. 3, pp. 1551–1559, 2016.

[157] G. C. Vanlerberghe, "Alternative oxidase: a mitochondrial respiratory pathway to maintain metabolic and signaling homeostasis during abiotic and biotic stress in plants," *International Journal of Molecular Sciences*, vol. 14, no. 4, pp. 6805–6847, 2013.

[158] K. Apel and H. Hirt, "Reactive oxygen species: metabolism, oxidative stress, and signal transduction," *Annu. Rev. Plant Biol.*, vol. 55, pp. 373–399, 2004.

[159] J. G. Scandalios, W.-F. Tong, and D. G. Roupakias, "Cat3, a third gene locus coding for a tissue-specific catalase in maize: Genetics, intracellular location, and some biochemical properties," *Molecular and General Genetics MGG*, vol. 179, no. 1, pp. 33–41, 1980.

[160] H. Willekens, D. Inzé, M. Van Montagu, and W. Van Camp, "Catalases in plants," *Molecular Breeding*, vol. 1, no. 3, pp. 207–228, 1995.

[161] C. Foyer and G. Noctor, "Oxygen processing in photosynthesis: regulation and signaling," *New Phytol*, vol. 146, pp. 359–388, 2000.

[162] O. Chew, J. Whelan, and A. H. Millar, "Molecular definition of the ascorbate-glutathione cycle in arabidopsis mitochondria reveals dual targeting of antioxidant defenses in plants," *Journal of Biological Chemistry*, vol. 278, no. 47, pp. 46869–46877, 2003.

[163] C. H. Foyer and G. Noctor, "Ascorbate and glutathione: the heart of the redox hub," *Plant physiology*, vol. 155, no. 1, pp. 2–18, 2011.

[164] M. Schwarzlnder, M. Fricker, C. Mller, L. Marty, T. Brach, J. Novak, L. Sweetlove, R. Hell, and A. Meyer, "Confocal imaging of glutathione redox potential in living plant cells," *Journal of Microscopy*, vol. 231, no. 2, pp. 299–316, 2008.

[165] M. Schwarzländer, T. P. Dick, A. J. Meyer, and B. Morgan, "Dissecting redox biology using fluorescent protein sensors," *Antioxidants & redox signaling*, vol. 24, no. 13, pp. 680–712, 2016.

[166] J. Hu, L. Dong, and C. E. Outten, "The redox environment in the mitochondrial intermembrane space is maintained separately from the cytosol and matrix," *Journal of Biological Chemistry*, vol. 283, no. 43, pp. 29126–29134, 2008.

[167] I. Tzafrir, R. Pena-Muralla, A. Dickerman, M. Berg, R. Rogers, S. Hutchens, T. C. Sweeney, J. McElver, G. Aux, D. Patton, *et al.*, "Identification of genes required for embryo development in arabidopsis," *Plant physiology*, vol. 135, no. 3, pp. 1206–1220, 2004.

[168] L. Marty, W. Siala, M. Schwarzländer, M. D. Fricker, M. Wirtz, L. J. Sweetlove, Y. Meyer, A. J. Meyer, J.-P. Reichheld, and R. Hell, "The NADPH-dependent

thioredoxin system constitutes a functional backup for cytosolic glutathione reductase in Arabidopsis.," *Proc. Natl. Acad. Sci. U. S. A.*, vol. 106, no. 22, pp. 9109–9114, 2009.

[169] D. C. Logan, "Plant mitochondrial dynamics," *Biochim. Biophys. Acta - Mol. Cell Res.*, vol. 1763, pp. 430–441, 2006.

[170] K. Mitra, C. Wunder, B. Roysam, G. Lin, and J. Lippincott-Schwartz, "A hyperfused mitochondrial state achieved at g1–s regulates cyclin e buildup and entry into s phase," *Proceedings of the National Academy of Sciences*, vol. 106, no. 29, pp. 11960–11965, 2009.

[171] J. M. Seguí-Simarro, M. J. Coronado, and L. A. Staehelin, "The mitochondrial cycle of arabidopsis shoot apical meristem and leaf primordium meristematic cells is defined by a perinuclear tentaculate/cage-like mitochondrion," *Plant physiology*, vol. 148, no. 3, pp. 1380–1393, 2008.

[172] G. Zinta, A. Khan, H. AbdElgawad, V. Verma, and A. K. Srivastava, "Unveiling the Redox Control of Plant Reproductive Development during Abiotic Stress," *Front. Plant Sci.*, vol. 7, no. June, pp. 1–6, 2016.

[173] C. J. Smart, F. Monéger, and C. J. Leaver, "Cell-specific regulation of gene expression in mitochondria during anther development in sunflower.," *Plant Cell*, vol. 6, no. June, pp. 811–825, 1994.

[174] L.-Y. Wen and C. D. Chase, "Mitochondrial gene expression in developing male gametophytes of male-fertile and s male-sterile maize," *Sexual Plant Reproduction*, vol. 11, no. 6, pp. 323–330, 1999.

[175] M. Sabar, D. Gagliardi, J. Balk, and C. J. Leaver, "Orfb is a subunit of f1 fo-atp synthase: insight into the basis of cytoplasmic male sterility in sunflower," *EMBO reports*, vol. 4, no. 4, pp. 381–386, 2003.

[176] K. Wang, F. Gao, Y. Ji, Y. Liu, Z. Dan, P. Yang, Y. Zhu, and S. Li, "ORFH79 impairs mitochondrial function via interaction with a subunit of electron transport chain complex III in Honglian cytoplasmic male sterile rice," *New Phytologist*, vol. 198, no. 2, pp. 408–418, 2013.

[177] P. Touzet and E. H. Meyer, "Cytoplasmic male sterility and mitochondrial metabolism in plants," *Mitochondrion*, vol. 19, pp. 166–171, 2014.

[178] D. Rhoads, C. Levings III, and J. Siedow, "URF13, a ligand-gated, pore-forming receptor for T-toxin in the inner membrane ofcms-T mitochondria," *J. Bioenerg. Biomembr.*, vol. 27, no. 4, pp. 437–445, 1995.

[179] R. Flavell, "A model for the mechanism of cytoplasmic male sterility in plants, with special reference to maize," *Plant Sci. Lett.*, vol. 3, no. 4, pp. 259–263, 1974.

[180] D. H. Gonzalez, E. Welchen, C. V. Attallah, R. N. Comelli, and E. F. Mufarrege, "Transcriptional coordination of the biogenesis of the oxidative phosphorylation machinery in plants," *The Plant Journal*, vol. 51, no. 1, pp. 105–116, 2007.

[181] C. P. Lee, H. Eubel, C. Solheim, and A. H. Millar, "Mitochondrial proteome heterogeneity between tissues from the vegetative and reproductive stages of arabidopsis thaliana development," *Journal of proteome research*, vol. 11, no. 6, pp. 3326–3343, 2012.

[182] L. Huang, J. Xiang, J. Liu, T. Rong, J. Wang, Y. Lu, Q. Tang, W. Wen, and M. Cao, "Expression characterization of genes for cms-c in maize," *Protoplasma*, vol. 249, no. 4, pp. 1119–1127, 2012.

[183] Y. Duroc, S. Hiard, N. Vrielynck, S. Ragu, and F. Budar, "The ogura sterility-inducing protein forms a large complex without interfering with the oxidative phosphorylation components in rapeseed mitochondria," *Plant molecular biology*, vol. 70, no. 1-2, pp. 123–137, 2009.

[184] P. González-Melendi, M. Uyttewaal, C. N. Morcillo, J. R. Hernández Mora, S. Fajardo, F. Budar, and M. M. Lucas, "A light and electron microscopy analysis of the events leading to male sterility in ogu-inra cms of rapeseed (brassica napus)," *Journal of Experimental Botany*, vol. 59, no. 4, pp. 827–838, 2008.

[185] S. Li, D. Yang, and Y. Zhu, "Characterization and Use of Male Sterility in Hybrid Rice Breeding," vol. 49, no. 6, pp. 791–804, 2007.

[186] S.-L. J. Lee, V. Gracen, and E. Earle, "The cytology of pollen abortion in c-cytoplasmic male-sterile corn anthers," *American Journal of Botany*, pp. 656–667, 1979.

[187] H. Warmke and S.-L. J. LEE, "Mitochondrial degeneration in texas cytoplasmic male-sterile corn anthers," *Journal of Heredity*, vol. 68, no. 4, pp. 213–222, 1977.

[188] J. Balk and C. J. Leaver, "The PET1-CMS Mitochondrial Mutation in Sunflower Is Associated with Premature Programmed Cell Death and Cytochrome c Release ," *Plant Cell*, vol. 13, no. 8, pp. 1803–1818, 2001.

[189] S. Fujii and K. Toriyama, "Molecular mapping of the fertility restorer gene for ms-cw-type cytoplasmic male sterility of rice," *Theoretical and applied genetics*, vol. 111, no. 4, pp. 696–701, 2005.

[190] S.-L. J. Lee, E. Earle, and V. Gracen, "The cytology of pollen abortion in s cytoplasmic male-sterile corn anthers," *American Journal of Botany*, pp. 237–245, 1980.

[191] S. Kaul, H. L. Koo, J. Jenkins, M. Rizzo, T. Rooney, L. J. Tallon, T. Feldblyum, W. Nierman, M. I. Benito, X. Lin, *et al.*, "Analysis of the genome sequence of the flowering plant arabidopsis thaliana," *nature*, vol. 408, no. 6814, pp. 796–815, 2000.

[192] . G. Consortium *et al.*, "1,135 genomes reveal the global pattern of polymorphism in arabidopsis thaliana," *Cell*, vol. 166, no. 2, pp. 481–491, 2016.

[193] N. Gobron, C. Waszczak, M. Simon, S. Hiard, S. Boivin, D. Charif, A. Ducamp, E. Wenes, and F. Budar, "A cryptic cytoplasmic male sterility unveils a possible gynodioecious past for arabidopsis thaliana," *PLOS ONE*, vol. 8, no. 4, pp. 1–13, 2013.

[194] M. Simon, *Genetic analysis of an hybrid sterility in Arabidopsis thaliana.* Theses, Université Paris-Saclay, 2015.

[195] M. Simon, S. Durand, N. Pluta, N. Gobron, L. Botran, A. Ricou, C. Camilleri, and F. Budar, "Genomic conflicts that cause pollen mortality and raise reproductive barriers in arabidopsis thaliana," *Genetics*, vol. 203, no. 3, pp. 1353–1367, 2016.

[196] J. Forner, B. Weber, S. Thuss, S. Wildum, and S. Binder, "Mapping of mitochondrial mrna termini in arabidopsis thaliana : t-elements contribute to 5 and 3 end formation," *Nucleic Acids Research*, vol. 35, no. 11, pp. 3676–3692, 2007.

[197] J. Kuhn and S. Binder, "RTPCR analysis of 5 to 3-end-ligated mRNAs identifies the extremities of cox2 transcripts in pea mitochondria," *Nucleic Acids Res.*, vol. 30, no. 2, pp. 439–446, 2002.

[198] B. Jing, S. Heng, D. Tong, Z. Wan, T. Fu, J. Tu, C. Ma, B. Yi, J. Wen, and J. Shen, "A male sterility-associated cytotoxic protein ORF288 in Brassica juncea causes aborted pollen development," *J. Exp. Bot.*, vol. 63, no. 3, pp. 1285–1295, 2012.

[199] Y. Duroc, C. Gaillard, S. Hiard, C. Tinchant, R. Berthomé, G. Pelletier, and F. Budar, "Nuclear expression of a cytoplasmic male sterility gene modifies mitochondrial

morphology in yeast and plant cells," *Plant Science*, vol. 170, no. 4, pp. 755–767, 2006.

[200] X. Ge, H. Wang, and K. Cao, "Transformation by t-dna integration causes highly sterile phenotype independent of transgenes in arabidopsis thaliana," *Plant cell reports*, vol. 27, no. 8, pp. 1341–1348, 2008.

[201] S. Behera, C. Wang, N.and Zhang, I. Schmitz-Thom, S. Strohkamp, S. Schltke, K. Hashimoto, L. Xiong, and J. Kudla, "Analyses of ca2+ dynamics using a ubiquitin-10 promoter-driven yellow cameleon 3.6 indicator reveal reliable transgene expression and differences in cytoplasmic ca2+ responses in arabidopsis and rice (oryza sativa) roots," *New Phytologist*, vol. 206, no. 2, pp. 751–760, 2015. 2014-18478.

[202] J.-L. Gallois, J. Drouaud, A. Lécureuil, A. Guyon-Debast, S. Bonhomme, and P. Guerche, "Functional characterization of the plant ubiquitin regulatory X (UBX) domain-containing protein AtPUX7 in Arabidopsis thaliana.," *Gene*, vol. 526, no. 2, pp. 299–308, 2013.

[203] R. Swanson, T. Clark, and D. Preuss, "Expression profiling of arabidopsis stigma tissue identifies stigma-specific genes," *Sexual Plant Reproduction*, vol. 18, no. 4, pp. 163–171, 2005.

[204] M. Borg, L. Brownfield, H. Khatab, A. Sidorova, M. Lingaya, and D. Twell, "The R2R3 MYB transcription factor DUO1 activates a male germline-specific regulon essential for sperm cell differentiation in Arabidopsis.," *Plant Cell*, vol. 23, no. 2, pp. 534–549, 2011.

[205] K. Khn, A. Weihe, and T. Brner, "Multiple promoters are a common feature of mitochondrial genes in arabidopsis," *Nucleic Acids Research*, vol. 33, no. 1, pp. 337–346, 2005.

[206] S. Binder, K. Stoll, and B. Stoll, "Maturation of 5 ends of plant mitochondrial rnas," *Physiologia Plantarum*, vol. 157, no. 3, pp. 280–288, 2016.

[207] S. Fujii, T. Toda, S. Kikuchi, R. Suzuki, K. Yokoyama, H. Tsuchida, K. Yano, and K. Toriyama, "Transcriptome map of plant mitochondria reveals islands of unexpected transcribed regions," *BMC Genomics*, vol. 12, no. 1, pp. 279–287, 2011.

[208] A. Barkan, M. Rojas, S. Fujii, A. Yap, Y. S. Chong, C. S. Bond, and I. Small, "A combinatorial amino acid code for rna recognition by pentatricopeptide repeat proteins," *PLOS Genetics*, vol. 8, no. 8, pp. 1–8, 2012.

[209] T. Kubo, A. Yoshimura, and N. Kurata, "Hybrid Male Sterility in Rice Is Due to Epistatic Interactions with a Pollen Killer Locus," *Genetics*, vol. 189, no. 3, pp. 1083–1092, 2011.

[210] S. Casson, M. Spencer, K. Walker, and K. Lindsey, "Laser capture microdissection for the analysis of gene expression during embryogenesis of arabidopsis," *The Plant Journal*, vol. 42, no. 1, pp. 111–123, 2005.

[211] S. Bonhomme, C. Horlow, D. Vezon, S. de Laissardière, A. Guyon, M. Férault, M. Marchand, N. Bechtold, and G. Pelletier, "T-dna mediated disruption of essential gametophytic genes in arabidopsis is unexpectedly rare and cannot be inferred from segregation distortion alone," *Molecular and General Genetics MGG*, vol. 260, no. 5, pp. 444–452, 1998.

[212] J. Mantis and B. W. Tague, "Comparing the utility of β-glucuronidase and green fluorescent protein for detection of weak promoter activity inarabidopsis thaliana," *Plant Molecular Biology Reporter*, vol. 18, no. 4, pp. 319–330, 2000.

[213] M. P. Yamamoto, H. Shinada, Y. Onodera, C. Komaki, T. Mikami, and T. Kubo, "A male sterility-associated mitochondrial protein in wild beets causes pollen disruption in transgenic plants," *The Plant Journal*, vol. 54, no. 6, pp. 1027–1036, 2008.

[214] H. Wintz, H.-C. Chen, C. A. Sutton, C. A. Conley, A. Cobb, D. Ruth, and M. R. Hanson, "Expression of the cms-associated urfs sequence in transgenic petunia and tobacco," *Plant Molecular Biology*, vol. 28, no. 1, pp. 83–92, 1995.

[215] Y. Kobayashi, H. Motose, K. Iwamoto, and H. Fukuda, "Expression and genome-wide analysis of the xylogen-type gene family," *Plant and Cell Physiology*, vol. 52, no. 6, pp. 1095–1106, 2011.

[216] D. Honys, S.-A. Oh, D. Reňák, M. Donders, B. Šolcová, J. A. Johnson, R. Boudová, and D. Twell, "Identification of microspore-active promoters that allow targeted manipulation of gene expression at early stages of microgametogenesis in arabidopsis," *BMC Plant Biology*, vol. 6, no. 1, pp. 31–39, 2006.

[217] J. A. da Costa-Nunes, "A novel arabidopsis marker line that strongly labels uninucleate microspores and the subsequent male gametophyte development stages," *SpringerPlus*, vol. 2, no. 1, pp. 237–244, 2013.

[218] C. Johns, M. Lu, A. Lyznik, and S. Mackenzie, "A mitochondrial DNA sequence is associated with abnormal pollen development in cytoplasmic male sterile bean plants.," *Plant Cell*, vol. 4, no. 4, pp. 435–49, 1992.

[219] D. C. Logan and C. J. Leaver, "Mitochondriatargeted gfp highlights the heterogeneity of mitochondrial shape, size and movement within living plant cells," *Journal of Experimental Botany*, vol. 51, no. 346, pp. 865–871, 2000.

[220] M. B. Smith, R. G. Palmer, and H. T. Horner, "Microscopy of a cytoplasmic male-sterile soybean from an interspecific cross between Glycine max and G. soya (Leguminosae)," *American Journal of Botany*, vol. 89, no. 3, pp. 417–426, 2002.

[221] A. Geitmann, V. E. Franklin-Tong, and A. C. Emons, "The self-incompatibility response in Papaver rhoeas pollen causes early and striking alterations to organelles," *Cell Death and Differentiation*, vol. 11, no. 8, pp. 812–822, 2004.

[222] I. Scott and D. C. Logan, "Mitochondrial morphology transition is an early indicator of subsequent cell death in arabidopsis," *New Phytologist*, vol. 177, no. 1, pp. 90–101, 2008.

[223] H. Imamura, K. P. Huynh Nhat, H. Togawa, K. Saito, R. Iino, Y. Kato-Yamada, T. Nagai, and H. Noji, "Visualization of ATP levels inside single living cells with fluorescence resonance energy transfer-based genetically encoded indicators," *Proc. Natl. Acad. Sci.*, vol. 106, no. 37, pp. 15651–15656, 2009.

[224] S. Ishiguro, Y. Nishimori, M. Yamada, H. Saito, T. Suzuki, T. Nakagawa, H. Miyake, K. Okada, and K. Nakamura, "The Arabidopsis FLAKY POLLEN1 gene encodes a 3-hydroxy-3-methylglutaryl-coenzyme A synthase required for development of tapetum-specific organelles and fertility of pollen grains.," *Plant Cell Physiol.*, vol. 51, no. 6, pp. 896–911, 2010.

[225] D. Maxwell, Y. Wang, and L. McIntosh, "The alternative oxidase lowers mitochondrial reactive oxygen production in plant cells," *Proceedings of the National Academy of Sciences of the United States of America*, vol. 96, no. 14, p. 82718276, 1999.

[226] P. Jiang, X. Zhang, Y. Zhu, W. Zhu, H. Xie, and X. Wang, "Metabolism of reactive oxygen species in cotton cytoplasmic male sterility and its restoration," *Plant Cell Reports*, vol. 26, no. 9, pp. 1627–1634, 2007.

[227] P. M. A. Kianian and S. F. Kianian, "Mitochondrial dynamics and the cell cycle," *Frontiers in Plant Science*, vol. 5, no. May, pp. 1–6, 2014.

[228] R. Mittler, S. Vanderauwera, N. Suzuki, G. Miller, V. B. Tognetti, K. Vandepoele, M. Gollery, V. Shulaev, and F. Van Breusegem, "ROS signaling: The new wave?," *Trends in Plant Science*, vol. 16, no. 6, pp. 300–309, 2011.

[229] J. a. Traverso, A. Pulido, M. I. Rodríguez-García, and J. D. Alché, "Thiol-based redox regulation in sexual plant reproduction: new insights and perspectives.," *Front. Plant Sci.*, vol. 4, no. November, p. 465, 2013.

[230] B. Zechmann, B. E. Koffler, and S. D. Russell, "Glutathione synthesis is essential for pollen germination in vitro," *BMC Plant Biology*, vol. 11, no. 54, pp. 1–11, 2011.

[231] F. Müller and I. Rieu, "Acclimation to high temperature during pollen development," *Plant Reprod.*, vol. 29, no. 1-2, pp. 107–118, 2016.

[232] M. Schwarzländer, M. D. Fricker, C. Müller, L. Marty, T. Brach, J. Novak, L. J. Sweetlove, R. Hell, and A. J. Meyer, "Confocal imaging of glutathione redox potential in living plant cells," *J. Microsc.*, vol. 231, no. 2, pp. 299–316, 2008.

[233] C. Carrie, E. Giraud, O. Duncan, L. Xu, Y. Wang, S. Huang, R. Clifton, M. Murcha, A. Filipovska, O. Rackham, *et al.*, "Conserved and novel functions for arabidopsis thaliana mia40 in assembly of proteins in mitochondria and peroxisomes," *Journal of Biological Chemistry*, vol. 285, no. 46, pp. 36138–36148, 2010.

[234] J. Dahan, G. Tcherkez, D. Macherel, A. Benamar, K. Belcram, M. Quadrado, N. Arnal, and H. Mireau, "Disruption of the cytochrome c oxidase deficient1 gene leads to cytochrome c oxidase depletion and reorchestrated respiratory metabolism in arabidopsis," *Plant Physiology*, vol. 166, no. 4, pp. 1788–1802, 2014.

[235] M. Sabar, J. Balk, and C. J. Leaver, "Histochemical staining and quantification of plant mitochondrial respiratory chain complexes using blue-native polyacrylamide gel electrophoresis," *Plant J.*, vol. 44, no. 5, pp. 893–901, 2005.

[236] M. P. Alexander, "Differential staining of aborted and nonaborted pollen," *Stain Technology*, vol. 44, no. 3, pp. 117–122, 1969. PMID: 4181665.

[237] V. De Col, P. Fuchs, T. Nietzel, M. Elsaesser, C. P. Voon, A. Candeo, I. Seeliger, M. Fricker, C. Grefen, I. M. Moller, A. Bassi, B. L. Lim, M. Zancani, A. Meyer, A. Costa, S. Wagner, and M. Schwarzlaender, "Atp sensing in living plant cells reveals tissue gradients and stress dynamics of energy physiology," *bioRxiv*, 2017.

[238] D. Ezeria, B. Morgan, and T. P. Dick, "Imaging dynamic redox processes with genetically encoded probes," *J. Mol. Cell. Cardiol.*, vol. 73, no. 0, pp. 43–49, 2014.

136

[239] S. Wagner, T. Nietzel, I. Aller, A. Costa, M. D. Fricker, A. J. Meyer, and M. Schwarzländer, *Analysis of Plant Mitochondrial Function Using Fluorescent Protein Sensors*, pp. 241–252. New York, NY: Springer New York, 2015.

[240] I. Aller, N. Rouhier, and A. J. Meyer, "Development of roGFP2-derived redox probes for measurement of the glutathione redox potential in the cytosol of severely glutathione-deficient rml1 seedlings.," *Front. Plant Sci.*, vol. 4, no. December, p. 506, 2013.

Titre : Analyse fonctionnelle d'une stérilité mâle cytoplasmique chez *Arabidopsis thaliana*

Mots clefs : Stérilité mâle cytoplasmique, pollen, mitochondries, roGFP2-Grx1, ATeam, microscopie confocale

Résumé : Les stérilités mâles cytoplasmiques (SMC) résultent d'une incompatibilité nucléo-cytoplasmique. Le cytoplasme (presque toujours la mitochondrie) peut porter un gène de stérilité mâle, et le noyau peut restaurer la fertilité pollinique ou non. Les mécanismes physiologiques conduisant à la mort pollinique restent largement incompris. Plusieurs hypothèses ont été proposées, parmi lesquelles une déficience en ATP. Une SMC gamétophytique a été découverte chez *A. thaliana*. Une phase ouverte de lecture codant possiblement un peptide de 117 acides aminés, appelée *orf117Sha*, a été identifiée comme facteur de stérilité candidat. Au cours de ma thèse, j'ai cherché à valider le rôle de l'*orf117Sha*, et à comprendre comment une anomalie mitochondriale pouvait induire cette SMC. Aucune différence n'a pu être détectée au niveau de l'ARNm de l'*orf117Sha* entre les lignées stérile et restaurée, mais sa protéine semble accumulée uniquement dans la lignée stérile. La phénocopie par transgénèse de la SMC a suggéré un effet délétère de l'ORF117SHA dans les gamétophytes mâle et femelle. La description cytologique de la SMC montre une mort pollinique progressive à partir du stade binucléé. Auparavant, les mitochondries du pollen gonflent puis éclatent, et le développement s'arrête. L'utilisation de senseurs génétiquement encodés mesurant la concentration en ATP (ATeam) et l'état redox du glutathion (roGFP2-Grx1) a permis la mesure de ces facteurs en microscopie confocale, dans des tissus végétatifs et dans le pollen. La production d'ATP ne semble pas affectée dans la lignée stérile, contredisant l'hypothèse de l'ATP. Le glutathion mitochondrial est suroxydé dans la lignée stérile, à la fois dans les tissus végétatifs étudiés et le pollen, qui serait liée à la SMC car annulée par la restauration génétique de fertilité. Avec cette étude, j'apporte des arguments en faveur de l'*orf117Sha* dans l'induction de la SMC Sha, et je décris les évènements préalables à l'avortement du grain de pollen. Mes résultats permettent de mieux comprendre les évènements physiologiques conduisant à la mort du pollen.

Title : Functional analysis of a cytoplasmic male sterility in *Arabidopsis thaliana*

Keywords : Cytoplasmic male sterility, pollen, mitochondria, roGFP2-Grx1, ATeam, confocal microscopy

Abstract : This work aims at better understand the events leading to pollen abortion in a recently discovered gametophytic cytoplasmic male sterility (CMS) in *Arabidopsis thaliana*. Although CMS have been widely used in hybrid seed production in many crops, the physiological mechanisms leading to pollen death by the mitochondrial sterilizing genes in the permissive (maintainer) nuclear backgrounds are poorly understood. Association genetics previously identified orf117Sha as a candidate mitochondrial CMS-associated gene. In a first part, I analyzed the expression of the *orf117Sha* gene in sterile plants and in fertile plants carrying nuclear genes restoring male fertility. I observed unusual features of its mRNA, but detected no difference at this level between sterile and restored plants. Oppositely, the ORF117SHA protein seems to be accumulated specifically in the sterile line, supporting its role in CMS. A phenocopy attempt by transgenesis suggested a possible link between a female and male gametophytic lethality and the ORF117SHA, even though few individuals could be analyzed. In a second part, I observed pollen development in sterile plants and fertile controls using different cytological approaches. My results show a progressive pollen death starting from the binucleate stage in the sterile. Prior to abortion, pollen mitochondria swell before rupture, and the development stops. I used confocal microscopy combined with genetically encoded sensors to explore specific physiological features in pollen and vegetative tissues of sterile plants. With ATeam, which allows the assessment of ATP content in the cytosol, I could challenge the generally accepted hypothesis of an ATP deficiency leading to pollen abortion in CMS. Indeed, the ATP production does not seem to be affected in the sterile line. With a mitochondria-targeted roGFP2-Grx1, I was able to assess the redox state of the glutathione pool in vegetative tissues and in the male gametophyte. I observed an overoxidation of the glutathione pool in mitochondria of the sterile line, in vegetative tissue investigated and in the pollen grain. This overoxidation seems to be linked to the CMS as it is annihilated by the presence of restorer genes. My results pave the way for further exploration of the links between the sterility protein, mitochondrial morphology changes, mitochondrial overoxidation, and pollen development arrest and death in the *A. thaliana* CMS.